The study of Force in Digitally Captured Signatures

By Nikolaos D. Kalantzis

PhD Thesis
Submitted September 2025

ABSTRACT

Digitally Captured Signatures (DCS) provide biometric data—typically X and Y pen positions, applied force (F), and time (T)—that allow forensic handwriting examiners to assess authenticity with greater precision than traditional pen-and-paper signatures (PPS). Among these parameters, force data is particularly significant: while PPS reveals pen pressure only indirectly through ink distribution and line quality, DCS records it quantitatively. However, a major obstacle arises from the inconsistency of how different devices register force. Many systems label outputs as "pressure levels," but these do not correspond to absolute values. The same "pressure level" can represent different actual forces across devices, rendering raw data incomparable.

To address this limitation, experimental calibration methods have been developed to link device-specific "pressure levels" to physical force values. The **Zeta Function** (and its inverse, the Zeta^{-1} Function) provides a mathematical model for this mapping. By applying known forces through a mechanical array and recording the corresponding sensor outputs, a logarithmic relationship is derived that characterizes the response curve of each digitizing device. This Zeta Function enables conversion from arbitrary "pressure levels" to standardized Newton values, while the inverse function allows re-normalization of raw data to the scale of another device.

The implications for forensic practice are substantial. In real-world casework, disputed signatures and reference samples may originate from different hardware platforms or software versions. Without normalization, cross-comparison of force data is unreliable, potentially undermining evidentiary conclusions. By applying the Zeta Function, examiners can standardize datasets, ensuring comparability and preserving the evidentiary value of dynamic biometric features. This approach parallels established forensic practices in other disciplines, where calibration and normalization safeguard the integrity of measurements.

Moreover, use of the Zeta Function enhances error detection. Calibration curves can reveal defective sensors, software misinterpretations, or anomalous scaling, preventing misattribution of irregularities to the writer. This provides both scientific reliability and legal robustness, particularly under frameworks such as the EU eIDAS Regulation and national laws (e.g., Greece's Law 4961/2022), which grant evidentiary force to advanced and qualified electronic signatures.

In summary, while DCS technology offers unparalleled access to dynamic writing features, its forensic utility depends on the reliable interpretation of force data. The Zeta Function serves as a normalization tool that bridges hardware inconsistencies, supports valid cross-platform comparisons, and strengthens the role of DCS in forensic handwriting examination. By standardizing force analysis, it advances both the scientific credibility and legal admissibility of DCS evidence.

Dedication/Acknowledgements

This work is dedicated to Butuna, Sarra, Emmeleia, Silouanos, Maximos, Porfyrios and Sofronios, without which the world would be colourless.

I also have to acknowledge my teachers, Dimitrios who planted the seed, Manfred who cultivated the tree, Andy who supported me for so many years, Philip Andrew Morton for his support and George Pappas for his help in various bits here and there, reminding me of our time as first year students at the Physics Department.

Authors declaration

This Thesis is the result of my own work and has not previously been submitted for any degree at Staffordshire University / University of Staffordshire or any other institution.

Nikolaos D. Kalantzis

Table of Contents

List of Tables and Figures

1. Digitally Captured Signatures (DCS)[1] and the importance of Force

The Digitally Captured Signature (DCS, a.k.a. electronic handwritten signatures or biometric signature) has been established over the last few years throughout the EU area and abroad, both in the government and private sectors. The adaptation of the eIDAS regulation (eIDAS Refulation, 2014) from the EU member states (in full force since end of September 2018) lead the way for the major financing institutions (e.g. vast majority of systemic banks in Greece), government structures (use of DCS in Citizen's Service Centres (Greece, Law 4961/2022) and in consumer outlets (all telecommunication providers etc.).

As a result, the question of whether the DCS is forensically suitable as a legal alternative to the traditional pen and paper signature (PPS) surfaces. For an authentication and identification medium to be legally valid, its forensic

[1] Parts of the contents of this chapter have been published in Kalantzis N.: THE ELECTRONIC HANDWRITTEN SIGNATURE (DIGITALLY CAPTURED SIGNATURE – DCS) AS AN EQUIVALENT COUNTERPART TO THE TRADITIONAL PEN & PAPER SIGNATURE. CRIMINALISTICA NR. 1-2024 (137), MARTIE 2024, VOL. XXV and Kalantzis N., Platt A.W.G.: Digitally Captured Signatures (Biometric signatures) and Forensic Handwriting Examination: A short introduction, Penal Justice/Ποινική Δικαιοσύνη, ΠοινΔικ 10/2020, pp 1006-1012

examination – i.e. the capability of determining authenticity – has to be established.

1.1. What is a Digitally Captured Signature?

A quick definition of a DCS would be the data produced from the capturing of the physical properties of a signature. The capturing requires the use of a digitizing device and appropriate software and the physical properties that can be captured are the XY position of the tip of the stylus, time, force etc. The DCS is one kind of Electronic Signature.

For example, in practice, when a person performs a transaction in front of a bank teller with such as system, the following actions take place:

a. the teller creates a digital file, which remains "open", waiting for the capturing of the biometric data of the signatory, as they will be captured by the DCS,

b. the signatory is asked to "execute" their signature with the use of the suitable stylus on the active area of the digitizer (which is usually made of glass), and

c. after completion of the signing formation, either the signatory by pressing the appropriate button on the digitizer with the stylus, or the teller through their terminal, embeds the biometric data inside the digital file, which is automatically encrypted, producing what is usually referred to as the biometric file (or biometric PDF).

After the embedding and encrypting of the file, the biometric data cannot be accessed without the use of the system decryption keys. The produced "biometric" PDF is still accessible as to its pictorial information by any user, but the biometric data are encrypted inside the file – accessing the biometric PDF as a PDF file may reveal a 2-dimensional representation of the shape of the executed DCS, but that image is captured and embedded as an image (no biometric data) only during the creation of the file, and its presence does not imply access to the encrypted biometric data every time the file is accessed as a PDF file.

It should be noted that some systems also produce a "flat" PDF file alongside the "biometric" PDF file, which is a version of the file without any biometric data.

1.2. DCS biometric data and visualizations

The most common biometric data selected to be captured during signature execution for the aforementioned reason, as adopted internationally, are the following:

A. The horizontal pen position coordinate on the active area, denoted as X.

B. The vertical pen position coordinate on the active area, denoted as Y.

C. The Pressure or Force coordinate as measured along the axis of the stylus, depending on the hardware technology and the software used. This can be denoted as P or F.

D. The time of collection of events (points), denoted as T[2].

These four data channels constitute the biometric data that are routinely captured. It should be noted that there are other/more parameters that may be captured, depending on the hardware and software combination, e.g. the Apple iPad Pro and Wacom Intuos Pro may capture two additional angles – called tilt and azimuth – allowing the recreation and calculation of the 3-dimentional position and orientation of the stylus during the execution of a signature. Still the four data channels X, Y, F and T are currently the standard as deployed by the industry – a more comprehensive list of possible data to be captured is mentioned in the ISO/IEX 19794-7 (ISO/IEC 19794-7:2021).

When a signature is executed on paper with the use of a writing instrument, depending on the dynamics of the writer's product, the tip of the writing instruments moves on the XY plane but also minutely along the Z axis (or to be more accurate along the axis of the writing instrument) pushing towards and pulling from the surface of the document.

In the DCS there is no Z axis movement (as the glass or other surface of the digitizer does not "move" or is not deformed); instead of this parameter in DCS the force exercised by the writer through the stylus along the axis of the stylus is measured using pressure sensors. Currently the force is recorded in arbitrary units

[2] Even though in the SI time is symbolized by the small letter "t", due to the ISO19794-7 abbreviations and its adoption by the industry, time will be denoted with the capital letter "T".

that are intuitively called “Pressure Levels” even though they refer to Force rather than Pressure.

Essentially, the DCS is a collection of four numbers per event, four parameters; the real “image” of the DCS is presented in Table 1.1.

X (mm)	**Y (mm)**	**Time (msec)**	**Pressure Levels (%)**
63.64	36	2365	61.97
63.63	36.16	2370	64.91
63.55	36.36	2375	66.76
63.43	36.61	2380	68.04
63.27	36.87	2385	68.52
63.09	37.13	2390	68.82
62.91	37.38	2395	68.91
62.74	37.61	2400	69.01

Table 1.1 - Biometric Data as numerical values.

As the forensic expert is not used to directly comprehend and compare the acquired numerical values, a series of representations based on the visualization of the same numerical values, that is more familiar to them, is usually created per DCS. The most common that are currently used in practice are the following:

a) *Point by point representation*: in this representation the X and Y data channels are positioned on the horizontal plane. The resulting image resembles the trace of an executed signature, but the points are not connected. The information included in this representation is also the T data channel as the distance between points will reveal the speed of execution – especially if a

constant frequency of collection is used (although not directly calculable). There are versions of this representation where the diameter of the points is associated to the F data channel and hence all four data channels are represented, one way or another.

b) *Point by point representation with in-air movements*: this representation is the same as the previous one, with the difference that the in-air movements (i.e. the position of the stylus when *not* in contact with the active area and in close proximity to the active area, for EMR solutions).

c) *Connected line representation*: in this representation the single points of the captured events are connected, forming a visible line that resembles the inked trace of a PPT. In this representation the F data channel values can be incorporated too if they are connected to the size of the line.

d) *Time graphs*: in this form, data channels are represented in the form of XY plots, with the T data channel usually used as the X axis.

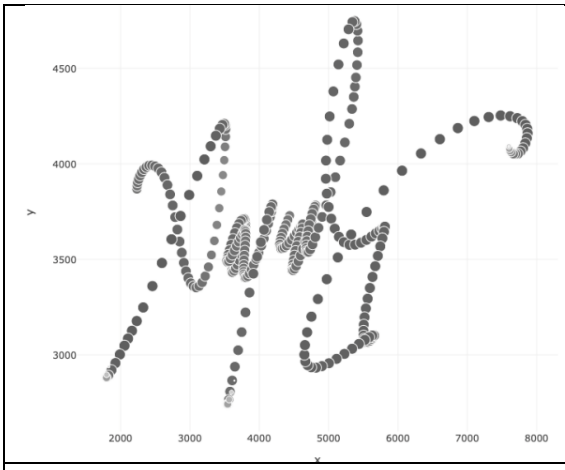

(a) Point by point representation

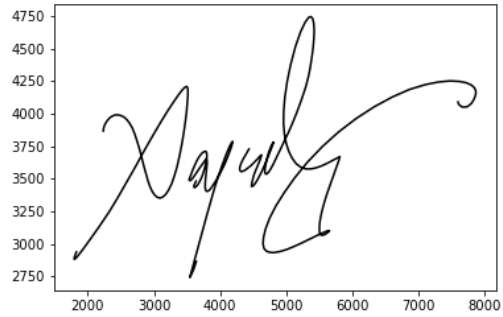

(b) Connected line XY representation (2 dimensional)

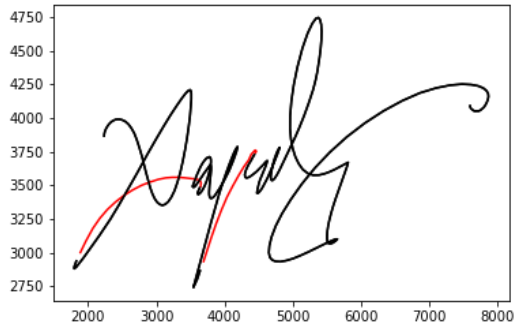

(c) Connected line XY representation (2 dimensional) with representation of the in-air movement of the stylus (in red color)

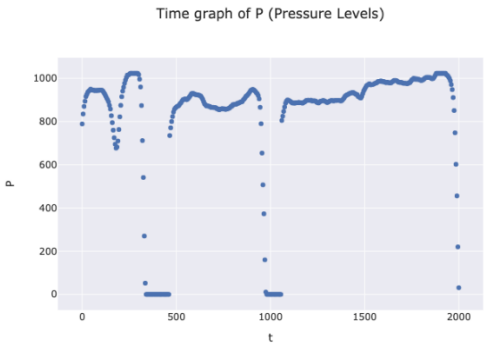

(d.1) Time graph (Pressure levels over time)

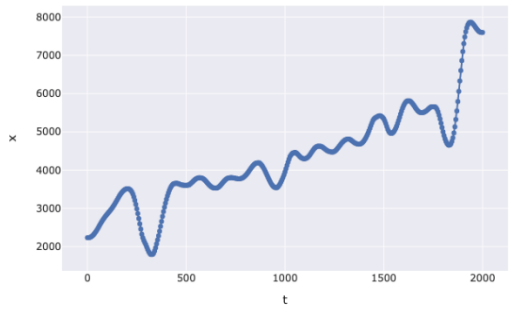

(d.2) Time graph (Movement on X axis over time)

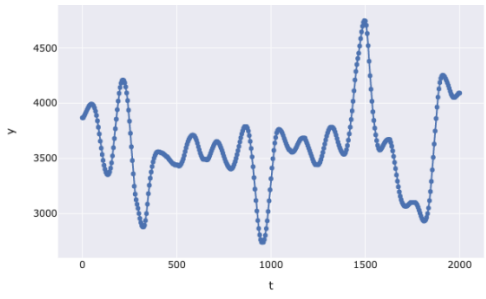

(d.3) Time graph (Movement on Y axis over time)

Figure 1.1 - Different visualizations of the same DCS.

e) *Colour representations*: In these representations, the data channels are represented either in point by point or connected line form, the F data channel is associated with the colour of the points/line and the representation can be visualized either in 2-dimensions or 3-dimensions. In the latter case, the user can interact with the representation by rotating it, allowing deeper study and appreciation of the data.

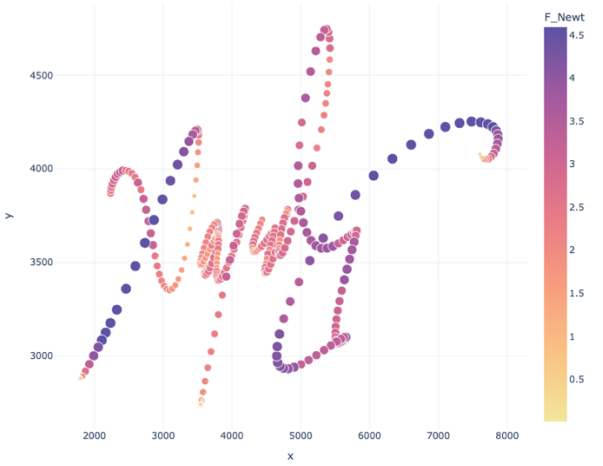	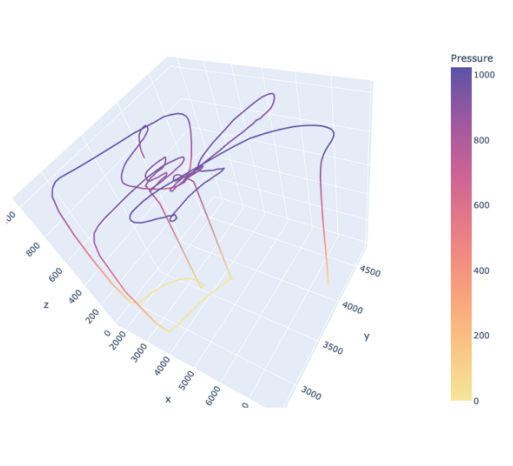
Connected line XY representation with color correlation of pressure levels (i.e. Force, in N)	3-dimensional point by point representation of the data channels X, Y and F. The size and colour of the points can be associated to the F data channel values.

Figure 1.2 - Different visualizations of the same DCS.

1.3. Forensic Examination of authorship for DCS

The DCS is a digitization of the handwritten motion, captured in numerical values, that can be visualized in familiar forms – similar to what the forensic expert

has been trained to examine. Using this parallel relationship, the methodology of examination of authenticity of a DCS resides in transforming and adapting the already established methodology for PPS.

A method for this type of examination has already been published by the European Network of Forensic Handwriting Experts since 2020 (ENFSI, 2020), and subsequently updated in 2022 (ENFSI, 2022). The concept of approach is based on adapting the already published method for determination of authenticity of PPS (Appendix no.3 of the Best Practice Manual (ENFSI, 2020, 2022)), to accommodate for the new features or new representations/visualizations of said features (Appendix no.5 (ENFSI, 2020) and then Appendix no.6 (ENFSI, 2022)).

A correlation of the correspondence of traditionally examined characteristics to their digital counterparts is presented in Table 1.2.

<table>
<tr><td colspan="3">Analysed Characteristics</td></tr>
<tr><td>PPS</td><td colspan="2">DCS Correspondence</td></tr>
<tr><td>Style and legibility</td><td colspan="2" rowspan="5">Spatial representations (e.g. point by point or connected line representations)</td></tr>
<tr><td>Size</td></tr>
<tr><td>Proportions</td></tr>
<tr><td>Spacing</td></tr>
<tr><td>Slant & Slope</td></tr>
<tr><td>Evidence of Tracing</td><td colspan="2">Not applicable[3]</td></tr>
<tr><td>Fluency & Pressure</td><td rowspan="5">Spatial representations</td><td rowspan="5">Dynamic Representations</td></tr>
<tr><td>Layout</td></tr>
<tr><td>Individual Character Shape</td></tr>
<tr><td>Individual Character Proportions</td></tr>
<tr><td>Individual Character Construction</td></tr>
</table>

Table 1.2 Analysed Characteristics

The visual representations of the DCS are not only equal to the 2-dimensional image of the PPS, but also allow for finer detail and greater accuracy to the calculations (as the spatial measurements are taking place based on the ppi[4] sensitivity of the digitizers which are very high in comparison to the detail perceivable by the human eye, which is about 84 μm (Betancourt and del Rio, 2006)). Furthermore, the numerical nature of the data allows for direct calculation of measures, which in turns allows integrated statistical calculations and measurements for the FHE.

[3] In case of DCS, the evidence of tracing is qualitative and to be found within the data, on contrast to PPS where it is mainly physical and can be found on the surface of the document.
[4] Point per inch analysis. e.g. for the Wacom DTU1141b has resolution of 540 lpi or 0.01 mm/pt.

Another important enhancement in the case of DCS vs. PPS is the quantitative capturing and representation of writing pressure (force) in contrast to the qualitative approach through microscopical examination of that dynamic parameter, as it currently takes place in PPS examinations. This enhancement allows the FHE to accurately study the exercised force during signature execution and perform the analysis, comparison and evaluation of this feature on a higher level. The additional recording of the in-air-trajectories (IATs) (Pertsinakis and Fernandes, 2018), when an EMR solution is used, provides with additional valuable information to the FHE, a feature that by default remains invisible in PPS. The recording of the time of execution (and the time of each event) also introduces a valuable dynamic aspect of the signature execution – available to the FHE. The time duration of the signature is directly connected to the natural execution of motion, the quality of the written line and therefore it is a factor that is largely differentiated in the event of forgery.

Therefore, it is obvious that DCS provide not only the same amount of information as the PPS to the FHE (as to the characteristics that should be analysed according to the BPM), but much more meaningful information than PPS.

1.4. Suitability of the DCS as a means of Authentication and Authorization

Regarding the suitability of DCS as a means of identification and authorization, a thorough research study (Heckeroth *et al*., 2020) financed[5] by the EU and the Internal Security Fund – Police (ISFP), investigated the variation of these various parameters when comparing PPS and DCS (through the examination of hybrid signatures), resulting amongst other deliverables to the aforementioned method of the ENFHEX BPM entitled "OVERVIEW PROCEDURE FOR FORENSIC EXAMINATIONS AND COMPARISONS OF DIGITALLY CAPTURED SIGNATURES AND HANDWRITTEN ENTRIES" (ENFSI, 2020, 2022), which deals with the method of determining the authenticity of disputed DCS, based on the preexisting method for PPS (which is also described in Appendix no.3 of the same document).

1.4.1. Suitability of DCS according to eIDAS

As it is thoroughly exhibited in the previous chapter, the DCS and its ability to capture the four biometric parameters (X, Y, F, T) is equivalent from the aspect of forensic examination of authenticity to that of the PPS and thus provides all the necessary tools to the trained expert to proceed to such an examination. Obviously, there are requirements that need to be met from the deployed DCS system; these are described in the relevant scientific literature (Čakovská *et al*.,

[5] "Steps Towards a European Forensic Science Area, STEFA, ISFP-2016-AG-IBA-ENFSI".

2020) as well as in the Annex II of eIDAS (eIDAS Regulation, 2014). From the aspect of definitions according to eIDAS, the DCS can constitute both an AES and a QES.

Article 26 of eIDAS stipulates that the Advanced Electronic Signature (AES) must meet the following requirements:

a) it is uniquely linked to the signatory;

b) it is capable of identifying the signatory;

c) it is created using electronic signature creation data that the signatory can, with a high level of confidence, use under his sole control; and

d) it is linked to the data signed therewith in such a way that any subsequent change in the data is detectable.

On point 12 of article 3 of eIDAS, the following is mentioned for Qualified Electronic Signatures (QES): «*'qualified electronic signature' means an advanced electronic signature, that is created by a qualified electronic signature creation device and is based on a qualified certificate for electronic signatures*».

Therefore, the difference between an AES and a QES lies on the additional use of a qualified certificate for electronic signatures during the creation of the digital file, which is sealed by it, and does not involve in any way the nature of the included biometric data or any other digitized characteristic of the stylus motion during the signature execution and subsequent capturing of motion parameters. The equivalence of DCS to PPS refers to the *manual* execution and correct

recording and parameterization of the movement of the stylus during the execution of the signature formation. As such, it is not affected by the use or not of a qualified certificate during the digital sealing of the electronic document.

The article 25 of eIDAS mentions that "*an electronic signature shall not be denied legal effect and admissibility as evidence in legal proceedings solely on the grounds that it is in an electronic form or that it does not meet the requirements for qualified electronic signatures*" and therefore a DCS in the form of an AES has legal effect and meets the requirements for a forensic examination and determination of authenticity.

1.4.2. Example of legal adaptation

In late summer of 2022, the Greek parliament voted law 4961/2022. The article 90 of this law states:

"1. The signing of applications and other documents bound to be processed at the K.E.P.[6] can be executed by using a digitized handwritten signature[7] on the document, which, solely for this purpose, has the same legal and evidentiary force as the handwritten signature[8] of a natural person. A digital handwritten signature is considered to be a handwritten signature placed in the physical presence of the signatory on a recording surface (tablet) using a stylus.

[6] Κεντρο Εξυπηρέτησης Πολιτών / Citizen's Service Center.
[7] i.e. DCS
[8] i.e. PPS

3. Paragraphs 1 and 2 also apply to the digitized handwritten signatures placed on any type of document with which a transaction is carried out within a credit or financial institution branch in the boundaries of the meaning of paragraphs 1 and 26 of paragraph 1 of article 4 of the Regulation (EU) 575/2013 on prudential requirements for credit institutions and investment firms and amending Regulation (EU) 648/2012 (L 176), respectively, in the physical presence of the signatory."

This law is a revision of the preexisting law 4821/2021 which recognized the legal validity of DCS executed for administrative applications and actions in Citizen Service Centers. This law was revisited, and paragraph 3 was added, allowing the use (& recognition of the legal validity) of DCS for all actions that are carried out within a credit or financial institution branch. This revision recognizes the DCS in its AES form, for all such transactions, with the caveat of the capturing to take place within the branch/building/premises of the institution. This law does not directly refer to AES, QES or the eIDAS regulation at all. Instead, it shifts the certification requirement of the QES (vs. the AES) to the physical location of the capturing (hence the caveat).

This approach deals in a direct and meaningful way with the QES substantial requirements that within eIDAS are expressed with the necessity of an additional certificate (from the client). This approach allows the full deployment of DCS (in

this AES manner) for full coverage of transactional needs, within the eIDAS requirements.

1.4.3. Lack of uniformity of DCS data

Having explored the various ways of visualizing and analysing the captured biometric data, in order to access the same amount of information as with the PPS and allow forensic examination of the DCS, it has to be stated that not all DCS solutions capture the same data or at the same detail and accuracy.

The necessary requirements from the point of view of the forensic expert has already been established (Čakovská *et al*., 2020), but the mere hardware specifications are not a safeguard. The DCS deployment involves both a hardware and a software component and both need to be confirmed that they are adequately capturing the necessary data. It has been shown (Kalantzis, 2023) that not only defective hardware has been deployed in the past but also defective software running properly designed hardware, that led to mislead opinions of experts as to the authenticity of the captured DCS. Furthermore, it has already been established (in a qualitative way) that different software and hardware combinations capture the same input (signature) differently (Zimmer *et al*., 2021).

1.5. First conclusions – Importance of Pressure/Force

The DCS can record with adequacy the characteristics of motion of the writing instrument/stylus during the execution of a signature formation and can therefore be the subject of the examination and determination of authenticity within the scope of Forensic Handwriting Examination (when specific qualitative conditions are met). The DCS and the corresponding recorded biometric data are represented in the same manner in AES and QES without loss of information, that would affect the capability of examining and determining its authenticity by a Forensic Handwriting Examiner in either form.

For the aforementioned reasons from both the theoretical approach of the Forensic Examination of Handwriting and Signatures as well as the practical application of the established method, DCS is treated as a suitable means of identification and authentication, allowing the forensic determination of authenticity, equivalently to the PPS. This inevitably means that the DCS will be the object of forensic examinations, following the same rules of Analysis – Comparison – Evaluation as PPS, which will certainly involve the examination of DCS captured from different software and hardware solutions. This eventuality requires the investigation of the unnormalized Force channel (provided in arbitrary Pressure Levels by the software and hardware manufacturers) and the establishment of a common representation system.

Forensic handwriting and signature examination rely on the analysis, comparison and evaluation of a series of characteristics that describe both the static (pictorial) as well as the dynamic aspects of a given handwriting product. Amongst these features, a very important one that allows the study of the dynamic aspects of handwriting, is pressure. Identified as one of the three aspects of pen control (as point load, the others being pen position and pen hold) (Huber and Headrick, 1999), pen pressure (point load or just pressure) can be defined as "the weight or pressure unconsciously applied to the pen during the act of writing" (Brewster, 1932), and this definition in itself includes some ambiguity. In the ENFHEX Best Practice Manual (BPM) (ENFSI, 2020), as part of the "General Characteristics" of handwriting and signatures that have to be taken into account during a forensic examination of authenticity, "fluency/pressure" is mentioned indirectly as a description of "whether the writing appears to be skilfully or poorly produced, whether there is hesitation in the pen line, whether the writing line is smooth flowing and whether the writing line has variable pressure, or constant, hard pressure" and the association of quality, penmanship and "pressure" becomes obvious. Still, pressure (in any of the above references) remains an aspect of writing that is evaluated by the qualified Forensic Handwriting Examiner (FHE) qualitatively and not quantitatively through inspection of the written line characteristics (preferably under the stereomicroscope).

1.6. The terms Force and Pressure

As it has already been discussed, in DCS the software and hardware solutions employed to digitize and encrypt the hand/stylus movements during signature execution produce sets of interconnected data. The mainstream coordinates currently captured by these solutions worldwide are identified as the X, Y, T and F channels (ISO/IEC 19794-7:2021). According to the ISO/IEC documentation (ISO/IEC 19794-7:2021), the X and Y channels capture the x and y spatial coordinates (i.e. the horizontal and vertical pen position on the surface of the digitizer) and the T channel captures the time data relative to the first data point. The pen tip force channel (or F channel) is defined as "recording pen forces (pressure) data". The ISO documentation goes one step further recognizing Newtons (N) as the unit of measurement. This is not necessarily reflected in the output of the currently available software and hardware solutions (as will be discussed later) and the terminology used in the application of this technology can be misleading. The ease with which different measures are interchanged creates problems of perception as pressure and force are treated as equals, and even though the ISO documentation describes the F channel values as "Force" to be measured in N, most solutions refer to the F channel values as "Pressure". Still, the definition is very clear, and in paragraph 7.7 of the standard it is stated that The F channel is for recording the magnitude of pen tip force. The unit of measurement is Newton (N). Furthermore, it is interesting to note the first edition (2007) of the

standard (ISO/IEC 19794-7:2007) in the corresponding paragraph (6.7 Pen tip force channel: F) mentioned “The F channel is defined for recording pen forces (pressure) data”. The term “pressure” in parenthesis was removed on the second edition (2017) (ISO/IEC 19794-7:2017).

When it comes to traditional (pen and paper) handwriting and signature examination, “pressure” is the term used to describe the effect of the dynamic parameter of the pen tip motion on paper. Huber and Headrick define pen pressure as “the average weight or pressure unconsciously applied to the writing instrument during the act of writing. The operative words in this definition are average weight,

which implies it is the average force with which the pen contacts the paper that determines whether a body of writing was written with light, medium, or heavy pen pressure” and “ When dealing with documents written with ballpoint pens, greater pressure applied during the writing process will cause the tip of the pen to push further into the paper, resulting in a slight thickening of the line and a depression of paper fibres under the written stroke.” (Huber and Headrick, 1999), exhibiting the ambiguity and empirical approach to the definition; in the glossary of the same book, the authors define pen pressure as “the force with which the writing instrument contacts the paper” (Huber and Headrick, 1999) referencing the corresponding ASTM standard (ASTM International, 2009), a definition which was repeated verbatim in the subsequent SWGDOC standard (SWGDOC, 2013).

1.7. How important is force?

The dynamic characteristics of handwriting and signature are very important for the examination and determination of authenticity. Huber and Headrick mention that "A person's pressure pattern is so unique that even if the letterforms are copied, the pen pressure usually betrays the forger", and carry on highlighting the importance of pen pressure by mentioning that "Regardless of the type of writing instrument used to prepare a document, a careful inspection of the questioned handwriting can reveal important details that speak volumes concerning the writing process. Heavy, consistent pen pressure frequently associated with slowly executed, drawn movements will quickly become apparent when dealing with forged signatures, as will other deficiencies, including tremor, retouching, pen lifts, and irregular pen strokes." (Huber and Headrick, 1999)

Ellen mentions that "Pressure variation is rarely consistent in forged signatures… Pressure habits are deeply ingrained and very difficult to simulate" (Ellen, 2005).

The importance of pen pressure as a feature that discriminates authentic from forges or disguised signatures is clearly and analytically described by Caliguiri and Mohammed (Caligiuri and Mohammed, 2012).

Having clarified that the term pressure in the relevant literature relates to the quantity of force (measured in Newtons) and not pressure (which is force over area

and is measure in Pascals), it is obvious that a clear definition of the units used in the capturing of said force is necessary.

1.8. The necessity for calibration testing

As it has been already discussed, force (mentioned as pressure) is a very important characteristic of writing, especially when the determination of authenticity is discussed. But how is force recorded in DCS systems?

The possibility of different software and hardware solutions to measure exercised force differently (and therefore attribute different Pressure Levels to the same amount of force) has already been hinted in the literature (Zimmer *et al*., 2021) but is largely left not considered. Multiple studies that deal with pressure (or rather force) are self-consistent as they process data from the same software and hardware solution (Mohammed *et al*., 2015; Mohammed *et al*., 2011; Li *et al*., 2018), which means even though their force data is unnormalized, it is captured on the same system (and hence comparable).

1.9. Characteristics of the mechanism

As it was made clear in the previous section, it is necessary to construct a calibration mechanism that will allow us to study the relation of exercised force to assigned pressure levels by the various software and hardware solutions for capturing DCS.

The necessary feature of this mechanism is that it has to provide at the same time the amount of applied force (in Newtons) and the assigned pressure levels, also providing control of the amount of exercised force. Such approaches have happened in the past, but a fresh approach was deemed necessary.

1.9.1. Experiment by Katrin Franke

Katrin Franke in her research (Franke, 2005) did construct an experimental array to study the relation of Force to assigned pressure levels in one software/hardware combination. In her approach, Franke uses springs and their displacement to calculate force (according to Hooke's law). This approach whilst accurate as to the measurement of the exercised force, proved to be very complex in construction, especially if multiple different hardware solutions are to be used and hence was not considered as a possible approach to the current research.

1.9.2. Experiment by Jonathan Heckeroth

Jonathan Heckeroth in his research (Heckeroth, Kerkhoff and Weyermann, 2019) modified a 3D printer and tried to control the exercised force by controlling the displacement of the arm of the printer (which hold the stylus) along the Z axis, and by inserting a set of scales underneath the digitizer to collect the measured weight and hence calculate the force. Still, this array proved unreliable as the ambiguity of the z axis movement of the 3D printer's arm as well as the stress tolerance of the construction had as a result the fluctuation of the measured force for the same z axis displacement and this approach was not considered at all.

1.9.3. Need for a new mechanism

The preexisting attempts were considered but eventually were deemed unsuitable for the purposes of this study. The Franke mechanism, although precise, was far too complex to replicate and an easier, more direct solution was selected. The Heckeroth mechanism captured (with unknown accuracy and repeatability) the position of the robot arm on the Z axis, having generated force data as a result of the resistance of the digitizer pad which is "blocking" the path of the stylus. This

approach involves questionable repeatability features from the aspect of exercised force as it is not the force per se that is repeated each time but the displacement of the arm/stylus on the z axis, or rather the effort to produce such a movement of the robot arm. The accuracy and repeatability of such a method relies on the tolerance of the physical construction, possible random minute movements of the positioning of the entire configuration etc. The importance of low tolerance in the various “parts” that transfer force was also observed in a first attempt to build such a mechanism.

1.9.4. Initial exploration of the F channel behaviour

The first attempt to create a calibrating mechanism involved the use of a XY plotter to “draw” a straight line and to use a small wedge underneath one side of the digitizer (Figure 1.3).

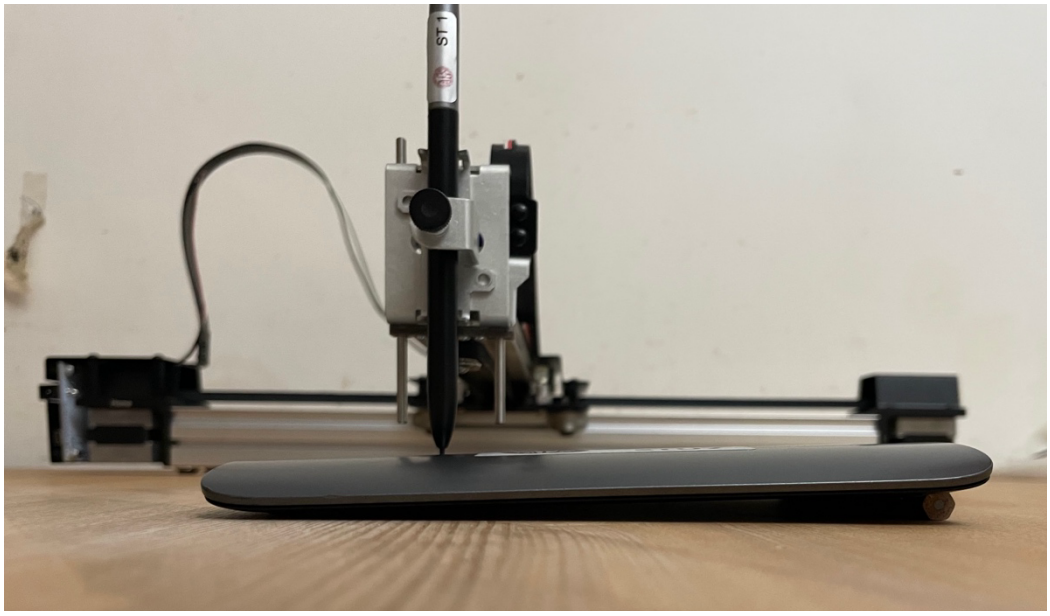

Figure 1.3 Spirals executed with the Axidraw and captured with the Wacom STU530. Wedge positioned under the digitizer.

The wedge raises one part of the digitizer; as the robot arm would move along the XY plane in a direction vertical to the placement of the wedge, continuous pressure level values would be collected (from 0 to the maximum of each tested solution). This initial attempt was more qualitative than quantitative, aiming at correlating a linear stimulus (the movement of the stylus held by the XY plotter over a slanted digitizer) with the corresponding pressure level attribution.
This method eventually proved to be unsuitable for the purposes of this study as it was primarily qualitative and could not allow for direct connection of the force values to the assigned pressure levels. Furthermore, it was discovered that when the slant of the digitizer was large (the wedge was high) the entire XY plotter had to be physically held down because the resistance from the digitizer to the stylus

was higher than the force from the weight of the entire plotter arm. Still some useful results were collected and presented (Kalantzis, 2020).

One of the initial tests was about repeatability and reproducibility of X, Y, F and T data of the Wacom STU530 digitizer; a total of 6 different Wacom STU530 digitizers and their corresponding default styli were used for this experiment. Additionally, to investigate the possible difference in force to pressure level correlation from different equipment, 4 Wacom Bamboo inking pens were also used for the collection. The XY plotter was programmed to execute a set of spirals for each of the combinations: for the flat condition it produced two spirals side by side, for the wedged condition it was programmed to execute only one spiral. Two conditions were selected (the digitizer lying flat – Figure 1.4 -and the digitizer with a wedge – Figure 1.5), and 10 samples were collected from each condition. This led to a total of 1200 samples collected (6 Wacom STU530 digitizers x (6 Default Styli + 4 Wacom Bamboo Inking Pens)) = 60 combinations x 2 Different Conditions x 10 samples per condition = 1200 samples).

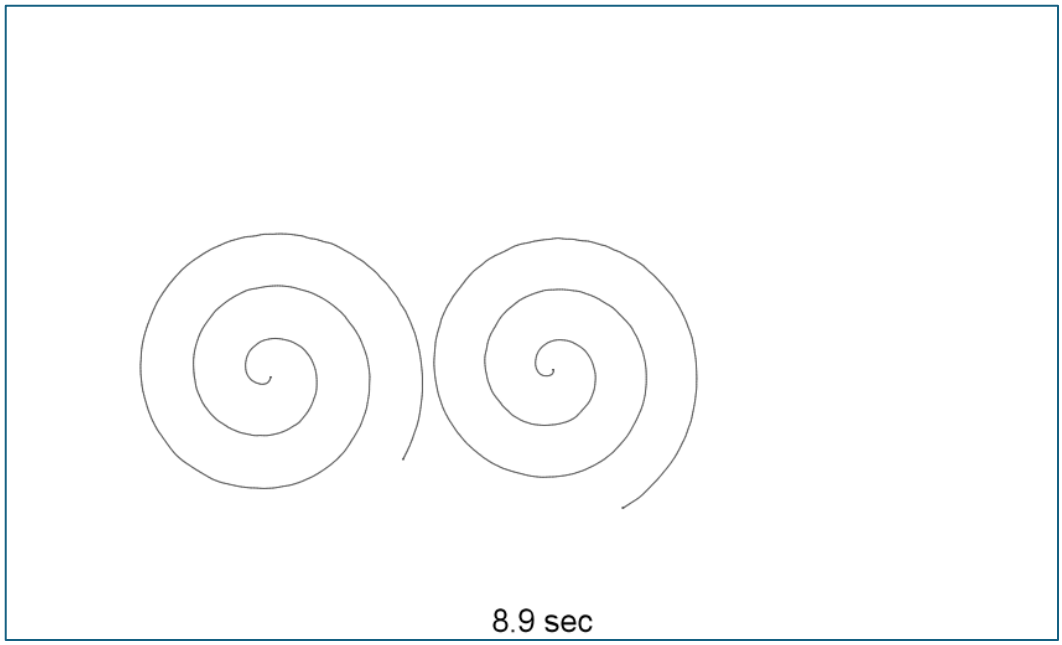

Figure 1.4 Example of execution of spirals. XY representation including time of execution.

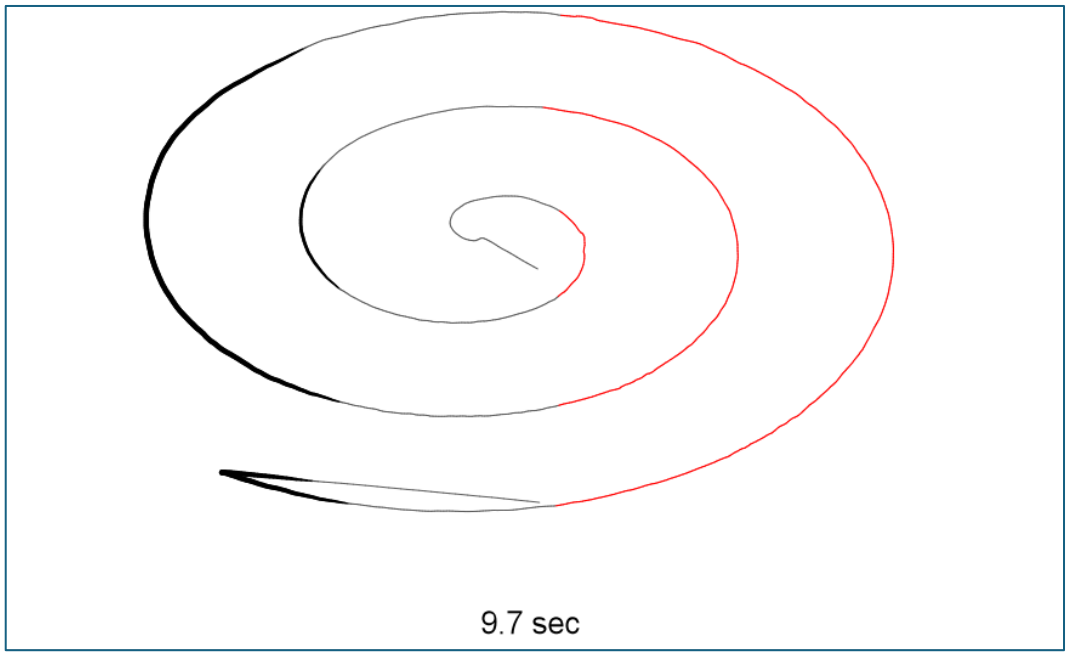

Figure 1.5 Example of execution of spiral with wedge positioned under the digitizer. XY representation including time of execution – IATs graphed in red colour.

For this experiment the Namirial Firma Certa Forensic analysis software was selected for the capturing and the subsequent analysis of the data.
From the selected devices only one was completely new – the rest of the devices were in use for several months and had different times of acquisition. Specifically, the devices were used for training in workshops, for research and for collecting samples from actual casework so it was impossible to accurately describe the age and wear of each device. Nonetheless, the oldest device digitizer and stylus was known.

During the first phase of the experiment (condition 1) it was observed that generally there was uniformity of the X, Y and T data. It was observed that the accuracy and reproducibility of the motion by the Axidraw XY plotter was less accurate that the capturing capabilities of the deployed digitizers, leading to slight differences (especially in the time of execution of up to 0.1 seconds) and hence the use of the Axidraw as the source of a motion for calibration purposes was abandoned on later stages of the experimental construction.
During the second phase of the experiment (condition 2) severe differences were observed amongst some of the solutions.
When collecting data with the same stylus and different digitizer no serious difference in the assigned pressure levels was observed (Figure 1.6).

Same Stylus – Different Digitizer / Condition 2

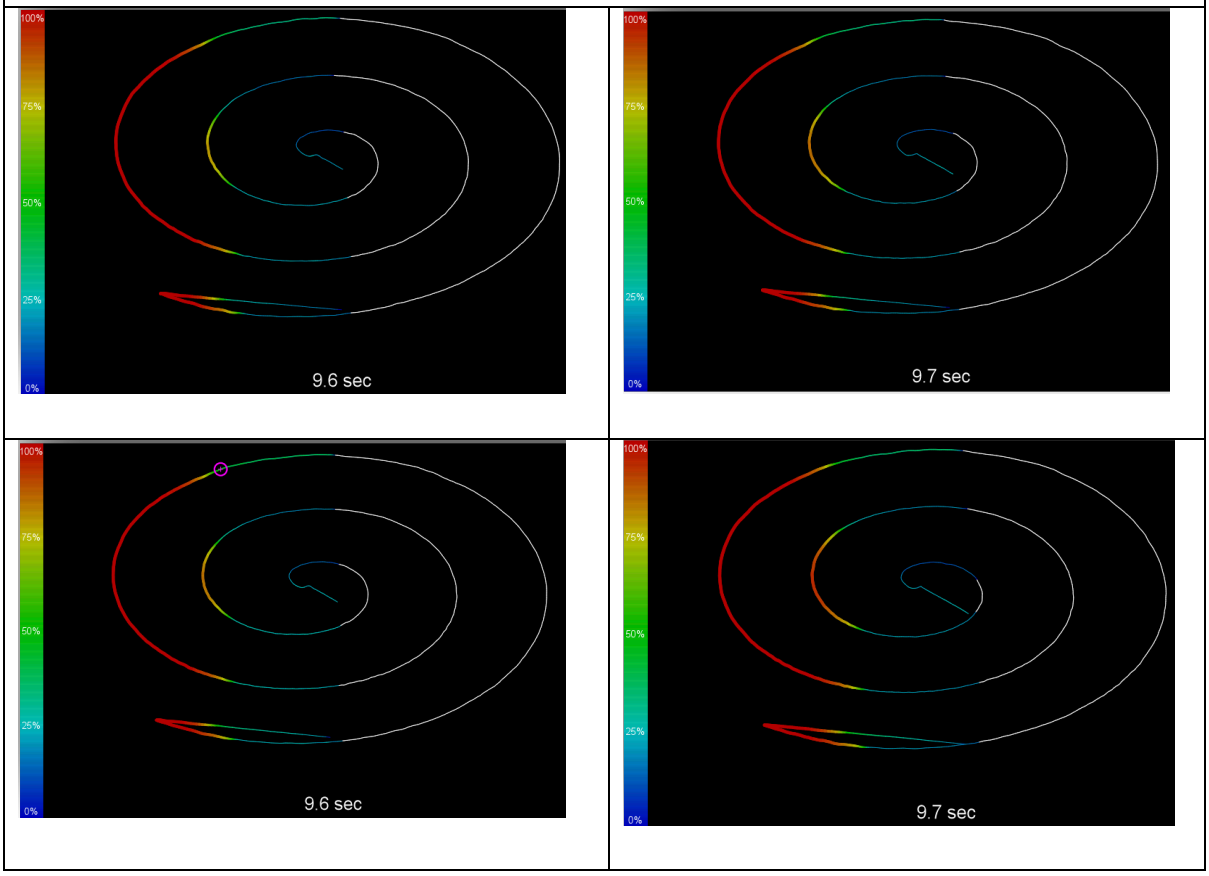

Figure 1.6 Example of execution of spiral with wedge positioned under the digitizer – same stylus different digitizer. XY representation including time of execution, Force values correlated to colour (see colour gradient on the left), IATs graphed in white colour.

When the digitizer was kept the same and the stylus changed, serious differences were noticed (Figure 1.7).

Same Digitizer – Different Stylus/ Condition 2

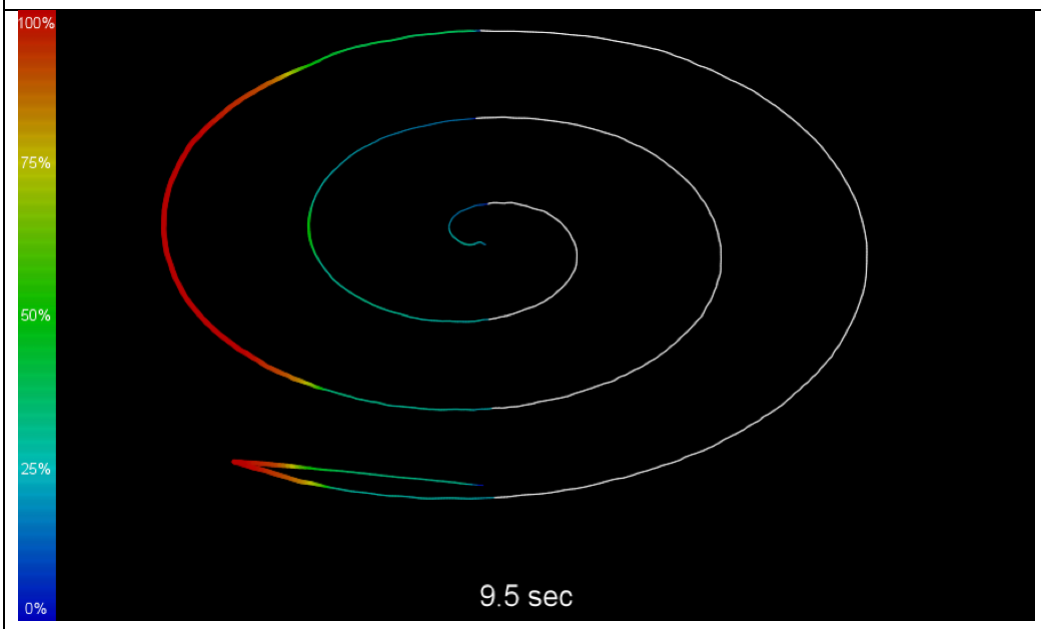

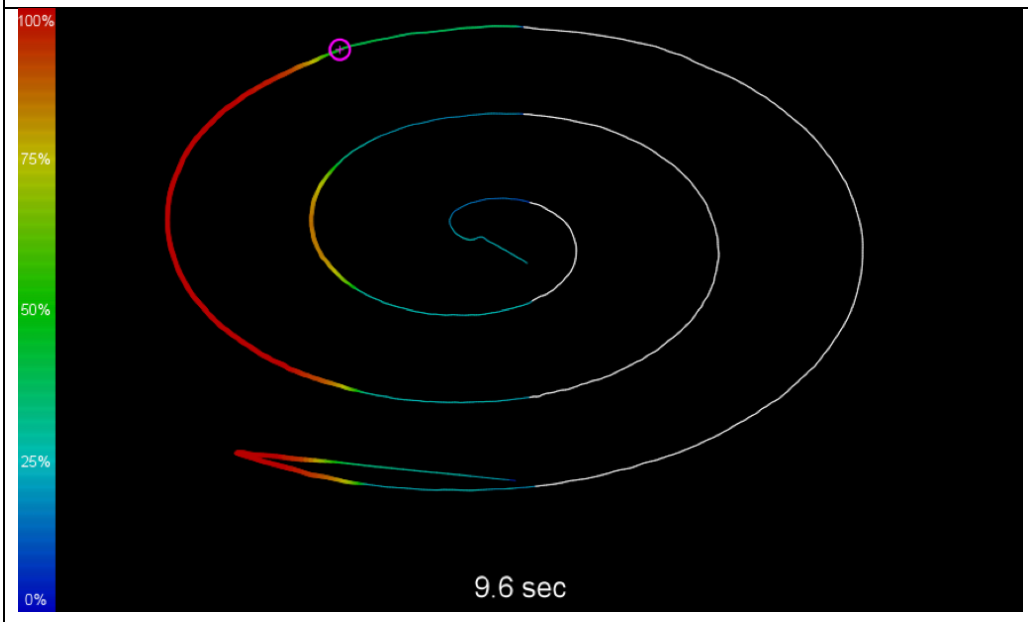

Figure 1.7 Example of execution of spiral with wedge positioned under the digitizer – same digitizer different stylus. XY representation including time of execution, Force values correlated to colour (see colour gradient on the left), IATs graphed in white colour.

The noticeable difference was observed only amongst the different types of styli (i.e. the default stylus of the Wacom STU530 vs the Wacom Bamboo Spark Inking Pen - Figure 1.7) but also amongst the same type of styli of different age – this was later confirmed during the finalization of the experimental mechanism.

This series of measurements highlighted the areas of interest of our research as it revealed that the properties of force / pressure level attribution lie with the stylus used rather than the digitizer (for the EMR solutions tested) and that age and use affect the sensitivity of the pressure sensor which is to be found inside the stylus. This conclusion was reached as it was the only condition that was different when collecting the different spiral data.
This experiment also highlighted the need for a more precise mechanism that would allow direct measurement of exercised force.

The next attempt to create the appropriate experimental setup involved the use of the z-axis mechanism of a stereomicroscope. It was considered that the mechanism would allow for absolute control of the z axis position and therefore allow for accurate measurements. For this purpose, a slate of the diameter of a stereoscope head was 3D printed with a holding mechanism in the middle to allow for positioning of a stylus.

A microscope boom stand was selected as the boom stand would allow easy positioning of the digitizer and a set of laboratory scales underneath for the measurements, without hindering the path along the Z axis (Figure 1.8).

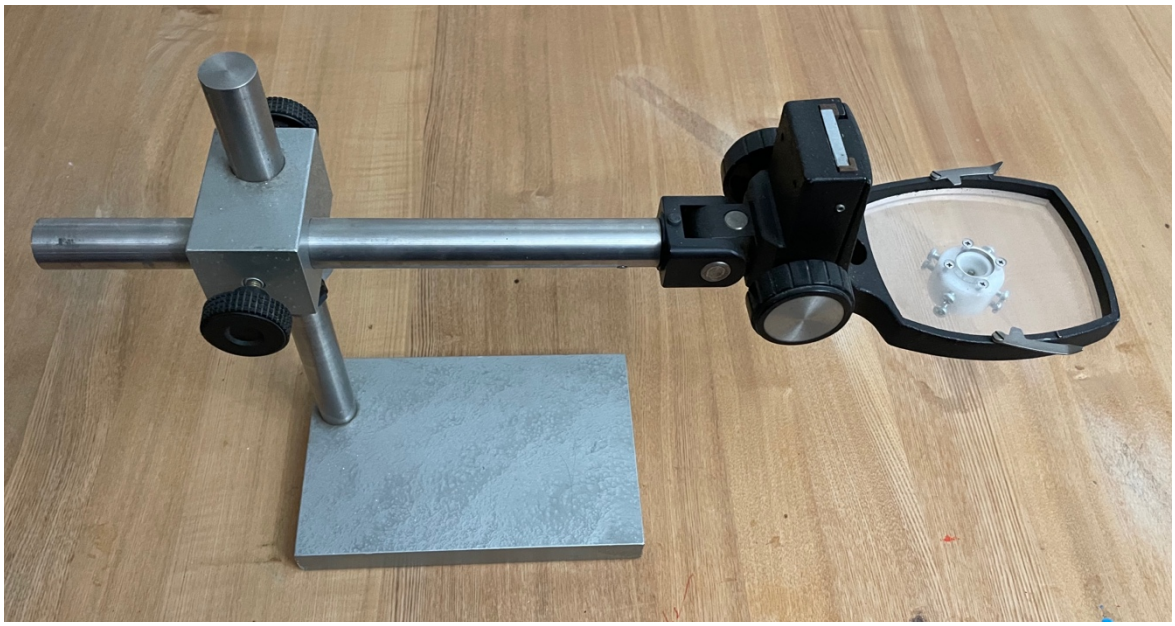

Figure 1.8 Experimental array – first attempt.

When collecting the first set of values it was noticed that the tolerance of the setup was not the desired one. When positioned and allowed for the stylus to rest on the digitizer over the scales, it was noticed that the measurement of the scales was

changing with time, hinting that parts of the array were moving and hence the applied force was changing values. Therefore, this setup was also abandoned.

1.10. Chapter 1 References

ASTM International (2009) *ASTM Standard E2195-09: Standard terminology relating to the examination of questioned documents*. West Conshohocken, PA: ASTM.

Betancourt, D. and del Rio, C. (2006) 'Study of the human eye working principle: An impressive high angular resolution system with simple array detectors', in *Proceedings of the Fourth IEEE Workshop on Sensor Array and Multichannel Processing*. Waltham, MA: IEEE, p. 93. doi:10.1109/SAM.2006.1706098.

Brewster, F. (1932) *Contested documents and forgeries*. Calcutta: The Book Company Ltd.

Caligiuri, M.P. and Mohammed, L.A. (2012) *The neuroscience of handwriting: Applications for forensic document examination*. Boca Raton, FL: CRC Press.

Čakovská, B.G. et al. (2020) 'Recommendations for capturing signatures digitally to optimize their suitability for forensic handwriting examination', *Journal of Forensic Sciences*, 00, pp. 1–5. doi:10.1111/1556-4029.14627.

Ellen, D.A. (2005) *The scientific examination of documents: Methods and techniques*. 2nd edn. Boca Raton, FL: CRC Press.

European Network of Forensic Science Institutes (ENFSI) (2020) *Best Practice Manual for the Forensic Examination of Handwriting*. Version 03. Wiesbaden: ENFHEX.

European Network of Forensic Science Institutes (ENFSI) (2022) *Best Practice Manual for the Forensic Handwriting Examination*. 4th edn. ENFSI-BPM-FHX-01.

Franke, K. (2005) *The influence of physical and biomechanical processes on the ink trace: Methodological foundations for the forensic analysis of signatures*. Doctoral dissertation. University of Groningen.

Greece (2022) *Law 4961/2022 on Emerging Information and Communication Technologies and Other Provisions*. OG A 146/2022.

Heckeroth, J. et al. (2020) 'Features of digitally captured signatures vs. pen and paper signatures: Similar or completely different?', *Forensic Science International*. doi:10.1016/j.forsciint.2020.11058.

Heckeroth, J., Kerkhoff, A. and Weyermann, C. (2019) 'German BKA's project "ESign" - How valid are pressure values', paper presented at the 12th ENFHEX Conference, Porto, Portugal.

Huber, R. and Headrick, A. (1999) *Handwriting identification: Facts and fundamentals*. 1st edn. Boca Raton, FL: CRC Press.

International Organization for Standardization (2007) *ISO/IEC 19794-7:2007 Information technology – Biometric data interchange formats – Part 7: Signature/sign time series data*. Geneva: ISO.

International Organization for Standardization (2017) *ISO/IEC 19794-7:2017 Information technology – Biometric data interchange formats – Part 7: Signature/sign time series data*. Geneva: ISO.

ISO/IEC (2021) *ISO/IEC 19794-7:2021 Information technology — Biometric data interchange formats — Part 7: Signature/sign time series data*. Geneva: International Organization for Standardization.

Kalantzis, N. (2020) 'The question of comparability of digitally captured signatures from the aspect of normalization & stability of used hardware/software solutions', paper presented at the 78th Annual General Meeting of the American Society of Questioned Document Examiners (ASQDE), Denver, CO, 10–14 August.

Kalantzis, N. (2023) *The necessity for calibration and normalization of DCS solutions: Unexpected findings*. FDE-Linked, 31 March.

Li, C.K., Wong, S.K. and Chim, L.J. (2018) 'A prototype of mathematical treatment of pen pressure data for signature verification', *Journal of Forensic Sciences*, 63(1), pp. 275–284. doi:10.1111/1556-4029.13491.

Mohammed, L., Found, B., Caligiuri, M. and Rogers, D. (2011) 'The dynamic character of disguise behavior for text-based, mixed, and stylized signatures', *Journal of Forensic Sciences*, 56(S1), pp. S136–S141.

Mohammed, L., Found, B., Caligiuri, M. and Rogers, D. (2015) 'Dynamic characteristics of signatures: Effects of writer style on genuine and simulated signatures', *Journal of Forensic Sciences*, 60(1), pp. 61–67.

Pertsinakis, M. and Fernandes, C.P. (2018) 'In-air trajectories: Forensic and graphonomical applications of an emerging handwriting characteristic', *Mannheimer Hefte für Schriftvergleichung*, 41(3–4), p. 141.

Regulation (EU) No 910/2014 of the European Parliament and of the Council (2014) on electronic identification and trust services for electronic transactions in the internal market and repealing Directive 1999/93/EC, *Official Journal of the European Union*, L 257/73.

SWGDOC (2013) *Standard terminology relating to the examination of questioned documents*. Version 2013-01.

Zimmer, J. et al. (2021) 'The challenge of comparing digitally captured signatures registered with different software and hardware', *Forensic Science International*, 327, p. 110945. doi:10.1016/j.forsciint.2021.110945.

2. Experimental[9]

2.1. The experimental array

To approach the issue of force recording in the case of DCS, an accurate mechanism of reproducible and measurable force load had to be constructed. This has been accomplished in the past (Franke, 2005; Heckeroth, Kerkhoff and Weyermann, 2019), but a simpler approach to apply measurable force was chosen. An XY-Plotter (the Axidraw V.3 from Evil Mad Scientist Laboratories) was used as a stable holding mechanism for the stylus. The height of the XY-plotter, the height of the stylus fixture and the relative height of the scales (PCE-BS 3000 from PCE Instruments which is calibrated) to the XY-plotter allow for different percentage of the actual weight of the XY-plotter to be applied by the stylus tip. The Furthermore, the selected XY-plotter allows the positioning of additional weight in the stylus holding part hence providing the capability to change the force load applied by the stylus tip (see figures 2.1 and 2.2).

[9] Parts of the contents of this chapter have been published in Kalantzis N, Platt AWG. Digitally captured signatures: A method for the normalization of force through calibration and the use of the zeta function. J Forensic Sci. 2021;00:1–18. https://doi. org/10.1111/1556-4029.14927

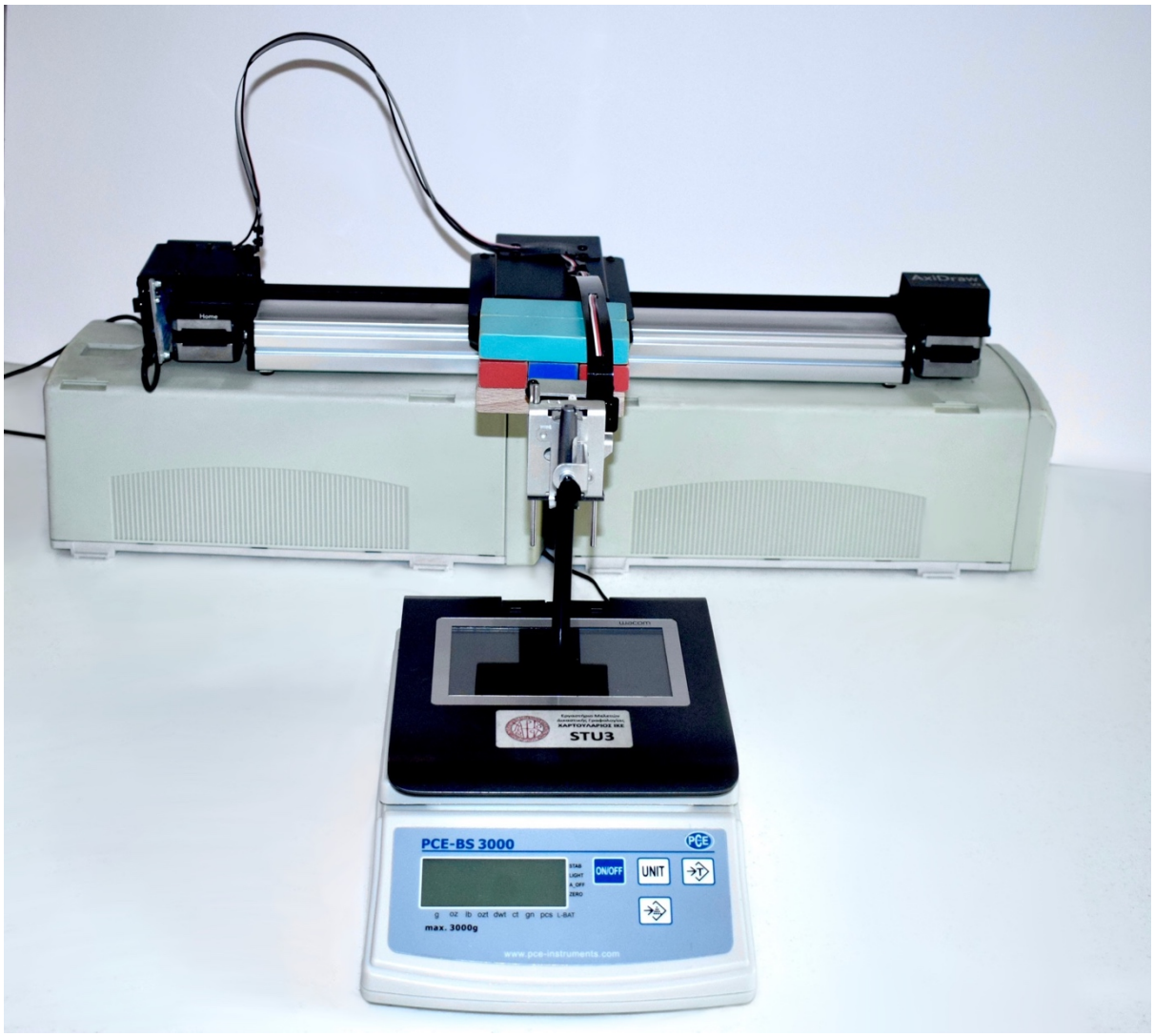

Figure 2.1 Experimental array – front.

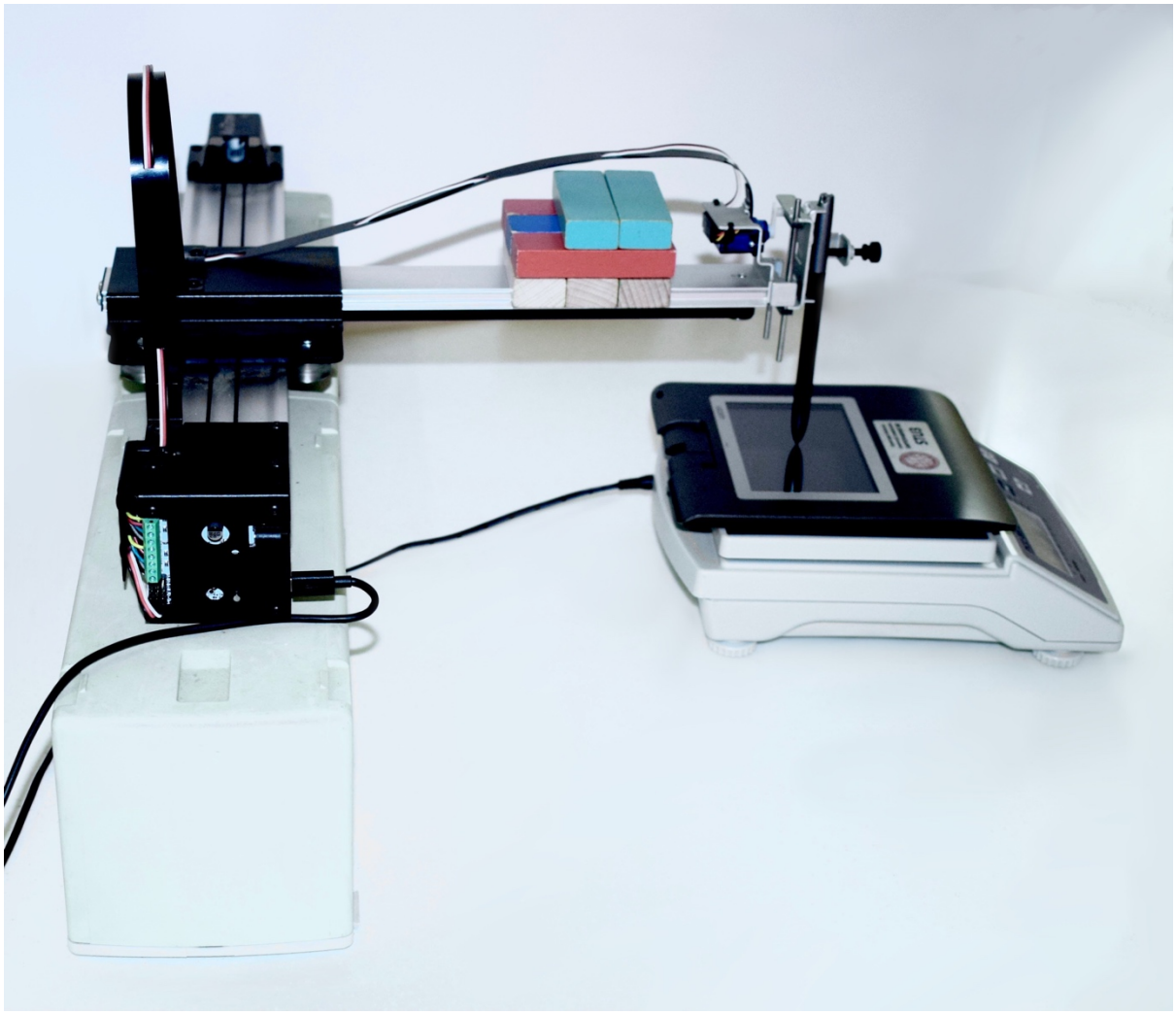

Figure 2.2 Experimental array – side.

For each set of measurements, the stylus was placed in the pen mount perpendicular to the digitizer, at the centre of the active area, and a measurement was recorded, noting the weight measurement. The collection per set was executed consecutively, adding weight from 0 to the maximum force threshold and back, adding or removing additional weight without changing the position of the plotter. The time interval between measurements was as long as it was required to collect the measurements (i.e. a few seconds). Initial tests were

conducted to determine the minimum and maximum force thresholds per combination, by gradually applying weight until the Force channel exhibited non-zero values, and then until the first instance that the Force channel exhibited the maximum value (i.e. 1023). The recorded values were subsequently transformed from weight (measured in grams) to force (measured in Newtons) through the formula F= m * g, where F is the force applied (in N), m is the mass (in Kg) and g is the acceleration of gravity on sea level (9.81 m/sec^2).

Preliminary testing and measurements proved that the selected mechanism provided stability, repeatability and reproducibility of the measurements as per the exercised (and subsequently measured) force.

2.2. Conducted experiments

Two different Electromagnetic Resonance (EMR) technology digitizers were selected, coupled with not only their default styli but also with a third-party compatible stylus and a compatible inking pen. Two different software solutions as well as the digitizer manufacturer's SDK (Software Developer's Kit) were used for the capturing and acquisition of the data of the aforementioned combinations. Furthermore, an Apple iPad Pro (1st Gen) coupled with an Apple Pencil (1st Gen) which uses conductive technology (Harley *et al*., 2014) was used in combination

with a dedicated DCS capturing application (Hecker, 2020). The different collection combinations are exhibited on Table 2.1.

Combination Number	Digitizer	Stylus	Software Used for Capturing
1	Wacom STU 540	Default (540)	Wacom SDK
2	Wacom STU 540	Default (540)	Wacom Signature Scope
3	Wacom STU 540	Default (540)	Namirial Firma Certa Forensic
4	Wacom STU 540	Wacom Bamboo Spark Inking Pen	Wacom SDK
5	Wacom STU 530	Default (530)	Wacom SDK
6	Wacom STU 530	Wacom Bamboo Spark Inking Pen	Wacom SDK
7	Wacom STU 540	LAMY AL-star black EMR (Glossy Surface)	Wacom SDK
8	Wacom STU 540	LAMY AL-star black EMR (Paper Surface)	Wacom SDK
9	Apple iPad Pro 9.7" (1st Gen)	Apple Pencil (1st Gen)	Forensic Signalyzer

Table 2.1 Combination of capturing conditions.

The three software programs (Wacom Co., Ltd., 2020a; Wacom Co., Ltd., 2020b; Namiral S.p.a., 2020) with the same hardware solution (combinations 1, 2 and 3) allowed the evaluation of how force is captured from the software aspect with the same default stylus and digitizer. The choice of different hardware from the same

manufacturer (combinations 1 and 5 for different digitizers with their default styli, combinations 1, 4, 7 and 8 for the STU 540 and 5 and 6 for STU 530 with different styli, but with the same digitizer and software, 4 and 6 with the same stylus over different digitizer) captured using the same software solution allowed the evaluation of how force is captured from the hardware aspect.

The selection of Wacom's Bamboo Spark inking pen was aimed at studies that compare signing behaviour on paper and on glass (DCS) by using the available EMR technology (Heckeroth *et al*., 2021). The inking pen is an EMR active stylus that also includes an inking cartridge thus allowing the pen to act as a traditional ballpoint pen (or felt tip, depending on the inking cartridge available), producing an ink trace on paper. The EMR circuit inside the inking pen allows the simultaneous capturing of the aforementioned four channels (X, Y, F and T) by the digitizer when the inking pen is moving over it and is within range. This technological advantage is used to study "Hybrid Signatures" which are created when executing a signature formation with an inking pen on a sheet of paper on top of the digitizer. Hybrid signatures are valuable for research purposes as they provide both a physical (paper) and a digital (DCS) representation of the same signature movement. This formation has been used before (Heckeroth *et al*., 2021) with the Wacom STU 530 digitizer and the Wacom Bamboo Inking pen, using a sticky note attached on the glass surface of the digitizer, and for that reason the authors chose to include a sticky note attached on the surface of the digitizer

during the measurement collection phase. The selection of the LAMY AL-star black EMR (which comes in two different versions which are equipped with different tips, a plastic one for the paper like surface variant and a rubber one for the glossy like surface variant– combinations 7 and 8) was aimed to the investigation of the forensic properties of a third party EMR pen, when used in combination with digitizers popular in the banking and government sector applications.

2.3. Chapter 2 References

Franke, K. (2005) *The influence of physical and biomechanical processes on the ink trace: Methodological foundations for the forensic analysis of signatures*. Doctoral dissertation. University of Groningen, Netherlands.

Hecker, T. (2020) *Forensic Signalyzer (Version 1.1)* [Mobile application software]. Available at: https://apps.apple.com/us/app/forensic-signalyzer/id1478881105

Heckeroth, J., Kerkhoff, A. and Weyermann, C. (2019) 'German BKA's project "ESign" - How valid are pressure values', paper presented at the 12th ENFHEX Conference, Porto, Portugal.

Heckeroth, J. *et al.* (2021) 'Features of digitally captured signatures vs. pen and paper signatures: Similar or completely different?', *Forensic Science International*, 318, p. 110587. doi:10.1016/j.forsciint.2020.110587.

Harley, J.A., Tan, L.-Q., Mukherjee, D. *et al.* (2014) *United States Patent No. US 8,638,320 B2*.

Namiral S.p.a. (2020) *Firma Certa Forensic (Version 1.2.9.0)* [Computer software].

Wacom Co., Ltd. (2020a) *STU SDK (Version 2.15.4)* [Computer software].

Wacom Co., Ltd. (2020b) *Wacom Signature Scope (Version 1.42.0)* [Computer software].

3. Results[10]

The experiment required the collection of a set of measurements or different forces applied to each of the chosen digitizers within the minimum and maximum threshold for applied force. The datasets were then graphed and fitted using RStudio (RStudio, Inc., 2020) and the resulting regressions were compared and discussed.

In preliminary testing, polynomials of different powers (3rd, 4th, 5th and 6th) as well as a logarithmic fit were applied and compared. From the different models the 6th degree polynomial fit provided the best fit not only for the main body of the data set but also for the extremities (i.e. pressure levels close to 0 or 1023) which are very important areas in the normalization process, hence the 6th degree polynomial fit was chosen for all calibrations.

For the EMR technology combinations (see Table 2.1), a hysteresis effect was observed as expected as it occurs in ferromagnetic and ferroelectric materials (Jackson, 1999). Hysteresis expresses the dependence of the state of a system on its history – and for the recorded force measurements on EMR digitizers this means

[10] Parts of the contents of this chapter have been published in Kalantzis N, Platt AWG. Digitally captured signatures: A method for the normalization of force through calibration and the use of the zeta function. J Forensic Sci. 2021;00:1–18. https://doi. org/10.1111/1556-4029.14927

that the assigned pressure level per exercised force is dependent on the previous value and specifically if the value is ascending or descending. This can clearly be observed in the calibration curve on figure 3.1. The recognition of the hysteresis effect in Wacom EMR digitizers should not be considered something new, as it is mentioned by Wacom in the relevant patent filings (Fukushima and Fujitsuka, 2013).

In order to calculate both phases of the hysteresis effect, two sets of measurements were collected between the minimum and maximum values, one set was collected with ascending weight load only and then one set was collected with descending weight load only.

For the seven EMR combinations the collected datasets were used to calculate the corresponding ascending load and descending load ZF and ZF^{-1}, whilst for the iPad Pro only one ZF and ZF^{-1} was calculated, presented in paragraph 3.9. The ZF^{-1} is calculated to allow computation of exercised force from assigned pressure level and is required for the normalization process as will be presented and discussed in the following chapter.

3.1. Wacom STU 540 with default stylus and Wacom SDK

The Wacom STU 540 with default stylus, using Wacom SDK recorded 1024 pressure levels (from 0 to 1023). During preliminary testing it was found that the device registers applied force between 0.14 and 4.9 N. Measurements were collected ascending from minimum to maximum and then descending from maximum to minimum and the results are shown in the following figure. As can be observed from figure 3.1, both datasets show a pseudo-logarithmic response.

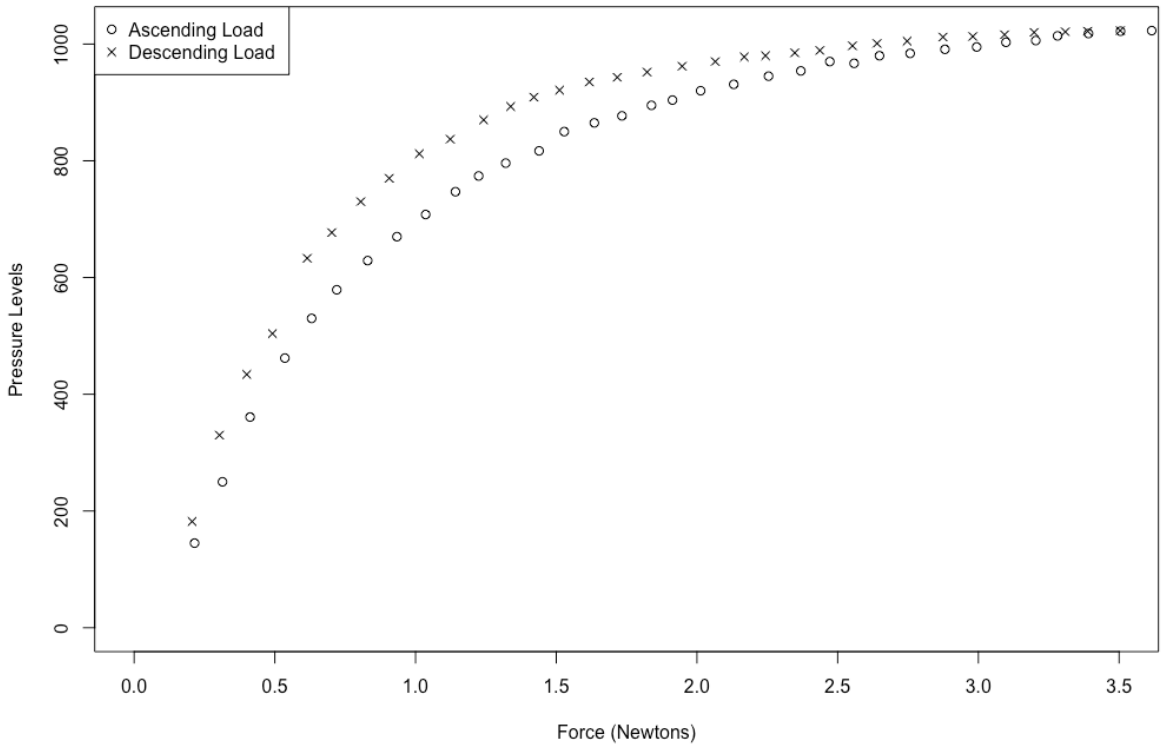

Figure 3.1 Calibration Curve

The datasets were fitted and the polynomial functions with the best fit were calculated:

Zeta Function for ascending load: $Z_u(x) = -131.5267 + 980.8542x - 282.4346x^2 - 17.9142x^3 + 28.158x^4 - 5.7823x^5 + 0.3858x^6$

Inverse Zeta Function for ascending load: $Z_u^{-1}(x) = 0.5604 - 8.463 * 10^{-3}x + 7.519 * 10^{-5}x^2 - 2.678 * 10^{-7}x^3 + 4.832 * 10^{-10}x^4 - 4.266 * 10^{-13}x^5 + 1.482 * 10^{-16}x^6$

Zeta Function for descending load: $Z_d(x) = -282.6441 + 2047.5107x - 1560.2461x^2 + 664.6895x^3 - 159.6381x^4 + 20.2146x^5 - 1.0508x^6$

Inverse Zeta Function for descending load: $Z_d^{-1}(x) = 5.729 - 9.391 * 10^{-2}x + 5.798 * 10^{-4}x^2 - 1.701 * 10^{-6}x^3 + 2.586 * 10^{-10}x^4 - 1.965 * 10^{-12}x^5 + 5.92 * 10^{-16}x^6$

The Zeta functions are plotted over the data points in the following figure (Figure 3.2.).

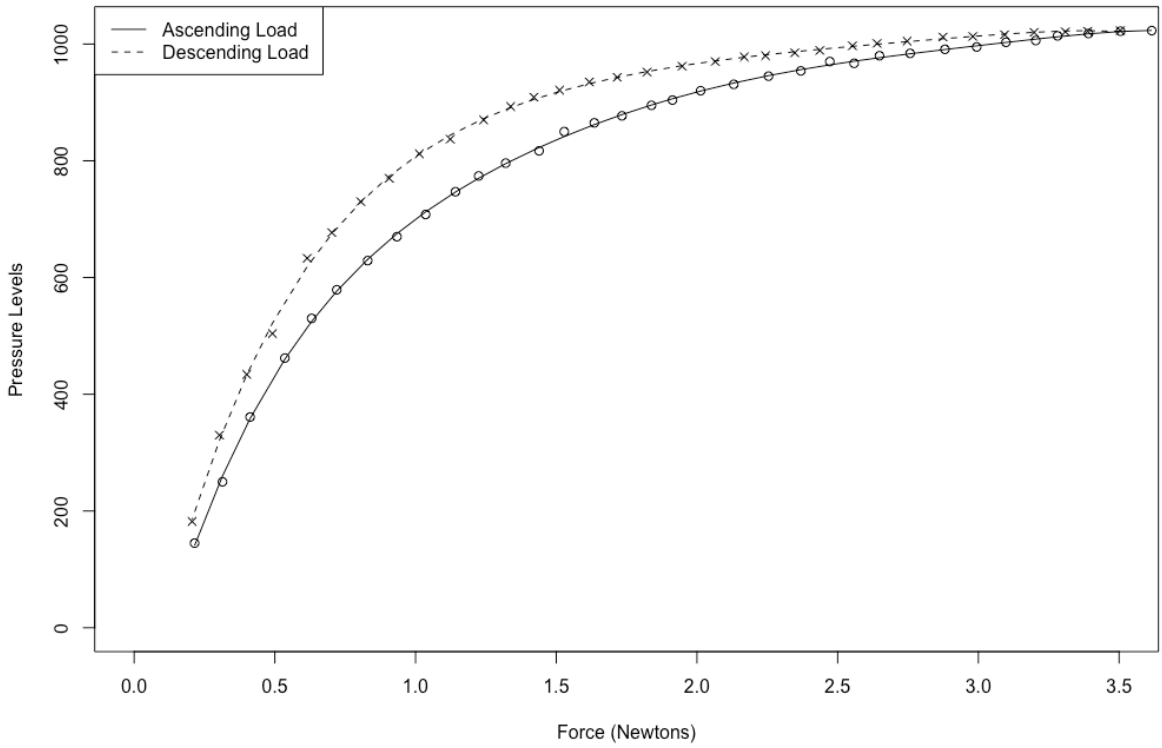

Figure 3.2 Calibration Curve with fitted function

3.2. Wacom STU 540 with default stylus and Wacom Signature Scope

The Wacom STU 540 with default stylus, using Wacom Signature Scope (WSS) recorded 1024 pressure levels (from 0 to 1023). During preliminary testing it was found that the device registers applied force between 0.14 and 3.8 N. Measurements were collected ascending from minimum to maximum and then

descending from maximum to minimum and the results are shown in the following figure. As can be observed in figure 3.3, both datasets show a pseudo-logarithmic response. The datasets were fitted and the polynomial functions with the best fit were calculated.

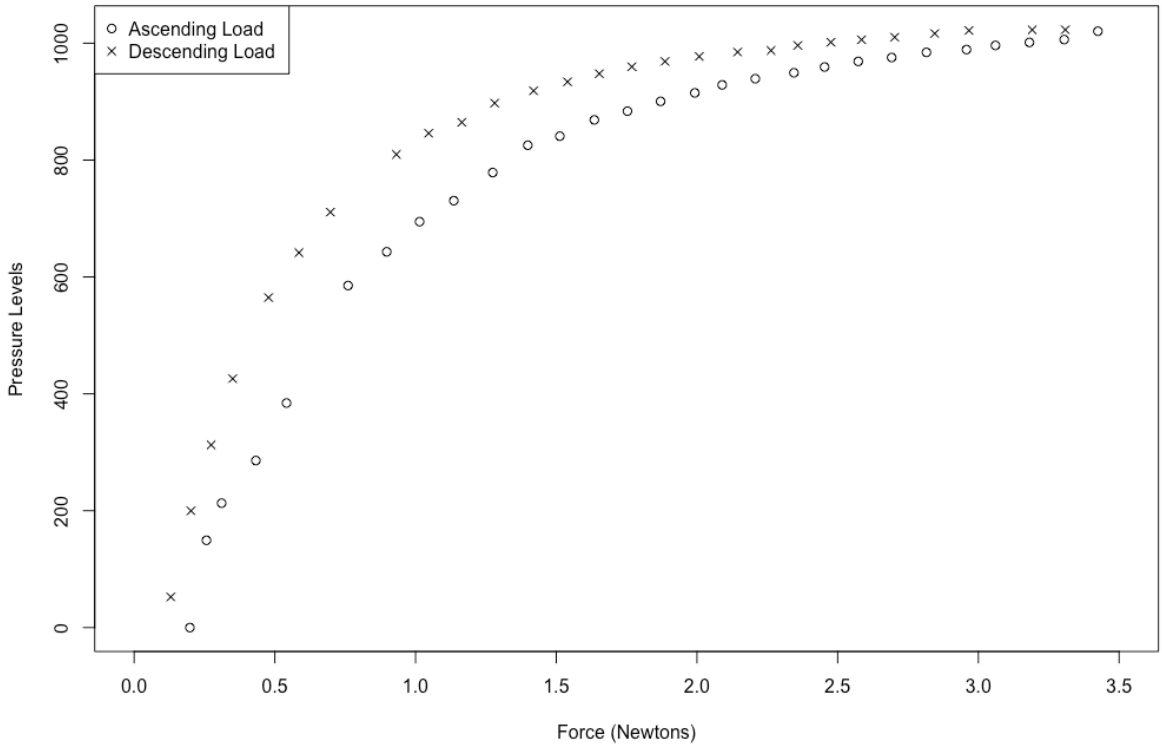

Figure 3.3 Calibration Curve

The datasets were fitted and the polynomial functions with the best fit were calculated:

Zeta Function for ascending load: $Z_u(x) = -285.902 + 1868.527x - 1364.392x^2 + 613.673x^3 - 169.38x^4 + 26.018x^5 - 1.673x^6$

Inverse Zeta Function for ascending load: $Z_u^{-1}(x) = 0.1989 - 2.47 * 10^{-3}x + 3.316 * 10^{-5}x^2 - 1.303 * 10^{-7}x^3 + 2.48 * 10^{-10}x^4 - 2.268 * 10^{-13}x^5 + 8.122 * 10^{-17}x^6$

Zeta Function for descending load: $Z_d(x) = -278.947 + 2968.945x - 3483.69x^2 + 2377.098x^3 - 927.931x^4 + 190.757x^5 - 15.946$

Inverse Zeta Function for descending load: $Z_d^{-1}(x) = 0.7408 - 1.847 * 10^{-2}x + 1.59 * 10^{-4}x^2 - 5.757 * 10^{-5}x^3 + 1.019 * 10^{-9}x^4 - 8.675 * 10^{-13}x^5 + 2.852 * 10^{-16}x^6$

The Zeta functions are plotted over the data points in figure 3.4.

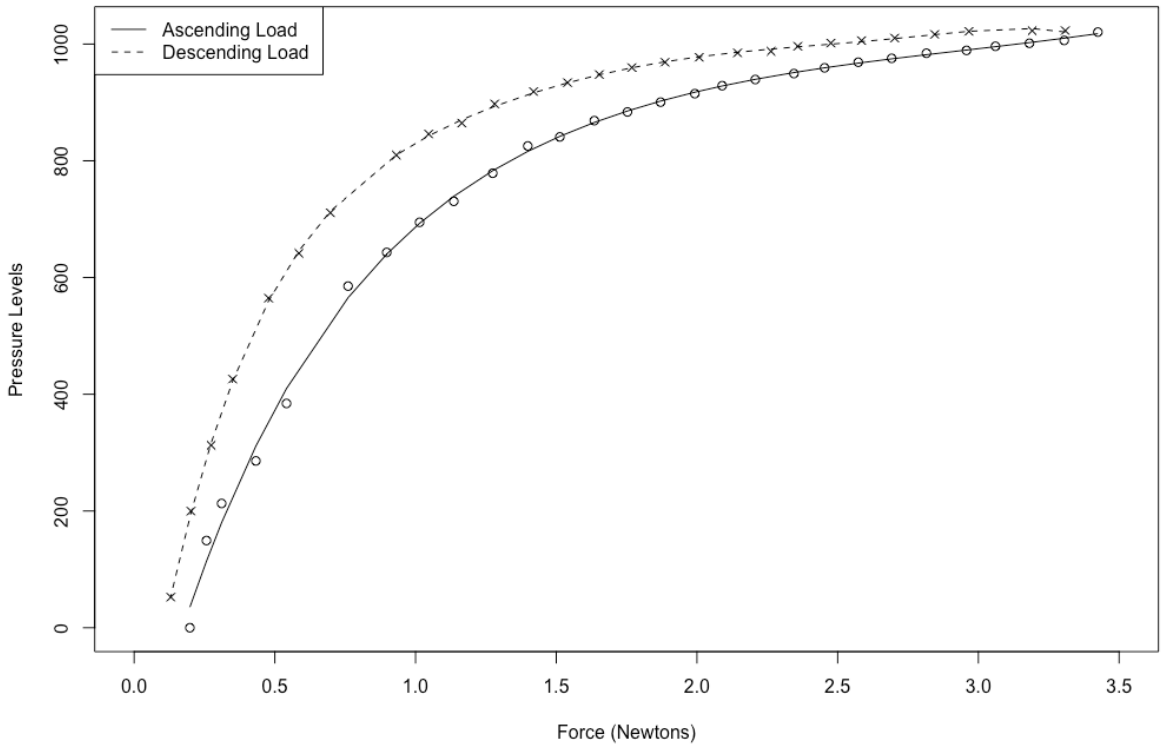

Figure 3.4 Calibration Curve with fitted function

3.3. Wacom STU 540 with default stylus and Namirial Firma Certa Forensic

The Wacom STU 540 with default stylus, using Namirial Firma Certa Forensic (FCF) recorded 1024 pressure levels (from 0 to 1023). During preliminary testing it was found that the device registers applied force between 0.14 and 3.8 N. Measurements were collected ascending from minimum to maximum and then descending from maximum to minimum and the results are shown in the following figure. As can be observed in figure 3.5, both datasets show a pseudo-logarithmic response. The datasets were fitted and the polynomial functions with the best fit were calculated.

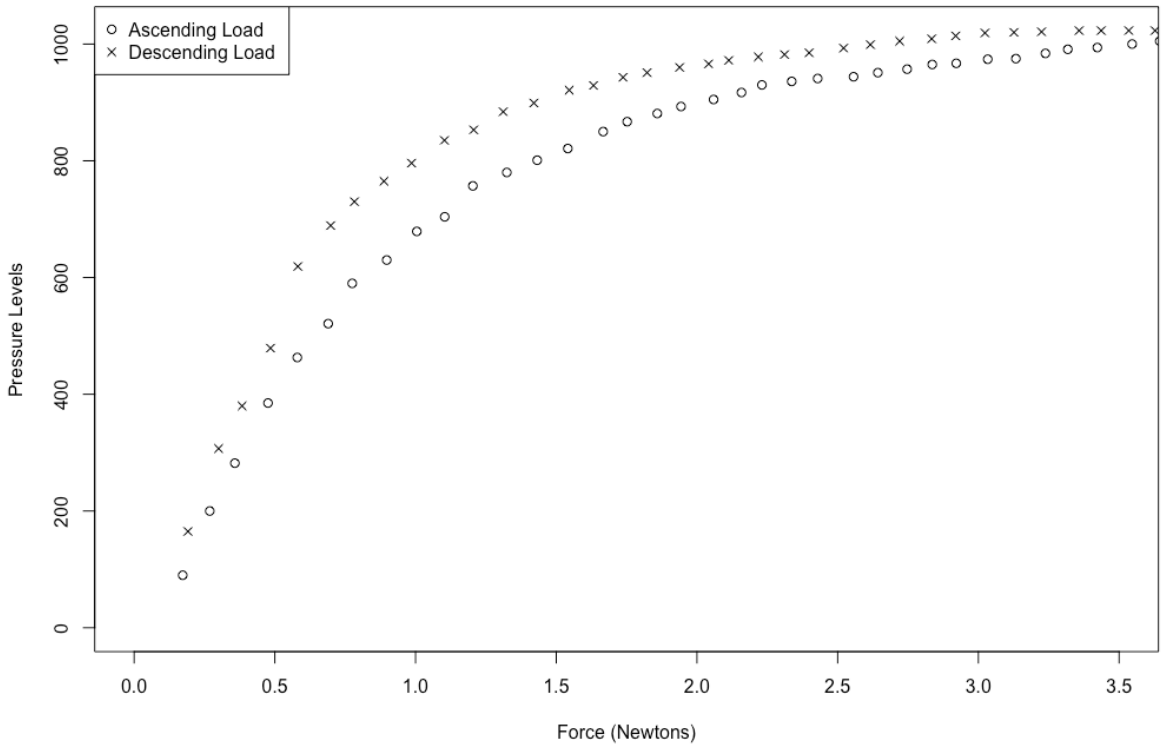

Figure 3.5 Calibration Curve

The datasets were fitted and the polynomial functions with the best fit were calculated:

Zeta Function for ascending load: $Z_u(x) = -128.4184 + 1426.6966x - 875.9802x^2 + 315.1193x^3 - 66.8796x^4 + 7.8297x^5 - 0.3933x^6$

Inverse Zeta Function for ascending load: $Z_u^{-1}(x) = 1.824 - 3.583 * 10^{-2}x + 2.629 * 10^{-4}x^2 - 8.648 * 10^{-7}x^3 + 1.437 * 10^{-9}x^4 - 1.171 * 10^{-12}x^5 + 3.738 * 10^{-16}x^6$

Zeta Function for descending load: $Z_d(x) = -200.386 + 2149.792x - 1756.524x^2 + 785.736x^3 - 194.391x^4 + 24.851x^5 - 1.28x^6$

Inverse Zeta Function for descending load: $Z_d^{-1}(x) = 26.50 - 3.889 * 10^{-1}x + 2.152 * 10^{-3}x^2 - 5.822 * 10^{-6}x^3 + 8.266 * 10^{-9}x^4 - 5.908 * 10^{-12}x^5 + 1.678 * 10^{-15}x^6$

The Zeta functions are plotted over the data points in figure 3.6.

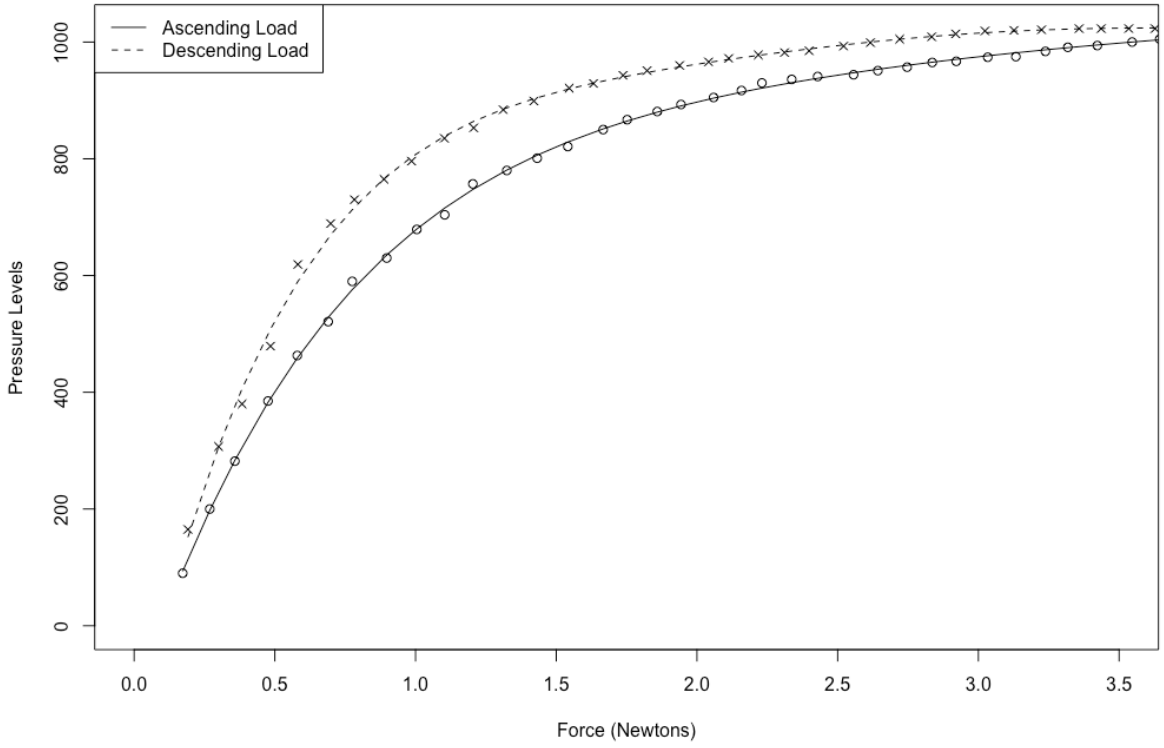

Figure 3.6 Calibration Curve with fitted function

3.4. Wacom STU 540 with Bamboo Spark Inking Pen and Wacom SDK

The Wacom STU 540 with Bamboo Spark Inking Pen, using Wacom SDK recorded 1024 pressure levels (from 0 to 1023). During preliminary testing it was found that the device registers applied force between 0.14 and 4.5 N. Measurements were collected ascending from minimum to maximum and then descending from maximum to minimum and the results are shown in the following figure. As can be observed in figure 3.7, both datasets show a pseudo-logarithmic response. The datasets were fitted and the polynomial functions with the best fit were calculated.

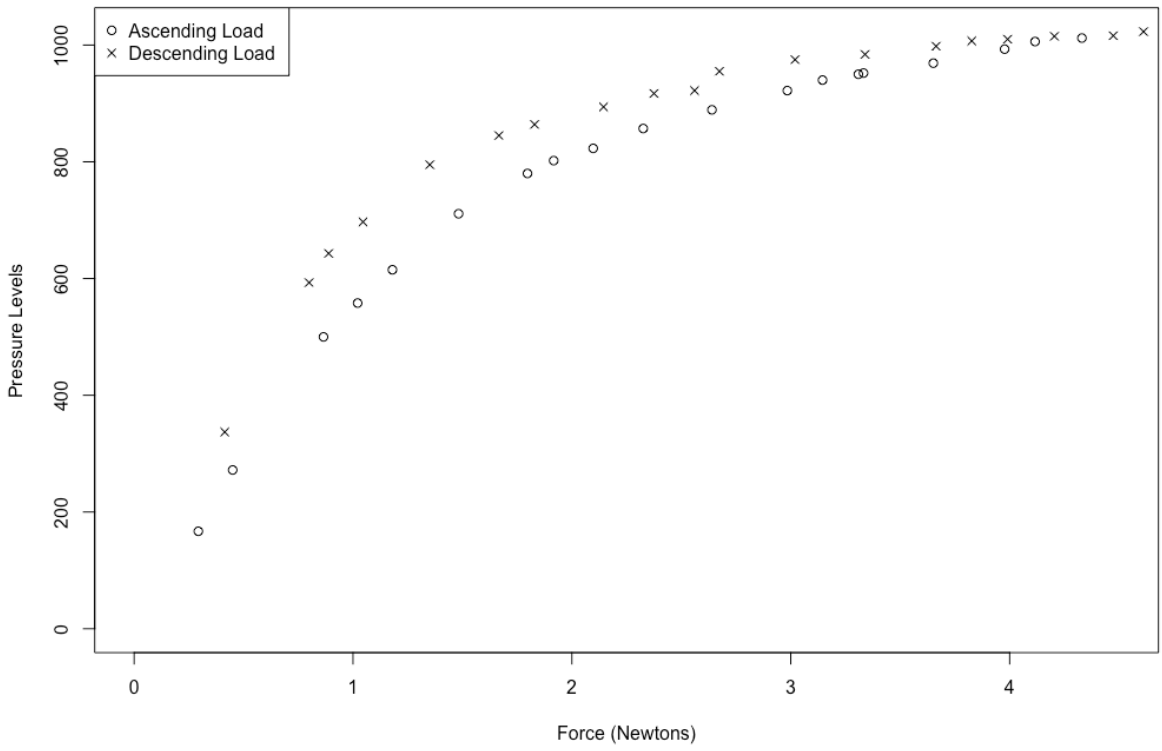

Figure 3.7 Calibration Curve

The datasets were fitted and the polynomial functions with the best fit were calculated:

Zeta Function for ascending load: $Z_u(x) = -151.6523 + 1264.8094x - 687.3093x^2 + 188.6995x^3 - 16.2854x^4 - 2.3297x^5 - 0.3846x^6$

Inverse Zeta Function for ascending load: $Z_u^{-1}(x) = 2.655 - 4.477 * 10^{-2}x + 2.841 * 10^{-4}x^2 - 8.305 * 10^{-7}x^3 + 1.252 * 10^{-9}x^4 - 9.391 * 10^{-13}x^5 + 2.79 * 10^{-16}x^6$

Zeta Function for descending load: $Z_d(x) = -152.0626 + 1660.6545x - 1249.2779x^2 + 570.4155x^3 - 153.1055x^4 + 22.07x^5 - 1.3165x^6$

Inverse Zeta Function for descending load: $Z_d^{-1}(x) = 1.314 - 2.968 * 10^{-2}x + 2.295 * 10^{-3}x^2 - 7.66 * 10^{-7}x^3 + 1.273 * 10^{-9}x^4 - 1.029 * 10^{-12}x^5 + 3.247 * 10^{-16}x^6$

The Zeta functions are plotted over the data points in figure 3.8.

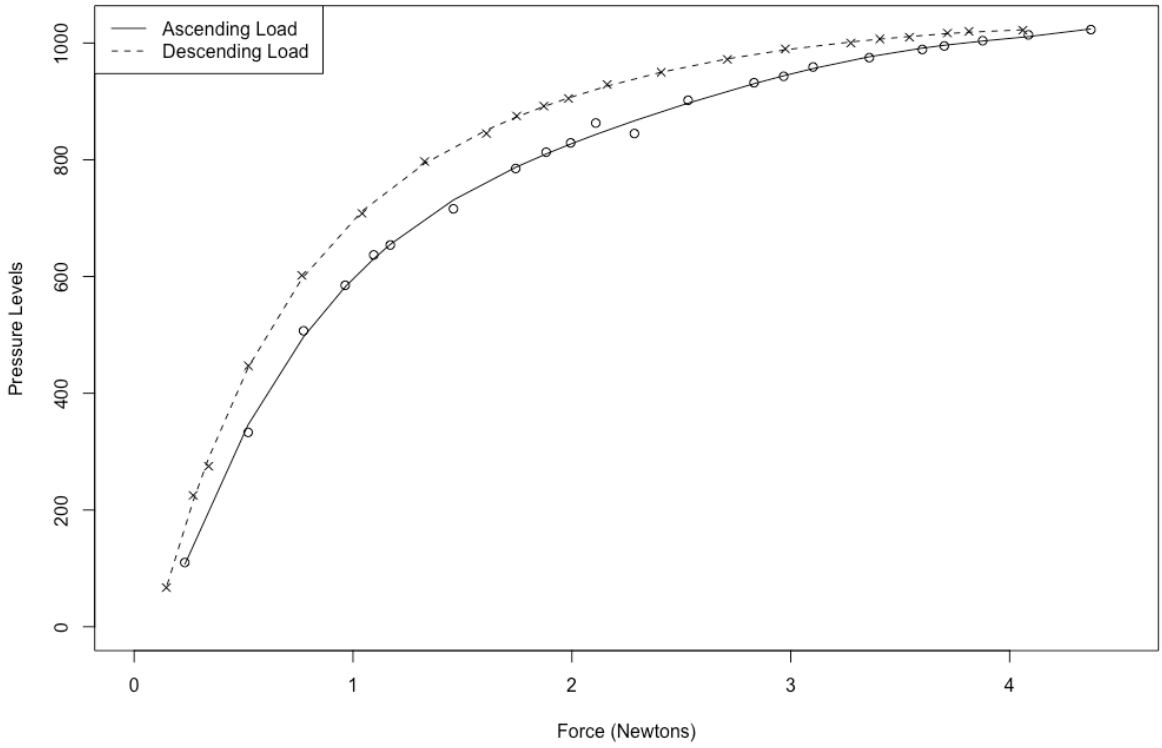

Figure 3.8 Calibration Curve with fitted function

3.5. Wacom STU 530 with default stylus and Wacom SDK

The Wacom STU 530 with default stylus, using Wacom SDK recorded 1024 pressure levels (from 0 to 1023). During preliminary testing it was found that the device registers applied force between 0.14 and 3.5 N. Measurements were collected ascending from minimum to maximum and then descending from maximum to minimum and the results are shown in figure 3.9. As can be observed in the figure, both datasets show a pseudo-logarithmic response. The datasets were fitted and the polynomial functions with the best fit were calculated.

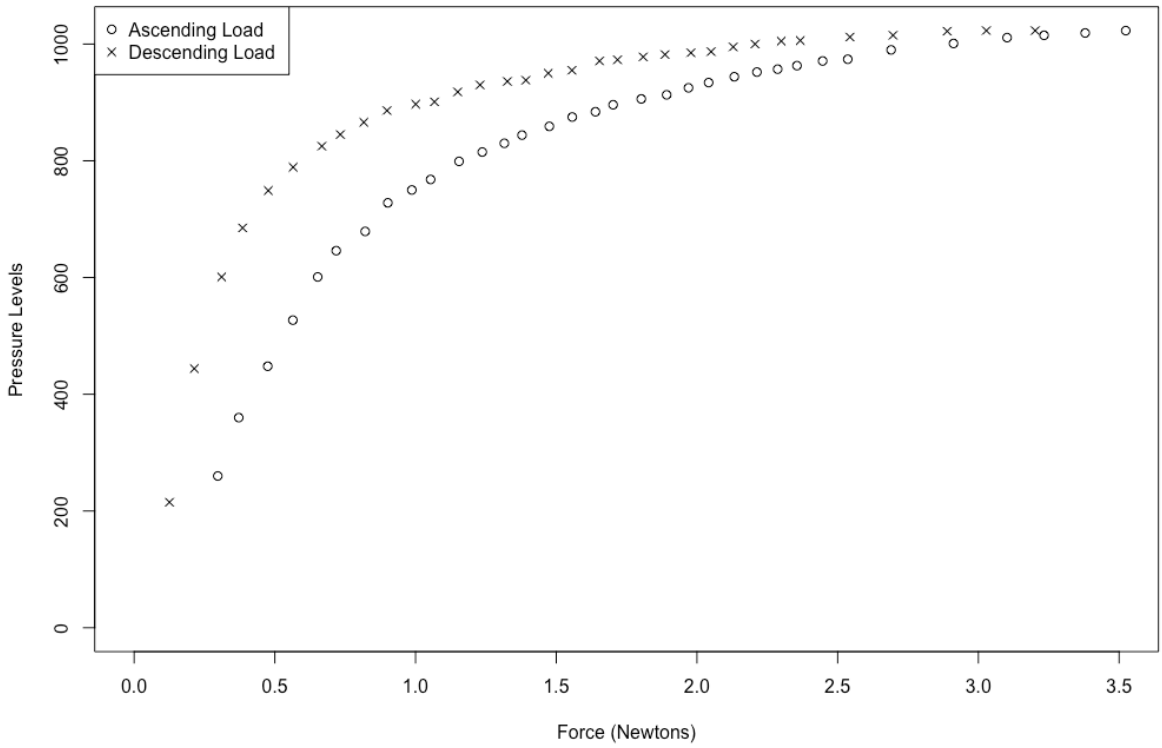

Figure 3.9 Calibration Curve

The datasets were fitted and the polynomial functions with the best fit were calculated:

Zeta Function for ascending load: $Z_u(x) = -273.122 + 2351.661x - 2182.893x^2 + 1150.935x^3 - 341.306x^4 + 53.126x^5 - 3.387x^6$

Inverse Zeta Function for ascending load: $Z_u^{-1}(x) = 14.74 - 1.713 * 10^{-1}x + 8.007 * 10^{-4}x^2 - 1.898 * 10^{-6}x^3 + 2.434 * 10^{-9}x^4 - 1.608 * 10^{-12}x^5 + 4.318 * 10^{-16}x^6$

Zeta Function for descending load: $Z_d(x) = -179.926 + 3971.228x - 6205.921x^2 + 5091.719x^3 - 2237.698x^4 + 498.409x^5 - 44.15x^6$

Inverse Zeta Function for descending load: $Z_d^{-1}(x) = 59.94 - 7.151 * 10^{-1}x + 3.279 * 10^{-3}x^2 - 7.547 * 10^{-6}x^3 + 9.327 * 10^{-9}x^4 - 5.926 * 10^{-12}x^5 + 1.524 * 10^{-15}x^6$

The Zeta functions are plotted over the data points in figure 3.10.

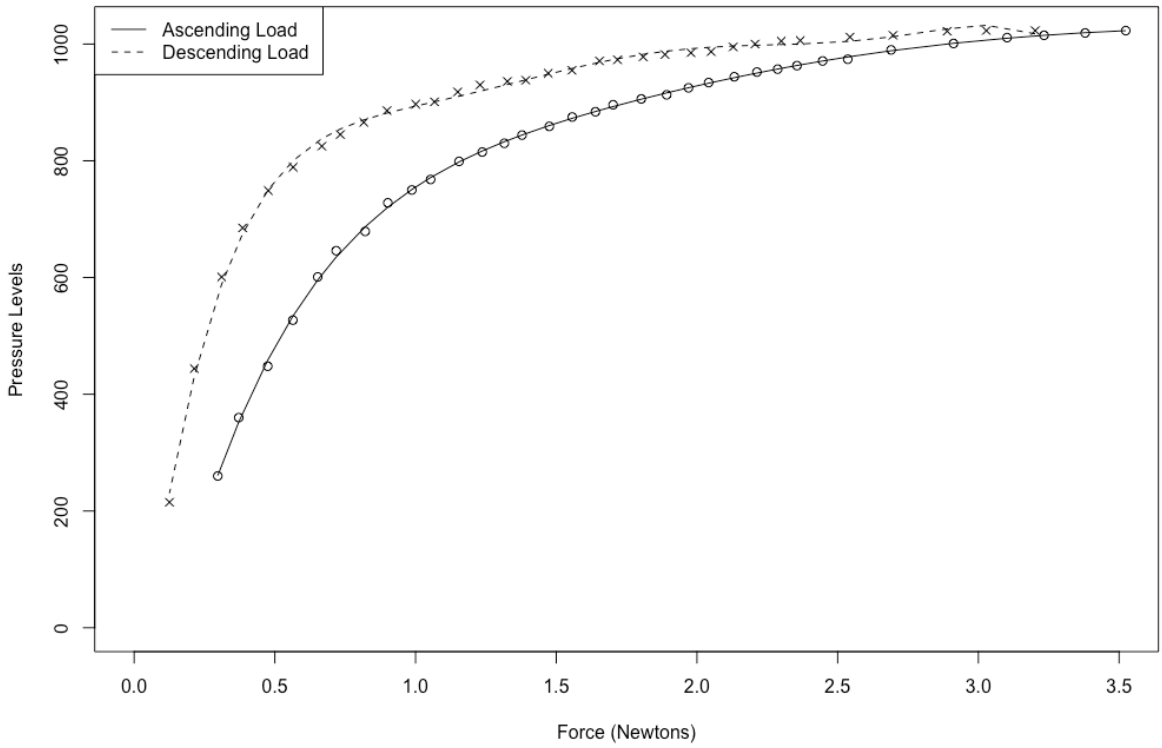

Figure 3.10 Calibration Curve with fitted function

3.6. Wacom STU 530 with Bamboo Spark inking pen and Wacom SDK

The Wacom STU 530 with Wacom Bamboo Spark inking pen, using Wacom SDK recorded 1024 pressure levels (from 0 to 1023). During preliminary testing it was found that the device registers applied force between 0.14 and 4.5 N. Measurements were collected ascending from minimum to maximum and then descending from maximum to minimum and the results are shown in figure 3.11.

As can be observed in the figure, both datasets show a pseudo-logarithmic response. The datasets were fitted and the polynomial functions with the best fit were calculated.

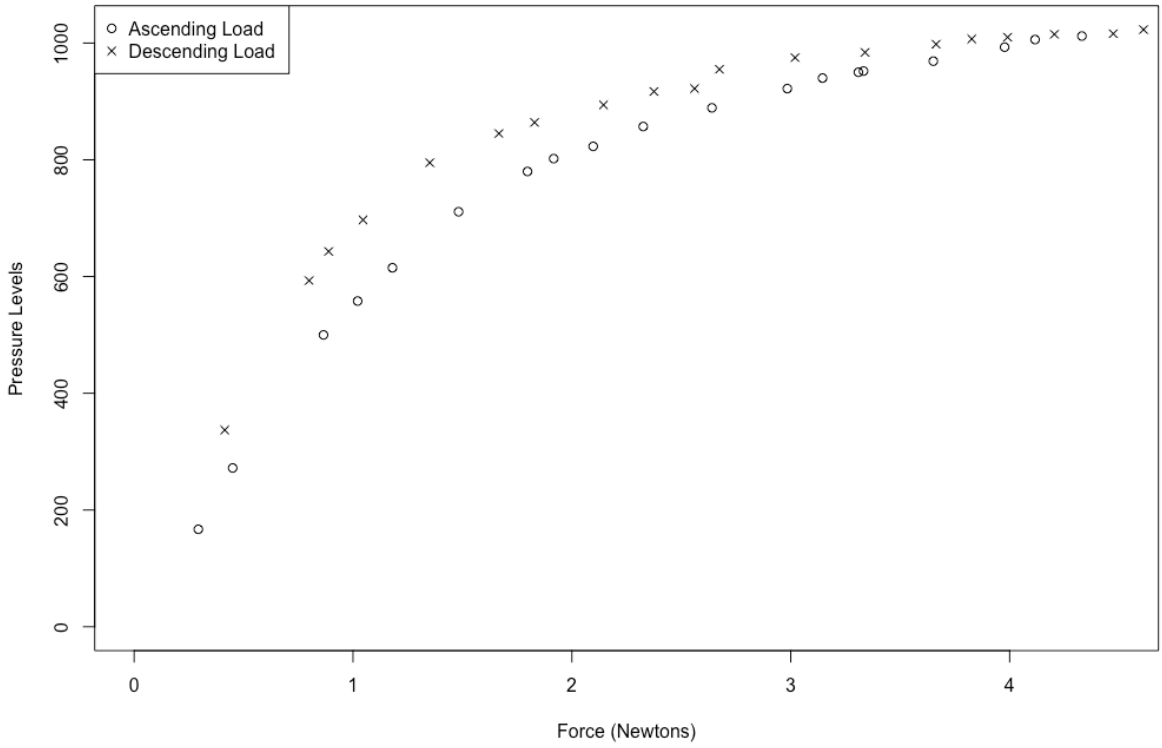

Figure 3.11 Calibration Curve

The datasets were fitted and the polynomial functions with the best fit were calculated:

Zeta Function for ascending load: $Z_u(x) = -65.8149 + 877.1544x - 294.7475x^2 + 31.6239x^3 + 6.1514x^4 - 1.7193x^5 + 0.1053x^6$

Inverse Zeta Function for ascending load: $Z_u^{-1}(x) = 4.036 - 5.824 * 10^{-2}x + 3.35 * 10^{-4}x^2 - 9.142 * 10^{-7}x^3 + 1.306 * 10^{-9}x^4 - 9.398 * 10^{-13}x^5 + 2.711 * 10^{-16}x^6$

Zeta Function for descending load: $Z_d(x) = -130.3994 + 1422.9675x - 796.1817x^2 + 203.8218x^3 - 11.67x^4 - 3.6521x^5 + 0.4728x^6$

Inverse Zeta Function for descending load: $Z_d^{-1}(x) = 833.31 - 7.848x + 2.971 * 10^{-2}x^2 - 5.825 * 10^{-5}x^3 + 6.269 * 10^{-8}x^4 - 3.525 * 10^{-11}x^5 + 8.112 * 10^{-15}x^6$

The Zeta functions are plotted over the data points in figure 3.12.

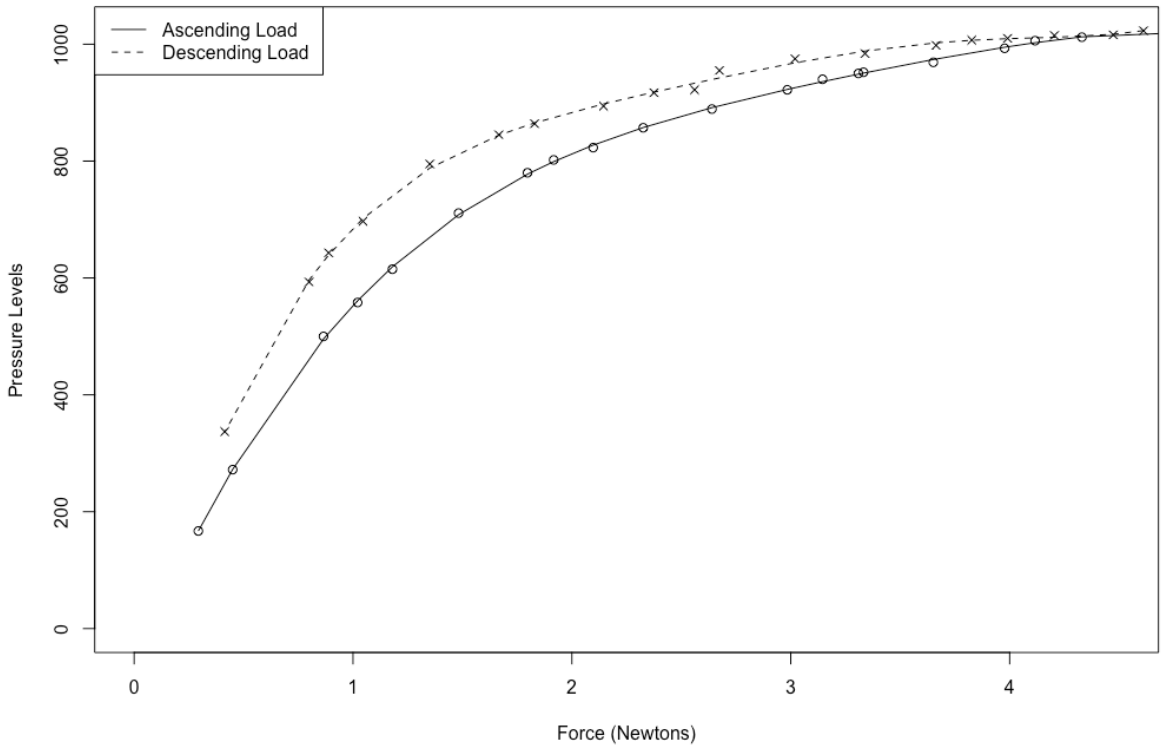

Figure 3.12 Calibration Curve with fitted function

3.7. Wacom STU 540 with LAMY AL-star black EMR (Glossy Surface) and Wacom SDK

The Wacom STU 540 with LAMY AL-star black EMR (Glossy Surface), using Wacom SDK recorded 1024 pressure levels (from 0 to 1023). During preliminary testing it was found that the device registers applied force between 0.14 and 6 N. Measurements were collected ascending from minimum to maximum and then descending from maximum to minimum and the results are shown in figure 3.13. As can be observed in from the figure, both datasets show a pseudo-logarithmic response. The datasets were fitted and the polynomial functions with the best fit were calculated.

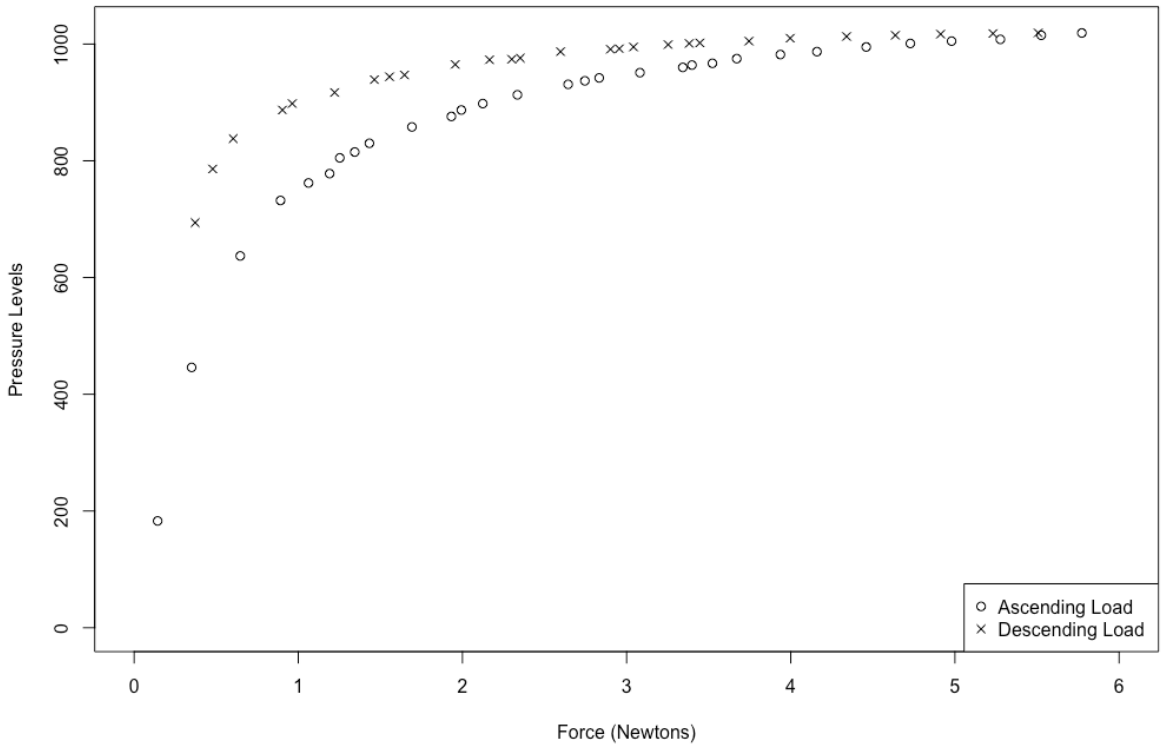

Figure 3.13 Calibration Curve

The datasets were fitted and the polynomial functions with the best fit were calculated:

Zeta Function for ascending load: $Z_u(x) = -18.5877 + 1696.0044x - 1431.4594x^2 + 653.7729x^3 - 161.1162x^4 + 20.1305x^5 - 0.9985x^6$

Inverse Zeta Function for ascending load: $Z_u^{-1}(x) = 6.335 - 8.087 * 10^{-1}x + 3.86 * 10^{-3}x^2 - 9.133 * 10^{-6}x^3 + 1.154 * 10^{-8}x^4 - 7.477 * 10^{-12}x^5 + 1.96 * 10^{-16}x^6$

Zeta Function for descending load: $Z_d(x) = 383.3673 + 1249.2542x - 1163.0723x^2 + 566.4673x^3 147.1668x^4 + 19.3046x^5 - 1.004x^6$

Inverse Zeta Function for descending load: $Z_d^{-1}(x) = 1.918 * 10^5 - 1.353 * 10^3 x + 3.964 * x^2 - 6.176 * 10^{-3} x^3 + 5.397 * 10^{-6} x^4 - 2.509 * 10^{-9} x^5 + 4.846 * 10^{-13} x^6$

The Zeta functions are plotted over the data points in figure 3.14.

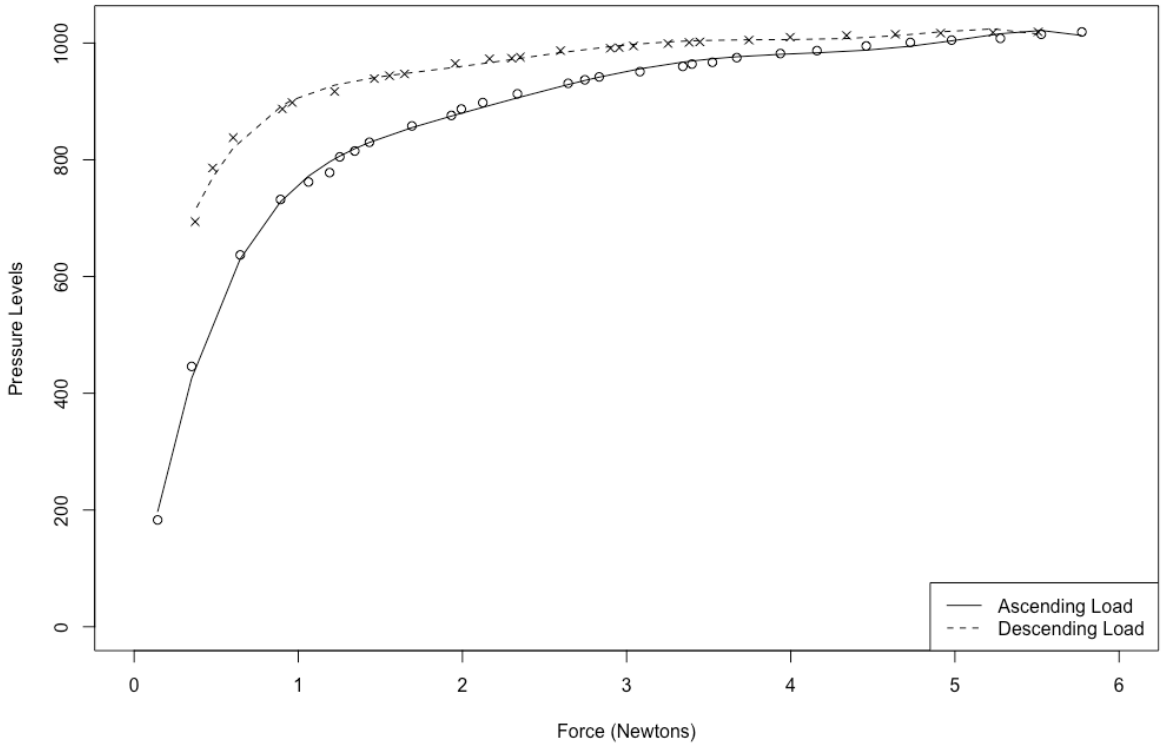

Figure 3.14 Calibration Curve with fitted function

3.8. Wacom STU 540 with LAMY AL-star black EMR (Paper Surface) and Wacom SDK

The Wacom STU 540 with LAMY AL-star black EMR (Paper Surface), using Wacom SDK recorded 1024 pressure levels (from 0 to 1023). During preliminary testing it was found that the device registers applied force between 0.14 and 6 N. Measurements were collected ascending from minimum to maximum and then descending from maximum to minimum and the results are shown in the following figure. As can be observed in figure 3.15, both datasets show a pseudo-logarithmic response. The datasets were fitted and the polynomial functions with the best fit were calculated.

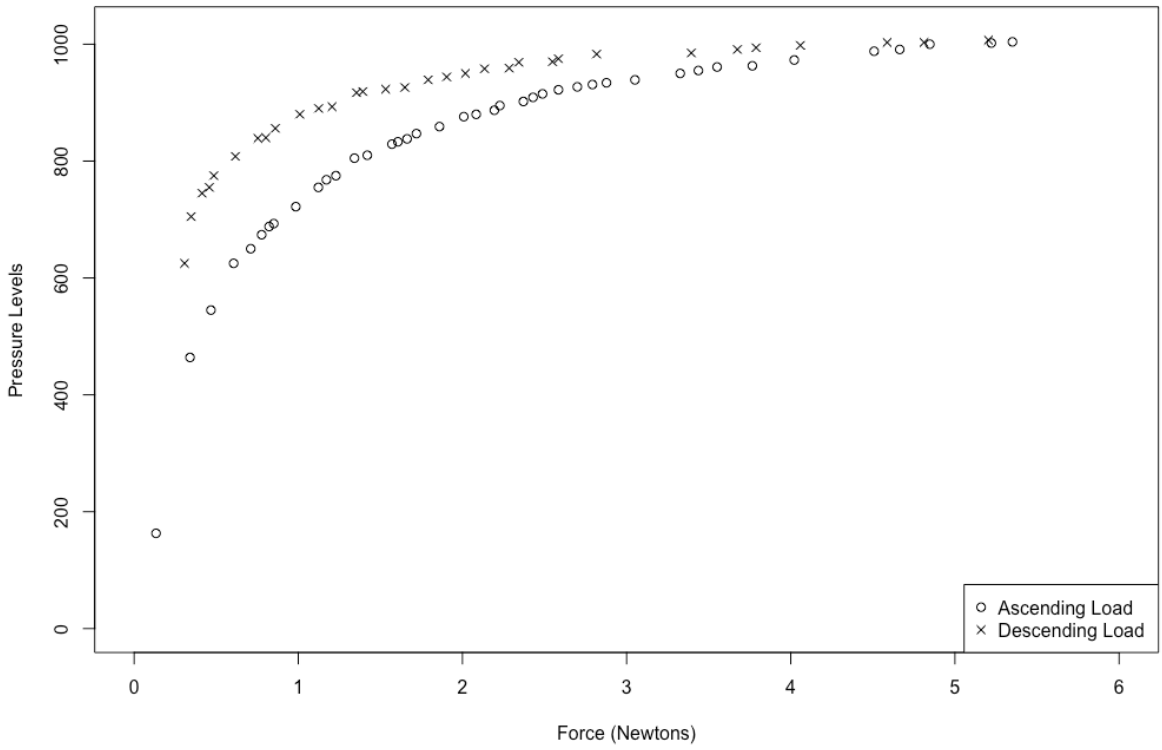

Figure 3.15 Calibration Curve

The datasets were fitted and the polynomial functions with the best fit were calculated:

Zeta Function for ascending load: $Z_u(x) = -26.551 + 1835.345x - 1767.667x^2 + 927.681x^3 - 261.062x^4 + 36.934x^5 - 2.058x^6$

Inverse Zeta Function for ascending load: $Z_u^{-1}(x) = 16.76 - 2.316 * 10^{-1}x + 1.192 * 10^{-3}x^2 - 3.038 * 10^{-6}x^3 + 4.142 * 10^{-9}x^4 - 2.898 * 10^{-12}x^5 + 8.217 * 10^{-16}x^6$

Zeta Function for descending load: $Z_d(x) = 380.0815 + 1251.73x - 1252.6155x^2 + 666.198x^3 - 188.567x^4 + 26.7721x^5 - 1.4973x^6$

Inverse Zeta Function for descending load: $Z_d^{-1}(x) = 2.836 * 10^4 - 2.151 * 10^2x + 6.769 * 10^{-1}\mathrm{x}^2 - 1.131 * 10^{-3}x^3 + 1.058 * 10^{-6}x^4 - 5.259 * 10^{-10}x^5 + 1.085 * 10^{-13}x^6$

The Zeta functions are plotted over the data points in figure 3.16.

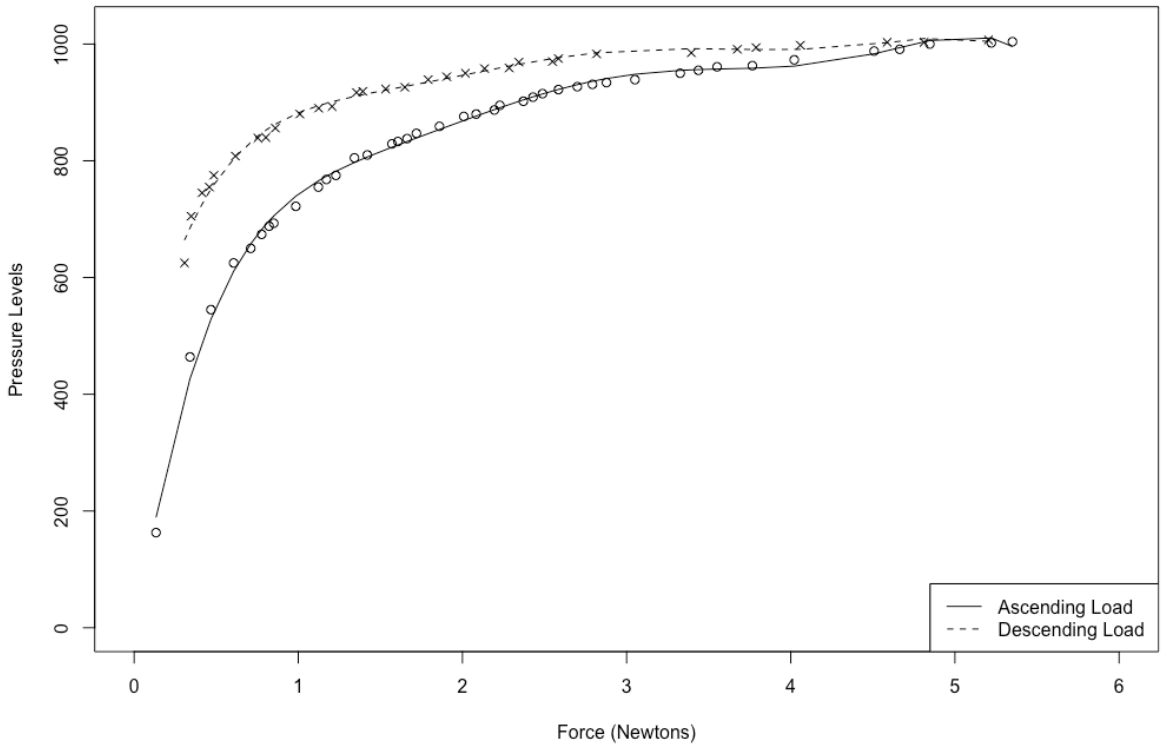

Figure 3.16 Calibration Curve with fitted function

3.9. iPad Pro 9.7" (1st Gen) with Apple Pencil (1st Gen), captured with Forensic Signalyzer app.

The Apple iPad Pro, using Forensic Signalyzer app recorded 4096 pressure levels (from 0 to 4095). During preliminary testing it was found that the device registers applied force between 0.085 and 4.8 N. Measurements were collected ascending from minimum to maximum and then descending from maximum to minimum and are plotted in the following figure. As can be observed from figure 3.17, both

datasets show a linear response and are identical. The datasets were fitted and the polynomial functions with the best fit were calculated.

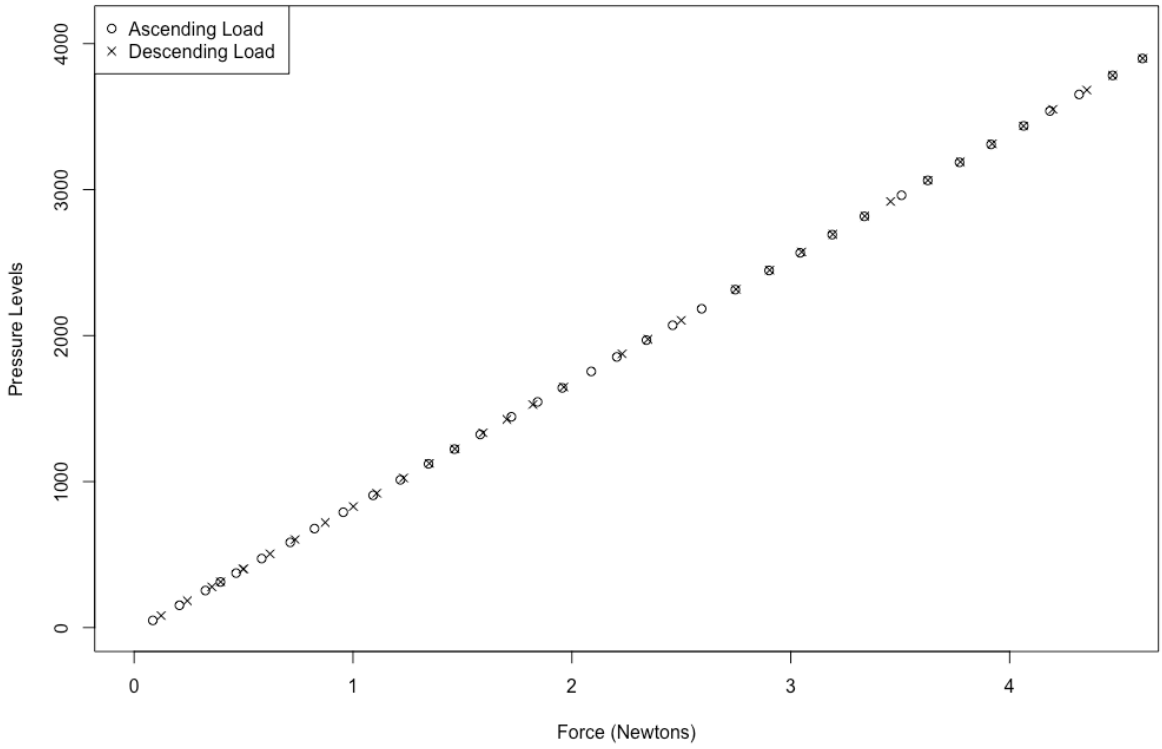

Figure 3.17 Calibration Curve

The ascending load Zeta function is $Z_u(x) = -23.47 + 851.3x$. The descending load Zeta function is $Z_d(x) = -23.47 + 851.3x$. For uniformity with the previous, the fitting function used was a 6th degree polynomial, which produced the linear equation. It is obvious that the iPad Pro does not exhibit a hysteresis effect (as expected as it is not EMR technology), since the difference of the two is zero. Therefore, there is only one Zeta function for the iPad Pro and there is need for the

calculation of only one inverse Zeta function, which is $Z^{-1}(x) = 2.757 * 10^{-2} + 1.175 * 10^{-3}x$.

The Zeta functions are plotted over the data points in figure 3.18.

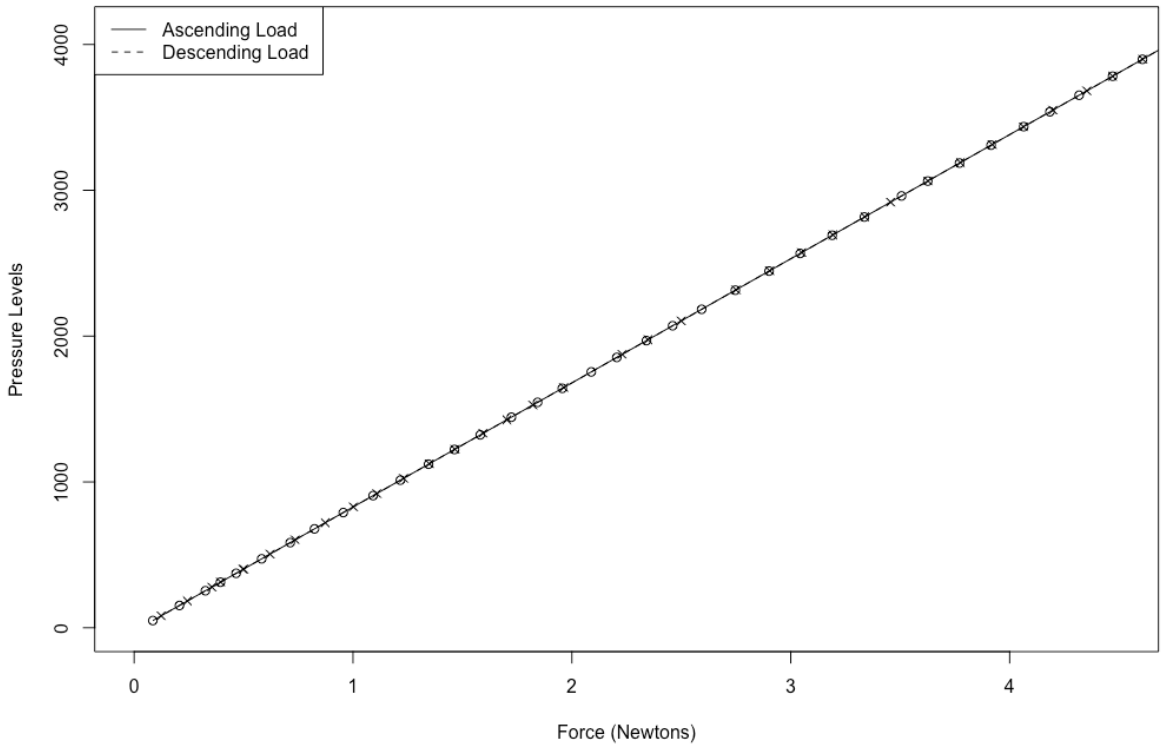

Figure 3.18 Calibration Curve with fitted function

3.10. Chapter 3 References

RStudio, Inc. (2020) *RStudio (Version 1.2.5042)* [Computer software].

Jackson, J.D. (1999) *Classical electrodynamics*. 3rd edn. New York, NY: John Wiley & Sons, Inc.

Fukushima, Y. and Fujitsuka, H. (2013) *United States Patent No. US 8,525,530 B2*.

4. Chapter 4 Discussion I

4.1. Initial observations

As highlighted in the previous chapter (e.g., Figures 3.2 and 3.17), various technologies can produce significantly different models for assigning pressure levels to force (e.g., linear versus pseudo logarithmic).

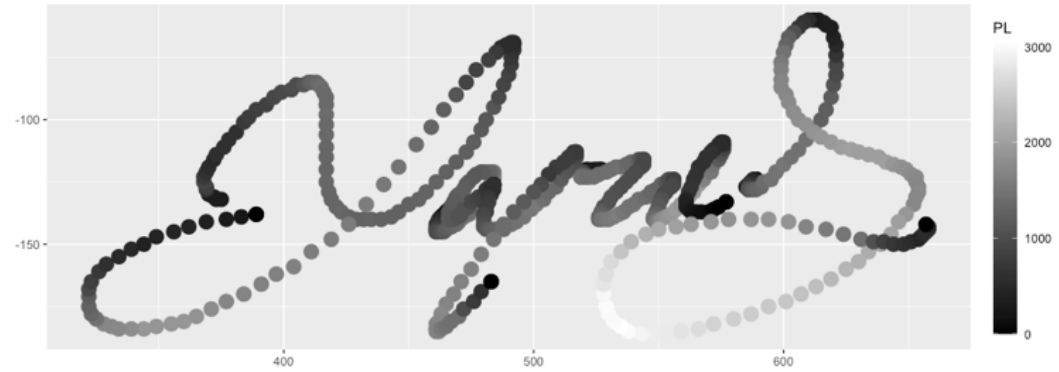

Signature with EMR solution, pressure levels are represented as shades of gray, with black for 0 and white for the maximum pressure level value.

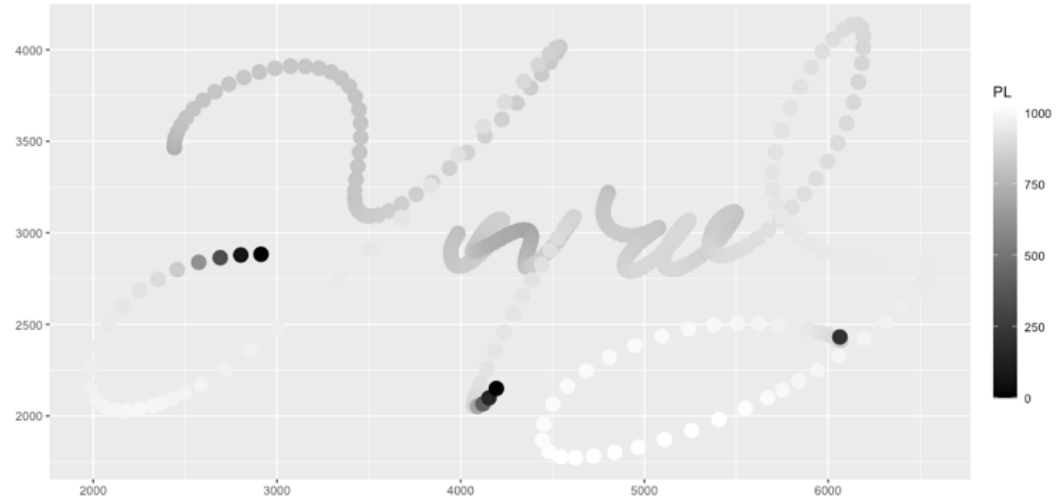

Signature (of the same author as above), captured with a capacitive solution. Pressure levels are represented as shades of gray, with black for 0 and white for the maximum pressure level value.

Figure 4.1. Example of vast difference of representation of Pressure Levels in two DCS of the same author captured with different technology equipment.

It is crucial to approach direct comparisons of unnormalized pressure levels for DCS captured using different technologies with caution in forensic contexts, as such comparisons can be misleading (as shown on Figure 4.1).

While the differences between solutions using the same EMR technology are less pronounced, they are still not insignificant across the tested combinations. As shown in Table 4.1, the same pressure level can correspond to vastly different force values, making unnormalized comparisons and evaluations potentially problematic. Therefore, the need for comparability in the F channel data is clear, and appropriate normalization strategies should be developed, as will be discussed in the following chapter. The observations allow the understanding of how the technology works and which factors play a key role to the pressure level assignment.

	Corresponding force in Newtons		
Pressure Levels	STU 540 with Default Stylus	STU 540 with Bamboo Spark Inking Pen	STU 530 with Default Stylus
300	0.54	0.43	0.28
600	1.07	0.93	0.79
800	1.77	1.68	1.62
1000	4.28	3.38	3.94

Table 4.1 Example of different pressure levels values assigned for the same force on different digitizers.

4.2. Comparison of same hardware with different software

Combinations 1, 2 and 3 calibrate the Wacom STU 540 with the default stylus, captured with three different software solutions, i.e. the Wacom SDK, the Wacom Signature Scope and Namirial's Firma Certa Forensic. As shown on figure 4.2, the calibration curves of the 3 combinations are similar, so the conclusion reached is that these three software attribute the same pressure level to the same applied force for the same device. This result cannot be generalized for software other than the aforementioned three, as the literature indicates that this is not always the case (Zimmer and Heckeroth, 2019; Zimmer *et al*., 2021; Geistová Čakovská *et al*., 2021).

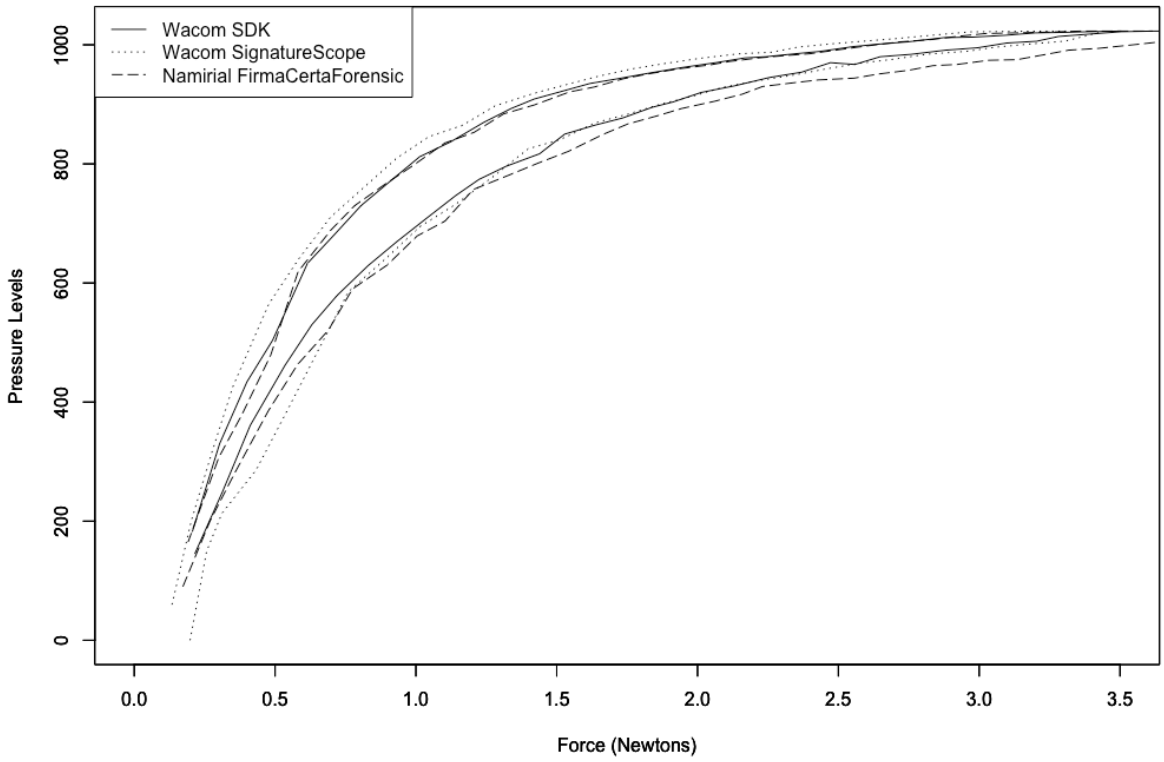

Figure 4.2 Superimposition of the calibration curves of Wacom STU540 using Wacom SDK, Wacom Signaturescope and Namirial Firma Certa Forensic software.

4.3. Comparison of different hardware with same software

4.3.1 Comparison of different digitizer with corresponding default stylus, same software

To explore the way pressure levels are allocated by different hardware solutions under the same software, the calibration curves of Wacom's STU 530 and Wacom's STU 540 with their default styli were compared, accordingly, captured with the Wacom SDK (combinations 1 and 5, Table 3.1). As shown in figure 4.3, the calibration curves are clearly different.

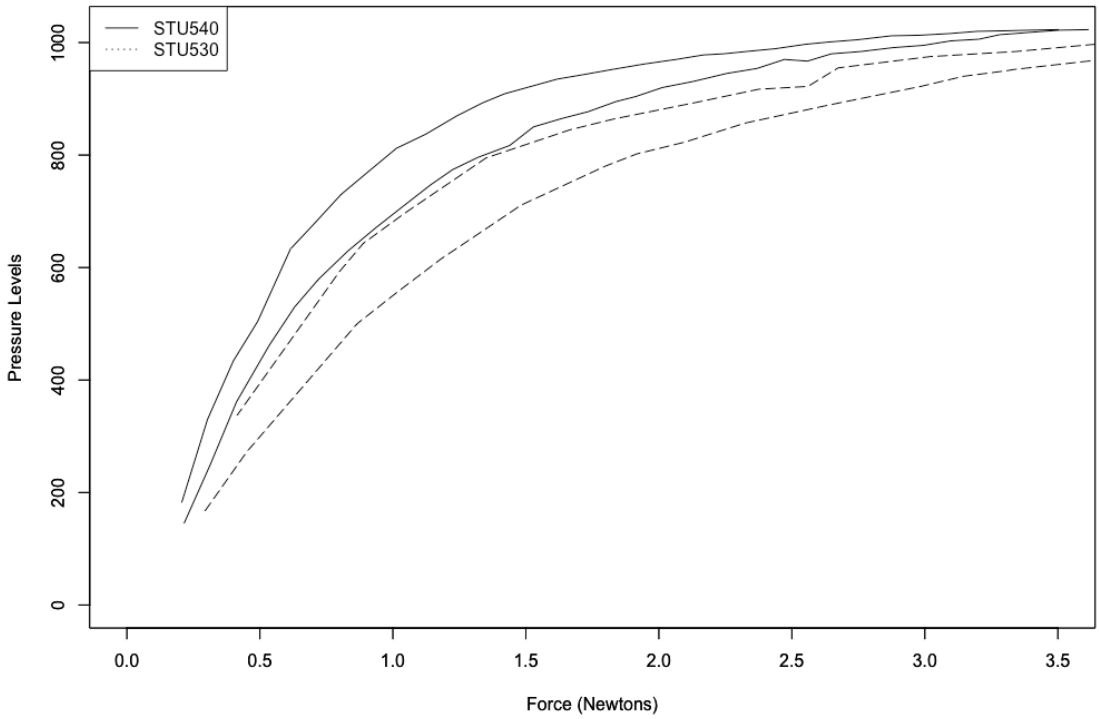

Figure 4.3 Superimposition of the calibration curves of Wacom STU530 and STU540.

The experiment shows that pressure levels are allocated in a similar (pseudo logarithmic) manner but at different levels, not allowing quantitative comparison of data captured with these two digitizers (without normalization).

4.3.2 Comparison of same digitizer, different stylus, same software

4.3.2.1 Wacom STU 530, Wacom SDK, default stylus vs. Wacom Bamboo Spark inking pen

To explore the way pressure levels are allocated when using different styli but the same digitizer under the same software, the calibration curves of Wacom's STU 530 with the default stylus and the Bamboo Spark inking pen captured with the Wacom SDK were compared (combinations 5 and 6). As shown in figure 4.4, the calibration curves are different.

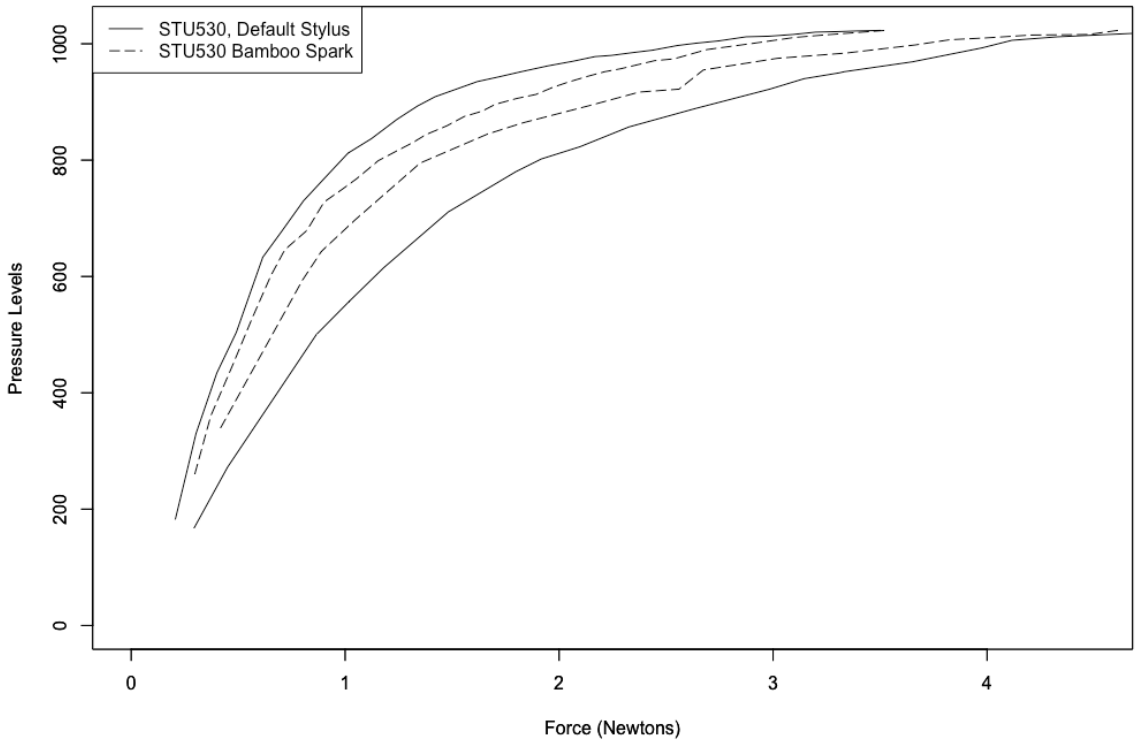

Figure 4.4 Superimposition of the calibration curves of Wacom STU530 with default stylus and Bamboo Spark stylus.

Pressure levels are allocated in a similar (pseudo logarithmic) but different model (see Table 3.1), not allowing quantitative comparison of data captured with these two styli (without normalization). These results can be explained by the fact that the correlation of exercised force to assigned pressure level is related to the pressure sensor inside the stylus and not the digitizer itself for the EMR technology solutions.

This result may explain the statistical difference observed by Heckeroth et al. (Heckeroth *et al.*, 2021) during the comparison of signatures collected on Wacom STU 530 digitizers both with the default stylus and the Bamboo Spark inking pen, exploring the characteristics of signature execution between DCS on glass and traditional signature on paper surfaces.

4.3.2.2 Comparison between Wacom STU 540, Wacom SDK, default stylus vs. Wacom Bamboo Spark inking pen vs. LAMY Al-Star black EMR (paper surface and glass surface variants)

To further explore the way pressure levels are allocated when using different styli but the same digitizer captured by the same software, the calibration curves of Wacom's STU 540 with the default stylus, the Bamboo Spark Inking Pen Wacom Bamboo Spark Inking Pen the two variants of the LAMY Al-Star black EMR (paper surface and glass surface), captured with the Wacom SDK were compared (combinations 1, 4, 7 and 8). As exhibited in figure 4.5, the calibration curves for the two variants of the LAMY Al-Star black EMR (combinations 7 and 8) are similar, so the conclusion can be drawn that both LAMY Al-Star black EMR styli attribute applied force to pressure levels in the same way, regardless of the variant (which has to do with the material at the tip of the stylus).

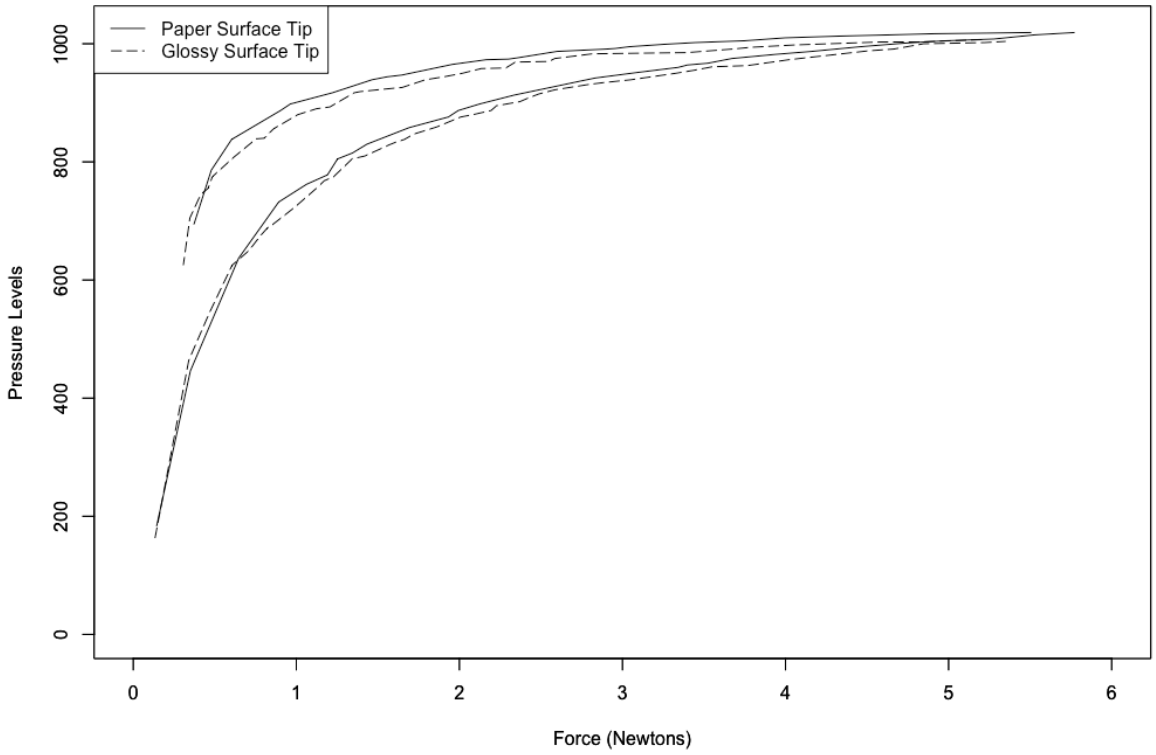

Figure 4.5 Superimposition of the calibration curves of the two variants of the LAMY Al-Star black EMR styli, on a Wacom STU540.

Proceeding with the comparison of the calibration curves of combinations 1, 4 and 7 (which also represents 8), strong differences were observed, as exhibited in figure 4.6. Pressure levels are allocated in a similar (pseudo logarithmic) but different model, not allowing quantitative comparison of data captured with these two styli (without normalization). These results can again be explained by the fact that the correlation of exercised force to assigned pressure level is related to the pressure sensor inside the stylus and not the digitizer itself.

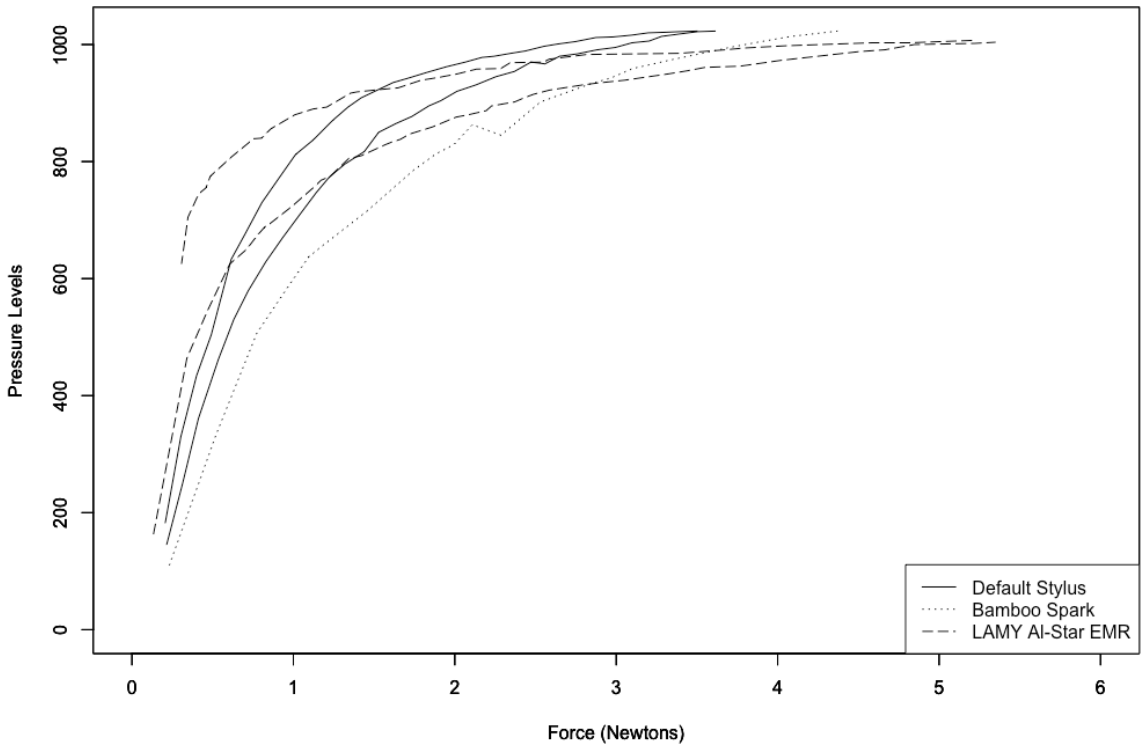

Figure 4.6 Superimposition of the calibration curves of the default stylus, the Bamboo Spark stylus and the LAMY Al-Star black EMR styli, on a Wacom STU530.

4.4. Limitations I

The calibration procedure collected measurements from the centre of the active area of each digitizer. Variations due to the position on the digitizer are therefore not expected for EMR technology, since the force sensor is positioned within the

stylus. This seems to be confirmed by prior research (Heckeroth, Kerkhoff and Weyermann, 2019). Furthermore, the direction of the stylus during collection of measurements was perpendicular to the active area of the digitizer, not exploring the possibility of variation of the registered force by the pressure sensor at an angle. This is not expected to change the accuracy of the force recording by the pressure sensor as this is positioned along the axis of the stylus (Hecker, 2020; Fukushima and Fujitsuka, 2013), although this was not confirmed. The measurements have been collected with the stylus being placed statically over the digitizer's active area, whilst the execution of a DCS would include a moving stylus. This is a limitation but again, due to the mechanics involved, the actual force exercised parallel to the axis of the stylus (which is what the pressure sensor registers force) should be recorded without issues. The reliability of the measurements was confirmed when comparing preliminary measurements, the data presented in the experiment and during repetition of some of the measurements, but repeatability was not exclusively tested. However, the results from the two variants of the LAMY Al-star EMR styli (which have a different tip but apparently the same pressure sensor) and the two versions of the S pen for the two variants of the Samsung device (presented on Chapter 7) suggest repeatability. Lastly, the aging of the pressure sensor (Kalantzis, 2021) was not examined in this experiment as new styli were used for the calibrations. The aging

factor is important as demonstrated in the literature (Kalantzis, 2021) and will be examined in further research.

4.5. Chapter 4 References

Zimmer, J. and Heckeroth, J. (2019) 'Creating a basis for the comparison of digitally captured signatures collected with different signing solutions', in European Network of Forensic Handwriting Experts (ed.) *Proceedings of the Twelfth Conference of the European Network of Forensic Handwriting Experts*. Porto, Portugal: ENFHEX, pp. 12–13.

Zimmer, J. *et al.* (2021) 'The challenge of comparing digitally captured signatures registered with different software and hardware', *Forensic Science International*, 327, p. 110945. doi:10.1016/j.forsciint.2021.110945.

Geistová Čakovská, B. *et al.* (2021) 'Recommendations for capturing signatures digitally to optimize their suitability for forensic handwriting examination', *Journal of Forensic Sciences*, 66, pp. 743–747. doi:10.1111/1556-4029.14627.

Heckeroth, J. *et al.* (2021) 'Features of digitally captured signatures vs. pen and paper signatures: Similar or completely different?', *Forensic Science International*, 318, p. 110587. doi:10.1016/j.forsciint.2020.110587.

Heckeroth, J., Kerkhoff, A. and Weyermann, C. (2019) 'German BKA's project "ESign" - How valid are pressure values', paper presented at the 12th ENFHEX Conference, Porto, Portugal.

Forensic Signalyzer

Hecker, T. (2020) *Forensic Signalyzer (Version 1.1)* [Mobile application software]. Available at: https://apps.apple.com/us/app/forensic-signalyzer/id1478881105

Fukushima, Y. and Fujitsuka, H. (2013) *United States Patent No. US 8,525,530 B2*.

Kalantzis, N. (2021) 'Normalization and comparability of digitally captured signatures (DCS)', in American Academy of Forensic Sciences (ed.) *Proceedings of the Seventy Third Annual Scientific Meeting of the American Academy of Forensic Sciences*. Held virtually, p. 717.

5. Normalization Method[11]

5.1. Necessity of Normalization through Calibration

As it was made clear in the previous Chapter (e.g. figures 4.2 and 4.17), different technologies can exhibit radically different models of pressure level assignment to force (e.g. linear vs. polynomial). It is evident that direct comparison of unnormalized assigned pressure levels for DCS captured with solutions using different capturing technology should only be undertaken and interpreted with the necessary care in a forensic context as it can be misleading (e.g. see figure 4.1). The difference between solutions of the same EMR technology is less dramatic but also not negligible between any of the tested combinations. As demonstrated in Table 4, the same pressure level may refer to significantly different force and hence their unnormalized comparison and evaluation may be problematic.

The necessity for comparability of the F channel data is hence apparent, and normalization strategies should be devised.

[11] Parts of the contents of this chapter have been published in Kalantzis N, Platt AWG. Digitally captured signatures: A method for the normalization of force through calibration and the use of the zeta function. J Forensic Sci. 2021;00:1–18. https://doi. org/10.1111/1556-4029.14927 and Kalantzis N, Fieldhouse S. Digitally Captured Signature solution errors revealed by calibration and testing: Two examples. *J Forensic Sci*. 2025; 00: 1–12. https://doi.org/10.1111/1556-4029.70100

5.1.1. Normalization Strategies

The given work-case scenario has a disputed DCS compared to known DCS (serving as reference material), and the problem anticipated is the disputed DCS being captured in a source (hardware and software) solution, different from the (hardware and software) solution of the known material (which will be identified as the target solution). Similarly multiple different solutions may be encountered within the reference material, for which case the same strategies can be employed (and will not be investigated further).

There are two normalization strategies that can be employed to solve the problem of accurately comparing the F channel data from different solutions; one is to convert all unnormalized F channel data (Pressure Levels) to a common reference system (i.e. SI in Newtons or millinewtons), and the other is to normalize the source solution data set to the target solution dataset. The first strategy is more straight forward and requires one type of calculations – i.e. from Pressure Levels to Newtons through the use of the inverse Zeta function - (per data set, for both source and target solutions) whilst the second strategy includes a second step – i.e. the calculation of the Pressure Levels in the target solution's system through the treatment of the resulting Force data (in Newtons) of the source system. The second strategy may be more efficient in real casework scenarios (in which there is

only one DCS dataset in the source solution and several DCS datasets – the known material - in the target solution).

5.1.2. Normalization to SI

With the strategy the goal is to normalize the force data of a solution (source or target, i.e. disputed DCS or known material DCS) so that it is straightforwardly comparable to any other *normalized to SI* dataset.

When a signature formation is executed and captured by the source solution, the exercised force on the source digitizer is unknown – only the assigned pressure levels are known and are assigned by use of the Zeta function. From the ZF, its inverse (ZF^{-1}) can be calculated, i.e. the function that given the value of the assigned pressure levels will calculate the initially exercised force, hence the initially exercised force values can be calculated in Newton. These values (now normalized in Newtons) can be directly compared to other such values.

For EMR solutions, this process must happen for both ascending and descending loads to consider the hysteresis effect, and a criterion needs to be set to distinguish which type of load (and hence ZF) is to be used. This criterion is the difference of force between two consecutive points (ΔF). If $\Delta F>0$ then the force is

increasing and the Ascending Load ZF should be used, if the ΔF<0 then the force is decreasing and the Descending Load ZF should be used.

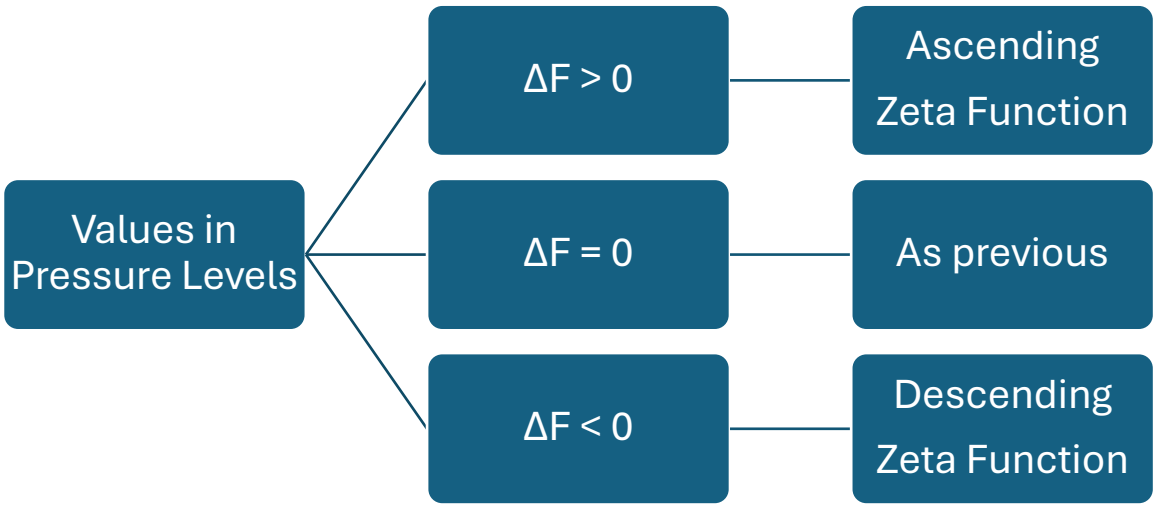

Figure 5.1 Force difference conditions.

The normalization process is exhibited on Figure 5.1, and as an example, for a DCS captured with Wacom STU540 the process is shown on Table 5.1 (for a small but indicative part of the data of the unnormalized signature).

Pressure Levels	Ascending Load Force Values	Descending Load Force Values	ΔF	Selection Operator	Zeta Function Selection
591	1.06663505	0.68439661	1	1	1.06663505
620	1.17161874	0.75112977	29	1	1.17161874
649	1.28303086	0.83059396	29	1	1.28303086
675	1.38802561	0.91177318	26	1	1.38802561
700	1.49350421	0.9973145	25	1	1.49350421
717	1.56793156	1.05889954	17	1	1.56793156
731	1.6310572	1.11132435	14	1	1.6310572
741	1.67727922	1.14959395	10	1	1.67727922
745	1.69605636	1.1650798	4	1	1.69605636
751	1.72455274	1.18849247	6	1	1.72455274
758	1.75833168	1.21608231	7	1	1.75833168
766	1.79769643	1.24797849	8	1	1.79769643
777	1.85328708	1.29250325	11	1	1.85328708
785	1.89490124	1.3254193	8	1	1.89490124
790	1.92146753	1.34624902	5	1	1.92146753
797	1.95944132	1.37578559	7	1	1.95944132
804	1.99839931	1.40581937	7	1	1.99839931
810	2.03264122	1.432019	6	1	2.03264122
816	2.06772951	1.4587035	6	1	2.06772951
822	2.10372751	1.48594332	6	1	2.10372751
825	2.12208861	1.49979634	3	1	2.12208861
831	2.15957926	1.5280244	6	1	2.15957926
835	2.1851721	1.54726927	4	1	2.1851721
836	2.19164846	1.55213823	1	1	2.19164846
839	2.21127101	1.56689208	3	1	2.21127101
841	2.22451772	1.57685592	2	1	2.22451772
840	2.21787761	1.57186084	-1	-1	1.57186084
843	2.23790003	1.5869274	3	1	2.23790003
844	2.24464302	1.59200498	1	1	2.24464302
843	2.23790003	1.5869274	-1	-1	1.5869274
847	2.26508413	1.60741237	4	1	2.26508413

Table 5.1 Biometric data

The resulting normalized DCS is visualized in figure 5.2 in XY point by point visualization with color correlation to the Pressure Level or Force values.

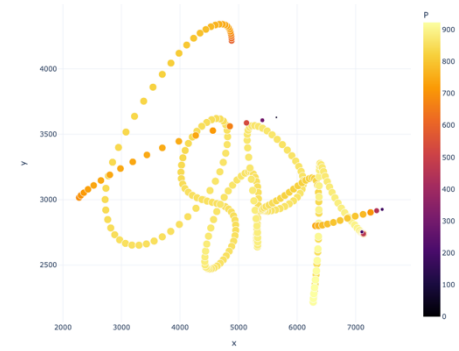

Unnormalized Pressure Level values representation of a DCS

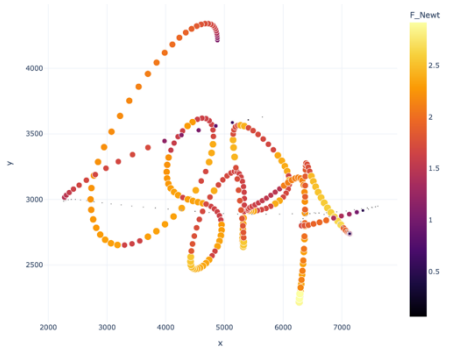

Normalized Newton Force values representation of a DCS

Figure 5.2 Difference in colour correlation between unnormalized and normalized biometric data.

5.1.3. Normalization of source solution to target solution

In this strategy, the goal is to normalize the force data of a source solution so that they are comparable to the force data of a target solution. When a signature formation is executed and captured by the source solution, the exercised force on the source digitizer is unknown – only the assigned pressure levels are known and are assigned by use of the Zeta function. From the ZF, its inverse (ZF^{-1}) can be calculated, i.e. the function that given the value of the assigned pressure level will

calculate the initially exercised force, hence the initially exercised force values can be calculated in N. Then, using these reconstructed force values with the target solution's ZF the pressure levels that would have been assigned by the target solution if the signature was captured by it can be calculated.

If any of the solutions involved is EMR, the process has to happen for both ascending and descending loads to take into account the hysteresis effect, and a criterion needs to be set to distinguish which type of load (and hence ZF) is to be used just like in the previous strategy. This criterion is the difference of force between two consecutive points (ΔF). If ΔF>0 then the force is increasing and the Ascending Load ZF should be used, if the ΔF<0 then the force is decreasing and the Descending Load ZF should be used. Finally, and in addition to what was employed in the previous strategy, different minimum and maximum force thresholds should be taken into account.

To demonstrate the importance of normalization two signatures were captured, and the process to normalize the data of the source solution to the target solution was applied. The source solution was chosen to be the Apple iPad Pro with the Apple Pencil captured with Forensic Signalyzer app, and the target solution was chosen to be the Wacom STU 530 with the default stylus captured with the Wacom SDK. The reference DCS, captured with the target solution, is visualized with R Studio in figure 5.2, with the pressure levels represented as shades of grey. The

unnormalized DCS, captured with the source solution, is visualized with R Studio in figure 5.2, with the pressure levels represented as shades of grey.

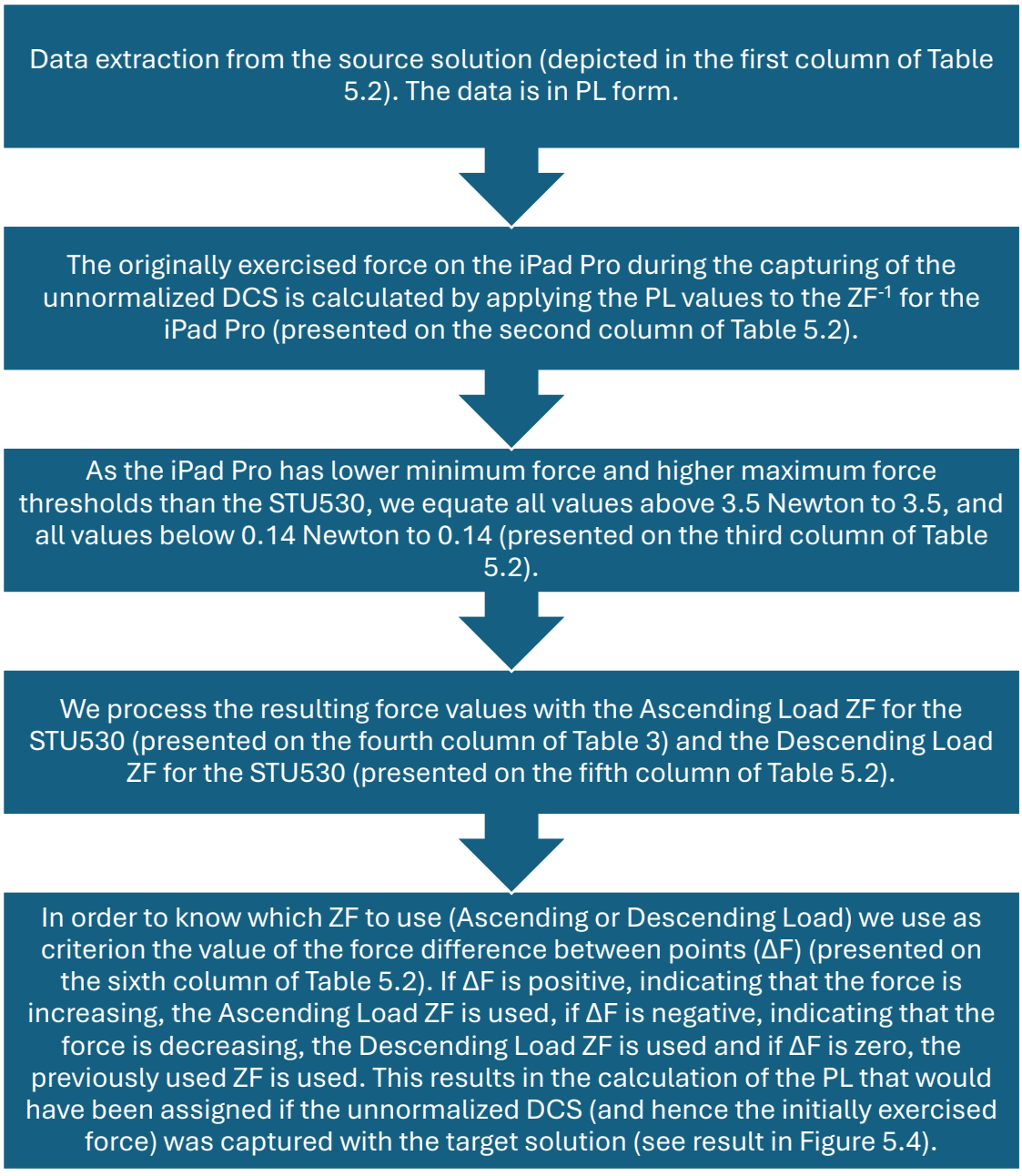

s

Figure 5.3 Normalization flowchart.

The normalization process is exhibited on Table 3 (for a small but indicative part of the data of the unnormalized signature), and the process is demonstrated in a flowchart (figure 5.3). The resulting normalized DCS is visualized in figure 5.4c.

F Data from iPad Pro	F (N)	F with STU 530 Thresholds	STU 530 Ascending	STU 530 Descending	ΔF	F Data Normalized to STU 530
2405	2.85	2.85	911	956	+	911
2439	2.89	2.89	914	959	+	914
2472	2.93	2.93	918	961	+	918
2464	2.92	2.92	917	961	-	961
2464	2.92	2.92	917	961	0	961
2497	2.96	2.96	920	964	-	920

Table 5.2 Example of pressure level values captured with the Apple iPad Pro with Pencil, and their transformation stages until they are normalized to Wacom's STU 530 and default stylus values.

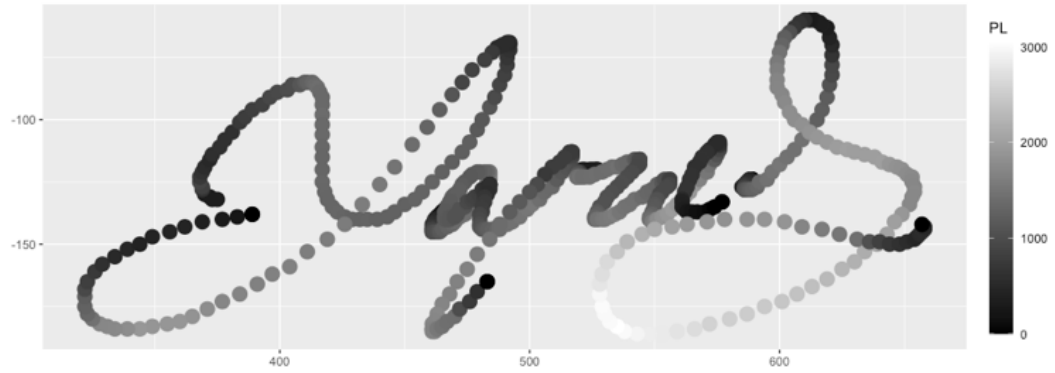

Figure 5.4 a. The reference DCS, captured with the target solution. pressure levels are represented as shades of grey, with black for 0 and white for the maximum pressure level value.

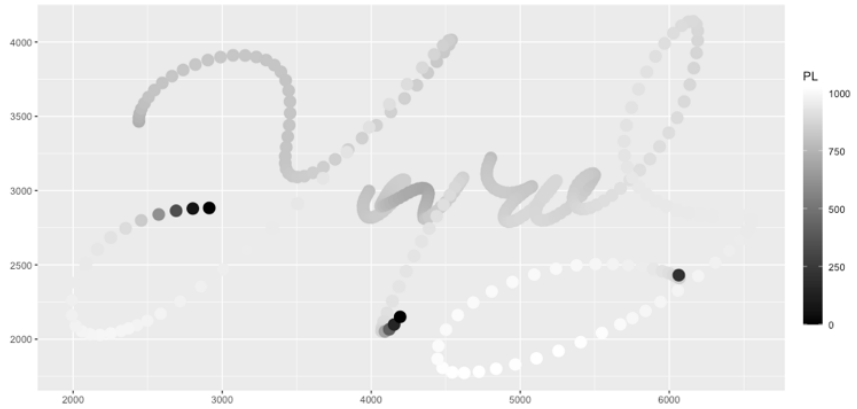

Figure 5.4 b. The unnormalized DCS, captured with the source solution. Pressure levels are represented as shades of grey, with black for 0 and white for the maximum pressure level value.

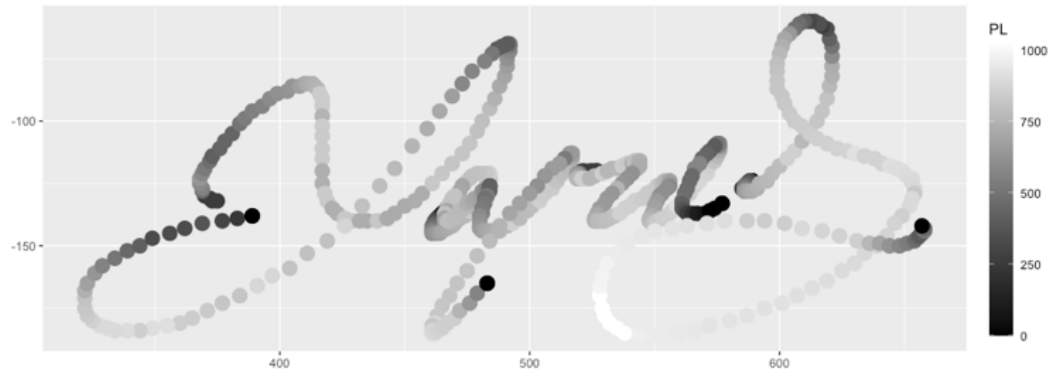

Figure 5.4 c. The normalized DCS, captured with the source solution but normalized to appear as if it was captured with the target solution. Pressure levels are represented as shades of grey, with black for 0 and white for the maximum pressure level value.

Figure 5.4 Examples of DCS from different sources that become normalized and comparable.

5.2. Normalization Tools

The available DCS forensic analysis tools (software suites) are using the captured biometric data (X, Y, F in pressure levels and T) to offer a series of visualizations to the forensic examiner for them to proceed with their analysis. Spatial coordinates X and Y are easily converted to SI units as the resolution is typically provided by the manufacturers (usually in points per inch – ppi), and time is always provided in msec. When looking at Force channel data, software solutions will either use the arbitrary and unnormalized Pressure Level values, or will offer a "normalized" version of these in percentage (e.g. a solution that offers 1024 pressure levels will be presented with values ranging from 0 to 100.00 instead of 0 to 1023) (Namiral S.p.a., 2020). Following what is stated in the previous paragraphs this is a problem, especially if the FHE is unaware of the necessity for normalization and assumes that the pressure levels (or even worse the percentage of) in different solutions represents the same exercised force.

To allow for appreciation of the normalization method – either within or outside of the specialized forensic software available –digital tools to allow the easy and

straight forward calculation of the normalized force values in Newtons were constructed.

Following the steps mentioned in paragraph 5.1.2, the calculation of the exercised force based on the assigned Pressure Levels is based by calculating the 6^{th} degree polynomial values which transforms the exercised Force to the assigned Pressure Levels, and this function is called the Zeta Function, and the processing of the given Pressure Levels with the inverse Zeta Function, again a 6^{th} degree polynomial, which will calculate the initially exercised Force. This would generally be a straightforward process, but for Electromagnetic Resonance (EMR) technology digitizers there are two Zeta Functions (and hence two inverse Zeta Functions) due to the Hysteresis effect. The Hysteresis effect, or Hysteresis phenomenon, is encountered in ferromagnetic materials and circuits, and describes how the state of a system depends on its history (Mayergoyz, 2003). In our case this means that for EMR digitizers, the assignment of Pressure Levels to a specific exercised Force value is affected by whether the previously exercised Force was higher or lower, which results in any EMR digitizer having two discrete Zeta Functions, one for increasing Force (ascending load) and one for decreasing force (descending load) (Kalantzis and Platt, 2022).

This complication does not allow the direct calculation of the exercised Force values from the assigned Pressure Levels, and requires the introduction of a new operator that takes into account the previous state of the system and calculates if

the Force is increasing or decreasing, this operator is the difference of the Pressure Levels and is symbolized with “DF”.

Three digital tools to assist the FHE with easy calculation of the Force values in Newtons provided the DCS solution has already been calibrated, and the inverse Zeta Functions are known, in Microsoft Excel, in Python and in R were developed.

5.2.1. Normalization with Excel

To facilitate the calculation of the initially exercised force through the processing of the assigned Pressure Levels with the inverse Zeta Functions with Microsoft Excel, a workbook with 3 spreadsheets is created.

The first spreadsheet is named “Inverse Zeta Function Values” and has polynomial factors of the Inverse Zeta Functions (An for the ascending load, and Dn for the descending load).

The second spreadsheet is named “Calculation of Force Values” and has 9 columns.

The first 4 columns are named “X Values”, “Y Values”, “T Values” and “F Values”; this is where the DCS data values should be imported (or pasted). Notice that depending on the source system CSV nomenclature, the positioning of these axes might be different.

For the rest of the columns of this spreadsheet, the functions will be copied and then pasted for a large number of lines (e.g. 1000), with the exception of the first value of the “ΔF” column – for reasons that will become apparent further down. As it is unknown how many data points the DCS file will have, to nullify all the rest of the lines with the pasted functions, the following is inserted in the beginning of all the functions.

For a function in a cell in line 2, with the Pressure Levels of the CSV in column D,

D2="", "",

This means that the Pressure Level column has a value, then whatever follows the coma of the above will take place, otherwise if there is no value then there will be no value in the function column too.

The fifth column processes the “F Values” column data through the ascending load inverse Zeta Function, called from the “Inverse Zeta Function Values” spreadsheet:

=IF(D2="", "", 'Inverse Zeta Function Values'!$A$5+'Inverse Zeta Function Values'!$B$5*D2+'Inverse Zeta Function Values'!$C$5*D2^2+'Inverse Zeta Function Values'!$D$5*D2^3+'Inverse Zeta Function Values'!$E$5*D2^4+'Inverse Zeta Function Values'!$F$5*D2^5+'Inverse Zeta Function Values'!$G$5*D2^6)

Similarly, the sixth column processes the “F Values” column data through the descending load inverse Zeta Function, called from the “Inverse Zeta Function Values” spreadsheet:

=IF(D2="", "", 'Inverse Zeta Function Values'!$A$8+'Inverse Zeta Function Values'!$B$8*D2+'Inverse Zeta Function Values'!$C$8*D2^2+'Inverse Zeta Function Values'!$D$8*D2^3+'Inverse Zeta Function Values'!$E$8*D2^4+'Inverse Zeta Function Values'!$F$8*D2^5+'Inverse Zeta Function Values'!$G$8*D2^6)

The seventh column named “ΔF” calculates the difference of the “F Values” column data, except for the first cell that should remain positive (e.g. 1):

=IF(D3="", "", D3-D2)

The eighth column named “Selection Operator” uses the values of the ΔF column to assign the number +1 if the Pressure Level difference is positive (ascending load), the number -1 if the Pressure Level difference is negative (descending load), or the same as the previous value if the Pressure Level difference is 0:

=IF(D2="", "", IF(G2>0, 1, IF(G2<0, -1, H1)))

Finally, the ninth column named “Zeta Function Selection” uses the Selection Operator column to select either the ascending or the descending load calculated values from the appropriate columns:

=IF(D2="", "", IF(H2>0, E2, F2))

The third and last spreadsheet is named “Force Values in Newtons” and features one column with the final values in Newtons, called from the “Calculation of Force Values” spreadsheet:

='Calculation of Force Values'!I2

5.2.2. Normalization with Python Code

This python snippet is used to import DCS data from a generic CSV file with columns X, Y, T and F, and calculate the initially exercised Force in Newtons by selecting the appropriate inverse Zeta Function.

First the inverse Zeta Functions for ascending and descending load are defined as “Z_inv_A(xi)” and “Z_inv_D(xi)”.

In order to properly select which inverse Zeta Function to use, an operator needs to be calculated. Initially the column of data named “dp” with the difference in Pressure Levels is created, having the first value be 1 by default:

```
data['dp'] = 1

data['dp'].iloc[1:] = data['F'].diff().iloc[1:]
```

Then a column of data named “Op” that gives +1 if the dp value is positive, -1 if the dp value is negative and the same as the previous entry if the dp value is 0 is created:

```
data['Op'] = np.where(data['dp'] > 0, 1, np.where(data['dp'] < 0, -1, np.nan))
for i in range(1, len(data)):
  if data['dp'].iloc[i] == 0:
    data['Op'].iloc[i] = data['Op'].iloc[i - 1]
data['Op'].fillna(method='ffill', inplace=True)
```

Following this, columns “Fa” for the ascending load zeta function values, and “Fd” for the descending load zeta function values are created, and the values of Op are used to select the proper one, and create the column named “F_Newtons” with the Force values in Newton:

```
data['Fa'] = data['F'].apply(Z_inv_A)
data['Fd'] = data['F'].apply(Z_inv_D)
data['F_Newtons'] = np.where(data['Op'] > 0, data['Fa'], np.where(data['Op'] < 0, data['Fd'], np.nan))
```

5.2.3. Normalization with R

The code for R requires the importing of the DCS data to R from the appropriate CSV file, and the creation of a data frame named “data”, and the Pressure Level values are imported as the “p” vector. Subsequently the inverse Zeta Functions for both ascending and descending load are set by defining their parameters (a_n for the ascending load, and d_n for the descending load).

Then the p vector values are processed through both ascending and descending inverse Zeta Functions, producing 2 new vectors, “Fa” and “Fd”.

To select the appropriate value (either Fa or Fd), a new vector named “DF” is initially created, that keeps the first value of p, and then calculates the difference of the p value from each previous:

```
data$DF <- c(data$p[1], diff(data$p))
```

The DF values cannot be immedietly used to select which inverse Zeta Function to use; even though positive or negative values of DF express whether the Force increases or decreases, it provides no information of the state of the system if the p values are the same. Therefore the “Op” vector is introduced, which will provide the value +1 if DF is positive, -1 if negative and the same as the previous value if 0:

```
data$Op <- ifelse(data$DF > 0, 1, ifelse(data$DF < 0, -1, NA))
```

```
for (i in 2:nrow(data)) {
 if (is.na(data$Op[i])) {
  data$Op[i] <- data$Op[i - 1]
 }
}
```

Finally the calculation of a new vector for the dataframe, named “F(Newtons)” can take place, by using the values of the Op vector for the selection:

```
data <- data %>% mutate(`F(Newtons)` = ifelse(Op > 0, Fa, ifelse(Op < 0, Fd, NA)))
```

5.3. Chapter 5 References

Namiral S.p.a. (2020) *Firma Certa Forensic (Version 1.2.9.0)* [Computer software].

Mayergoyz, I.D. (2003) *Mathematical models of hysteresis and their applications*. Amsterdam: Elsevier.

Kalantzis, N. and Platt, A.W.G. (2022) 'Digitally captured signatures: A method for the normalization of force through calibration and the use of the zeta function', *Journal of Forensic Sciences*, 67, pp. 651–668. doi:10.1111/1556-4029.14927.

Chapter 6 Discussion II[12]

6.1. Validation and use of method

The findings of the calibration and the method for normalization has been presented internationally since the completion of the experiment (Kalantzis, 2020, 2021a–i, 2022a–b, 2023). As a result, the main publications of the experiment, findings and method for normalization (Kalantzis and Platt, 2020, 2022) have been included in the latest edition of the Best Practice Manual of ENFHEX (ENFSI, 2022).

6.1.1. Polish example

Following the publication of the STEFA work regarding the compatibility problems for the data captured with different solutions (Zimmer *et al*., 2021), Dzieździc et al. published a study with respect to the problem of compatibility of different DCS software and hardware solutions deployed by the same authority in Poland (Dzieździc and Ferenc, 2020). In that study, three different solutions are studied as

[12] Parts of the contents of this chapter have been published in Nikolaos Kalantzis, George Pappas, Sarah Fieldhouse, Calibration and Zeta Functions for the Wacom DTU1141b, Science & Justice, Volume 65, Issue 1, 2025, Pages 1-4, ISSN 1355-0306, https://doi.org/10.1016/j.scijus.2024.11.002.

per their captured DCS data, and the authors state “Due to the fact that the pressure for signatures from type three cards is given in levels, a comparison of this feature with that of signatures from type one and two cards would require conversion of this unit into percentages. However, in order to do this, information would be needed on the number of levels of pressure recognised by the digitizer. Furthermore – as other studies have shown – a comparison of pressure levels captured by different digitizers (Heckeroth, Kerkhoff, Weyermann, 2019; Kalantzis, 2020) is burdened by other limitations and requires extreme caution.” (Dzieździc and Ferenc, 2020).

Following this, Dzieździc et al. started developing a tool for automatic normalization of force data by applying the aforementioned and published method detailed in Chapter 6 (Dziedzic and Radwan, 2024).

The acceptance and application of the developed method by the Polish research shows how the method has been validated and accepted by the international FHE community.

6.2. The way forward – Wacom DTU1141b

Given the fact that different software and hardware solutions exhibit different Zeta Functions, the way forward requires calibration and publication of the Zeta Functions and their inverse for use in the industry or FHEs. To exhibit the recommendation for how to generally apply the method, a new Wacom DTU1141b was selected for calibration, paired with its default stylus (Wacom UP7724 stylus). Wacom Wintab data collector application (2022 edition) was used for the collection of data points. It is noted that the Wintab data collector application provides raw Pressure Level values in the form of values from 0 to 32767, even though not all values are registered (as the actual sensitivity of Force Channel for this solution is 1024 levels).

The results are shown on Table 6.1, and the calibration curve on Figure 6.1.

Software used for measurements	Wintab data collector 2022 Wacom Company Limited		
# Pressure Levels	1024 (expressed in 32bits – 32768 levels)		
Minimum Force Threshold (Newtons)	0.25	Maximum Force Threshold (Newtons)	3.6
Ascending Load Zeta Function			
$Z_{ascending}(x) = -11171.8 + 53854.8x - 39361.5x^2 + 20839.6x^3 - 7233.7x^4 + 1402.5x^5 - 112.6x^6$			
Ascending Load Inverse Zeta Function			
$Z^{-1}_{ascending}(x) = 2.4 * 10^{-1} + 3.003 * 10^{-5}x + 1.78 * 10^{-9}x^2 - 4.021 * 10^{-13}x^3 + 3.775 * 10^{-17}x^4 - 1.4 * 10^{-21}x^5 + 1.929 * 10^{-26}x^6$			
Descending Load Zeta Function			
$Z_{descending}(x) = -18194.85 + 90717x - 86913.56x^2 + 50382.41x^3 - 17114.54x^4 + 3121.29x^5 - 235.66x^6$			
Descending Load Inverse Zeta Function			
$Z^{-1}_{descending}(x) = 4.584 * 10^{-1} - 2.02 * 10^{-4}x + 6.317 * 10^{-8}x^2 - 7.477 * 10^{-12}x^3 + 4.277 * 10^{-16}x^4 - 1.163 * 10^{-20}x^5 + 1.22 * 10^{-25}x^6$			

Table 6.1 Calibration measurements for Wacom DTU1141b.

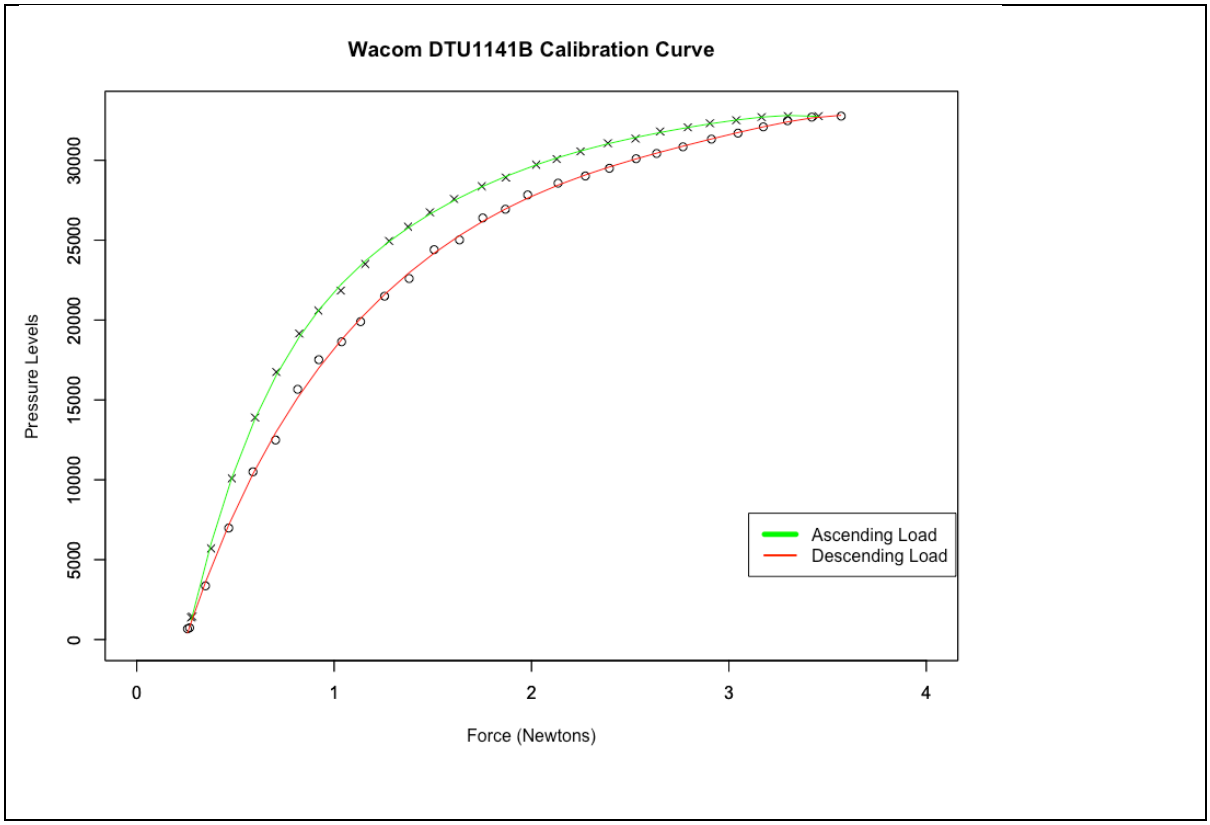

Figure 6.1 Graph of calibration curve for the Wacom DTU1141b.

During testing it was also observed that there is interoperability between the Wacom DTU1141b digitizer and a range of Wacom styli – or 3rd party EMR styli that include a Wacom pressure sensor. The range of compatible styli is included in Table 6.2.

Manufacturer	Model	Compatible with DTU1141b
Kaweco	KAWECO AL SPORT connect EMR	Yes
Lamy	LAMY AL-star black EMR pen Digital Writing	Yes
Lamy	LAMY safari twin pen all black EMR Digital Writing	Yes
Samsung	Samsung Galaxy Tab S6 Lite S Pen EJ-PP610BJEGU	Yes
Wacom	Wacom UP61089A1 pen	Yes
Wacom	Wacom UP6710 pen	Yes
Wacom	Wacom UP7724 pen (default DTU1141b Stylus)	Yes

Table 6.2 Compatible styli for the Wacom DTU1141b.

The normalization of pressure level values acquired from the Wacom DTU1141b to Force in Newtons can take place by applying the inverse Zeta Functions provided in Table 1. As there are two inverse Zeta Functions provided (one for ascending and one for descending load), a criterium has to be implemented in order to choose the correct one; the criterion is the change in Pressure Level values which can be expressed by the operator ΔPL. If ΔPL>0 then the load is ascending, if ΔPL<0 then the load is descending, and if ΔPL=0 then the previous state (ascending or descending) should be kept.

The calibration of the Wacom DTU1141b digitizer through the Zeta Function method provided the Zeta Functions for both ascending and descending loads. This expresses the relationship between exercised force and assigned pressure levels as well as the inverse Zeta Functions for both loads, allowing the calculation of the exercised force from the assigned Pressure Levels. The process of normalizing the values is clearly defined, and an example of how to apply the method in Python is provided in Table 6.3, using Namirial Firma Certa Forensic's ISO standard CSV files (Namirial, no date) as the source of the raw data:

```
def Z_inv_A(xi):
    a_0=0.24
    a_1=3.003e-5
    a_2=1.78e-9
    a_3=-4.021e-13
    a_4=3.775e-17
    a_5=-1.4e-21
    a_6=1.929e-26
    return a_0+a_1*xi + a_2*pow(xi,2.0) + a_3*pow(xi,3.0)+ a_4*pow(xi,4.0)+
a_5*pow(xi,5.0)+ a_6*pow(xi,6.0)


def Z_inv_D(xi):
    a_0=4.584e-1
    a_1=-2.02e-4
    a_2=6.317e-8
    a_3=-7.477e-12
    a_4=4.277e-16
    a_5=-1.163e-20
    a_6=1.22e-25
    return a_0+a_1*xi + a_2*pow(xi,2.0) + a_3*pow(xi,3.0)+ a_4*pow(xi,4.0)+
a_5*pow(xi,5.0)+ a_6*pow(xi,6.0)
```

```
inputDataFile = 'AS'

dataFile = open('RawData.csv')
dataReader = csv.reader(dataFile, delimiter =';')
dataCSV = list(dataReader)          # this makes a list of the file to be manipulated

print(len(dataCSV))

# itter = 0
# while itter <50 :
#     display(dataCSV[itter])
#     itter=itter+1

cwd = os.getcwd()                # This reads the current working folder which is the
same as the notebook's

display(cwd)

display(dataCSV[0+1])            # This line indicates the number of signatures

sig_N = int(dataCSV[0+1][1])
print(sig_N)

loop0 = 2
stepL = 1

while stepL < sig_N+1:

   #display(dataCSV[loop0+1])            # First line of the signature
   #display(dataCSV[loop0+22])            # This line indicates the number of data
points in the signature
   N_max = int(dataCSV[loop0+22][1])
   loopEnd = loop0 + 23 + N_max
   collumNames = dataCSV[loop0+23]          # 26th line of the file has the names
of the columns
   #display(collumNames)

   #display(dataCSV[loop0+24])            # 27th line is the first row of the table

##################################################################
#
   # Here we read the different columns from the Namirial ISO standard csv file.
```

```
    # the color column is just -Pressure
    # we also calculate the gradient, the 2D velocity and the Force (normilised
output)

    x_1 = []
    y_1 = []
    p_1 = []
    color_1 = []
    t_1 = []
    v_x = []
    v_y = []
    dP = []
    Force = []

    itter = loop0+24
    n=1
    while n <N_max+1 :
        x_1.append(float(dataCSV[itter][1]))  # The input is in the frm of a string
        y_1.append(float(dataCSV[itter][2]))  # so it needs to be converted to float
        p_1.append(float(dataCSV[itter][4]))
        t_1.append(float(dataCSV[itter][3]))
        color_1.append(-float(dataCSV[itter][4]))
        itter=itter + 1
        n=n+1



    step = 0

    v_x.append((x_1[step+1]-x_1[step])/(t_1[step+1]-t_1[step]))
    v_y.append((y_1[step+1]-y_1[step])/(t_1[step+1]-t_1[step]))
    dP.append((p_1[step+1]-p_1[step])/(t_1[step+1]-t_1[step]))

    step = 1

    while step <len(t_1)-1 :
        v_x.append((x_1[step+1]-x_1[step-1])/(t_1[step+1]-t_1[step-1]))
        v_y.append((y_1[step+1]-y_1[step-1])/(t_1[step+1]-t_1[step-1]))
        dP.append((p_1[step+1]-p_1[step-1])/(t_1[step+1]-t_1[step-1]))
        step = step + 1

    step = len(t_1)-1
```

```
    v_x.append((x_1[step]-x_1[step-1])/(t_1[step]-t_1[step-1]))
    v_y.append((y_1[step]-y_1[step-1])/(t_1[step]-t_1[step-1]))
    dP.append((p_1[step]-p_1[step-1])/(t_1[step]-t_1[step-1]))



    step = 0
    while step <len(t_1) :
        if p_1[step] < 256 :
            f_1 = 0.0
        elif dP[step]>0 :
            f_1 = Z_inv_A(p_1[step])
        elif dP[step]==0:
            f_1 = f_1
        else :
            f_1 = Z_inv_D(p_1[step])
        Force.append(f_1)
        step = step + 1

#####################################################################
#
# # # From the imported list we create a DataFrame object to use in the plots
# # # each column is identified by the name given in "frame"

    frame = {'t': t_1, 'x': x_1, 'y': y_1, 'P': p_1, 'color':color_1, 'v_x': v_x, 'v_y': v_y,
'grad_P': dP\
            , 'F_Newt': Force}
    data_frame=pd.DataFrame(data=frame, index=None, columns=None,
dtype=None, copy=False)

    data_frame.reset_index(drop=True, inplace=True)

    #display(data_frame)

    data_frame.to_csv(inputDataFile + str(stepL) + '_output.csv') # saving an
output file
```

Table 6.3 Python code for normalization.

6.3. Application in the banking sector

The calibration and normalization method has been recognized by the banking industry as a necessity, especially in environments where more than one software and hardware solutions have been deployed. The calibration of devices was requested for a specific bank deployment in which a new set of solutions would be integrated together with the pre-existing infrastructure.

The new deployment included two devices, devices (Samsung SM-P610 and Samsung SM-P615) for the purposes of capturing and recording biometric data during contractual agreements; in the same bank environment Wacom STU-530 digitizers were already deployed (running with a different software provider's solution).

For the purposes of examination, the devices were identified according to the following table.

Device Identifier	Device Type
S1	Samsung Tab S6 Lite SM-P610
S2	Samsung Tab S6 Lite SM-P615
SP1	Samsung Galaxy Tab S6 Lite S Pen EJ-PP610BJEGU – default pen for S1
SP2	Samsung Galaxy Tab S6 Lite S Pen EJ-PP610BJEGU – default pen for S2
UP4	Wacom UP61089A1 pen
UP5	Wacom UP6710 pen
LM1	LAMY AL-star black EMR pen Digital Writing
LTW1	LAMY safari twin pen all black EMR Digital Writing

Table 6.4 Examined devices.

The devices were delivered for the evaluation and testing without any type of mounting or support. This form allows for the unobstructed access of the stylus to the active area, in a natural way, rested flat on the working area (desktop), just like in a PPS situation.

These properties are in accordance with the international recommendations for the capturing of biometric data – under the scope of Forensic Handwriting Examination and the examination of authenticity of signatures – as described in the relevant literature (Kalantzis, 2021h). The writer can freely access the active area of the devices without problems, and the size of the active area is big enough to accommodate large sized signature formations without constraints.

Styli SP1 and SP2 that accompany the two digitizers are simple design, relatively lightweight with a polygon shape, and were easily mounted on the experimental array.

As already mentioned on table 6.4 devices S1 and S2 are accompanied by the same model of stylus. Styli S1 and S1 are EMR technology (Electromagnetic Resonance – EMR) and include components manufactured by Wacom. As a result, styli SP1 and SP2 are compatible[13] with a series of digitizers of the same technology manufactured by Wacom (e.g. Wacom STU540, Wacom STU430, Wacom DTU1141b etc.). Similarly, digitizers S1 and S2 are compatible with other Wacom technology styli (e.g. LTW1, UP4 etc.).

The Force channel exhibits 100 pressure levels when captured by the STYLUSIS[14] application, whilst it exhibits 4096 channels when captured with the App GraphoSign application.

[13] See Chapter 5, paragraph 5.1.
[14] Idea Matters (13.05.2018).

Calibration Table

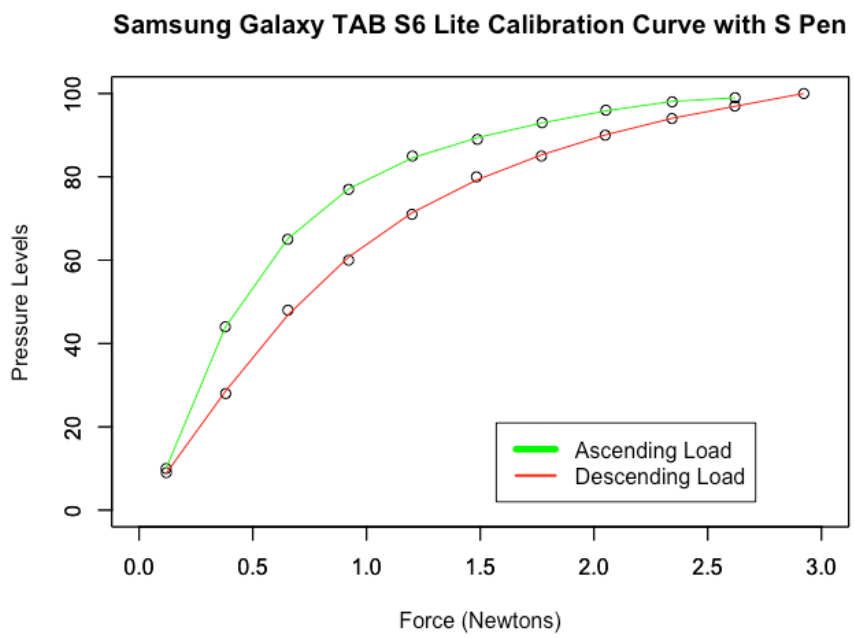

Ascending Load Zeta Function

$$Z_{ascending}(x) = -11171.8 + 53854.8x - 39361.5x^2 + 20839.6x^3 - 7233.7x^4 + 1402.5x^5 - 112.6x^6$$

Ascending Load Inverse Zeta Function

$$Z^{-1}_{ascending}(x) = 2.4 * 10^{-1} + 3.003 * 10^{-5}x + 1.78 * 10^{-9}x^2 - 4.021 * 10^{-13}x^3 + 3.775 * 10^{-17}x^4 - 1.4 * 10^{-21}x^5 + 1.929 * 10^{-29}x^6$$

Descending Load Zeta Function

$$Z_{descending}(x) = -18194.85 + 90717x - 86913.56x^2 + 50382.41x^3 - 17114.54x^4 + 3121.29x^5 - 235.66x^6$$

Descending Load Inverse Zeta Function

$$Z^{-1}_{descending}(x) = 4.584 * 10^{-1} - 2.02 * 10^{-4}x + 6.317 * 10^{-8}x^2 - 7.477 * 10^{-12}x^3 + 4.277 * 10^{-16}x^4 - 1.163 * 10^{-20}x^5 + 1.22 * 10^{-25}x^6$$

Figure 6.2 Calibration Table.

The relation of writing force / measurements on the F channel was normalized using the STYLUSIS[15] application, by applying the method exhibited on Chapter 6. The calibration of digitizer S1 with stylus SP1 produces the same Zeta function as the one for digitizer S2 with stylus SP2.

The calculation of the Zeta function allows the transition from Pressure Levels (either 100 or 4096, depending how these are captured) to physical units (i.e. Newtons in the SI system). With this method, the F data channel measurements of the biometric data can be normalized in the SI system and therefore compared with data captured by other solutions (which follow a different Zeta function) that have also been normalized.

Tests and measurements carried out with the Graphologist application proved that the exercised force is recorded following the same Zeta[16] function as in the case of the STYLUSIS app and therefore the same calculated functions presented on Table 3 are valid for the applications tested in this report.

Devices S1 and S2 will be tested and evaluated as per the software application that will run within the bank environment deployment. The devices that were delivered for testing, included the specific bank application, and subsequently the testing application "Graphologist" was provided as a tool to record and access

[15] Idea Matters (13.05.2018).
[16] See paragraph 2.4.

captured biometric data, in the same manner as with the bank dedicated application.

The F channels values are produced in percentage, with accuracy of two digits. This percentage refers to the maximum sensitivity value of the pressure sensor, and constitutes a "normalization" according to the equation $Force\ Values\ P[\%] = \frac{Raw\ Data\ Values}{4096}$.

If normalization of the percentage to Newtons is required, then the values will have to be normalized according to the calculated Zeta Functions (and their inverse), as presented in Figure 6.2.

As it has already been mentioned, digitizers S1 and S2 and styli SP1 and SP2 that accompany them, are EMR technology and are partially manufactured/supplied by Wacom; therefore, they exhibit interoperability with other parts that use the same technology.

This means that there is a vast selection of compatible styli that can be chosen for use or replacement of the S pen (styli SP1 and SP2), depending on the context of use. Calibration of the digitizers S1 and S2 with a series of compatible styli was performed (see Table 6.4). Styli UP5, Up4, LM1 and LTW1 worked with the S1 and S2 digitizers without problems. These styli were calibrated, and the corresponding Zeta functions are included in the Appendix.

The examined solution was subsequently deployed parallel to a pre-existing deployment for the capturing of DCS, which uses the STU530 digitizer and the

UP4 stylus. The preexisting solution captures biometric data adequately (see Appendix), and the accompanying software can produce the captured data in similar units (i.e. X and Y channel data in mm, T channel data in sec and F channel data in percentage). It should be stated that stylus UP4 obeys (Kalantzis, 2021i) a different Zeta function than styli SP1 and SP2, which means that the same percentage for Force data corresponds to a different exercised force per device. To achieve compatibility of the devices and comparability of data captured from both solutions, the corresponding Zeta functions and their inverse can be used either to normalize the values in percentages or to transform the values of both solutions to Newtons.

6.4. Necessity of calibration

The calibration of devices for the purposes of establishing a normalization method can also reveal errors in deployment, either hardware or software related (or both). During application of the method for calibration and testing of deployed solutions, two commercially deployed solutions that had errors in their original form were discovered, and were then corrected by their providers. The first case refers to a hardware issue that was discovered during the calibration of the Force Channel data. The second case refers to a software issue that caused corrupted data capturing even though the hardware component was functioning according to specifications. For legal reasons the hardware of the first case will be

anonymized and referred to as Digitizer 1 with the testing software referred to as Software 1, and the software of the second case will be anonymized and referred to as Software 2.

6.4.1. Case 1: Hardware error

6.4.1.1. Method

In this deployment case, the suitability of Hardware 1 run with Software 1 was investigated. Hardware 1 was an Electromagnetic Resonance (EMR) DCS solution. Part of the investigation involved the examination of the Force channel data capturing capabilities and the calibration and the normalization of this solution, according to the available method presented in Chapter 5.

6.4.1.2. Results

During calibration of the F Channel data, an error was detected; specifically, when Force reached a specific value, a "anomaly" would appear in the assigned Pressure Level values (see Figure 6.3).

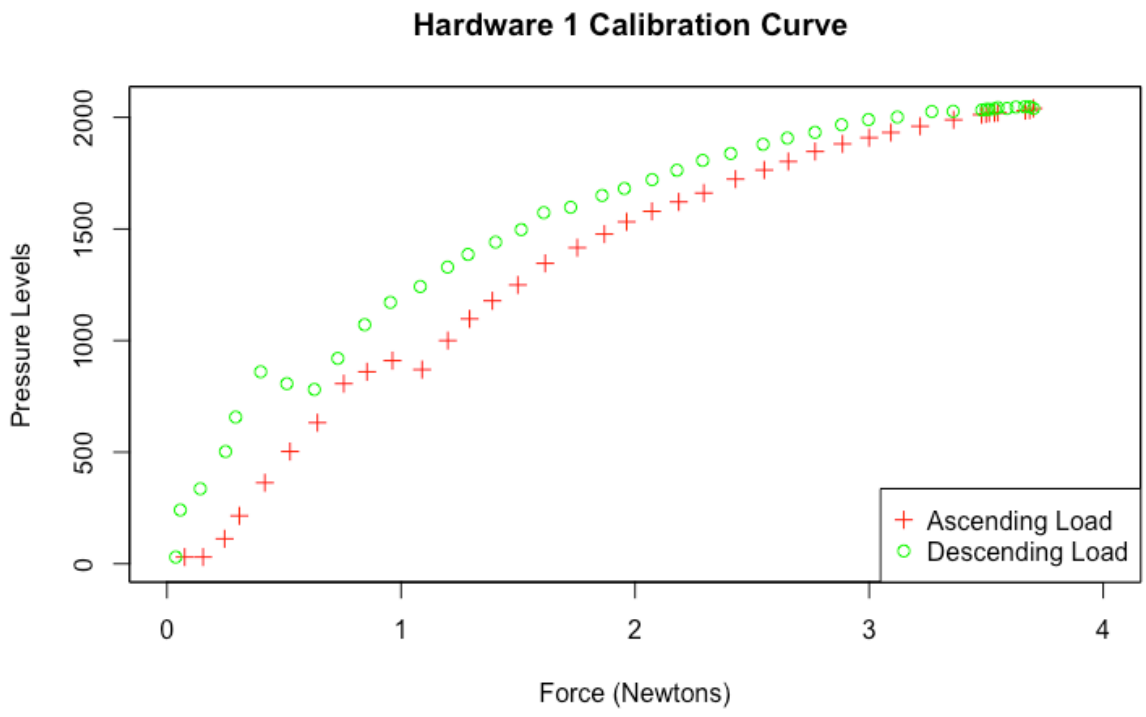

Figure 6.3 Calibration measurements.

As can be seen in detail in Figure 2 and in the raw data in Table 1, there is a point in the ascending load calibration (Force = 0.821 N) and a different point in the descending load calibration (Force = 0.758 N) where a "anomaly" is observed. In the ascending load part, the assigned Pressure Level values fall from 790 for 0.798

N to 643 for 0.821 (when they should be only increasing), and for the descending load part, the assigned Pressure Level values jump from 640 for 0.774 N to 790 for 0.758 (when they should be only increasing).

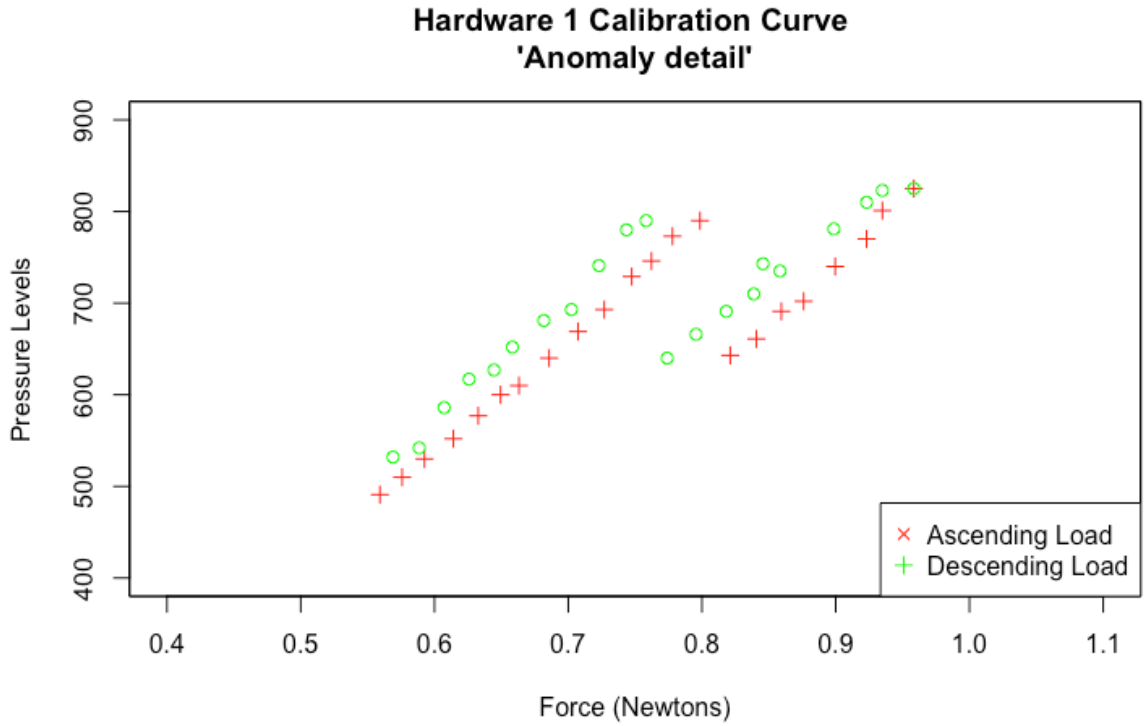

Figure 6.4 Calibration measurements – anomaly.

This is a serious problem because the same Pressure Level values are assigned to two different exercised force values, as can be observed on Figure 6.4 (e.g. for Pressure Level 700 there are two different Force values).

This error also affects the calculation of a Zeta Function for Hardware 1. DCS solutions provide the Force Channel data in arbitrary Pressure Levels; in order for those Pressure Levels to be comparable between different DCS solutions, it is necessary to calibrate the devices and calculate the Zeta Function, i.e. the

Function that calculates the assigned Pressure Levels from the exercised force. From the Zeta Function, the inverse Zeta Function can then be calculated which can provide the originally exercised force from the assigned Pressure Levels, thus normalizing the Force Channel data into Newtons. In this case, the assignment of the same Pressure Levels to more than one Force values render the Zeta Function for Hardware 1 a non one-to-one function, which subsequently means that there can be no inverse Zeta Function calculated. Consequently, the assigned Pressure Levels cannot accurately be normalized into Force values in Newtons.

These findings were communicated to the manufacturer of the hardware, and after a series of testing the firmware of the digitizer was identified as the source of the error, and it was updated to accommodate for this error.

6.4.2. Case 2: Software Error

6.4.2.1. Method

In this deployment case, the suitability of a Samsung SM-P610 Galaxy S6 Lite (and the corresponding S pen stylus) was investigated for the purposes of capturing and recording biometric data within a banking environment. The (already deployed) software is identified as “Software 2” and was an Android application

installed on the device. Furthermore, two additional applications were installed in the device for calibration and testing purposes, namely Namirial's GraphoSign App and IdeaStorm Labs' Stylusis App.

6.4.2.2. Results

During the initial testing and evaluation of the solution two errors were detected. The Samsung SM-P610 Galaxy S6 Lite uses Wacom technology (Harley *et al*., 2014) for the stylus applications, and therefore other Wacom component styli are compatible. The compatible styli used for testing are mentioned in Table 6.5

Device Identifier	Device Type
SP1	Samsung Galaxy Tab S6 Lite S Pen EJ-PP610BJEGU
UP4	Wacom UP61089A1 pen
UP5	Wacom UP6710 pen
LM1	LAMY AL-star black EMR pen Digital Writing
LTW1	LAMY safari twin pen all black EMR Digital Writing

Table 6.5 Tested devices.

6.4.2.2.1. Error 1: No capturing of In Air Trajectories

Testing and measurements that were conducted with Software 2 showed that the movement of the stylus on air (i.e. without the tip of the stylus being in contact with the glass surface of the digitizer), a.k.a. In Air Trajectories (IATs) was not captured, even though the digitizer technology of the hardware is EMR and supports it. Further testing of the same device with the application Namirial GraphoSign App proved that the device and its stylus were able to capture IATs; therefore it was deducted that the source of the problem was the software.

As mentioned in the relevant international literature (ENFSI, 2022; Geistová Čakovská *et al*., 2021), examination of the IATs is an important part of the process for the determination of authenticity of a DCS, and capturing IATs constitutes one of the main advantages of EMR technology; therefore, IATs should be captured. These findings were communicated to the software manufacturer, and the error was corrected in a subsequent version update of Software 2.

6.4.2.2.2. Error 2: Observation of discontinuity

During testing discontinuity of the capturing of events with Software 2 was observed when the stylus remained static or slowed down. This situation is reflected in the captured data, exhibiting large segments of loss, but also in the visual feedback provided by the applications (see Figure 6.5).

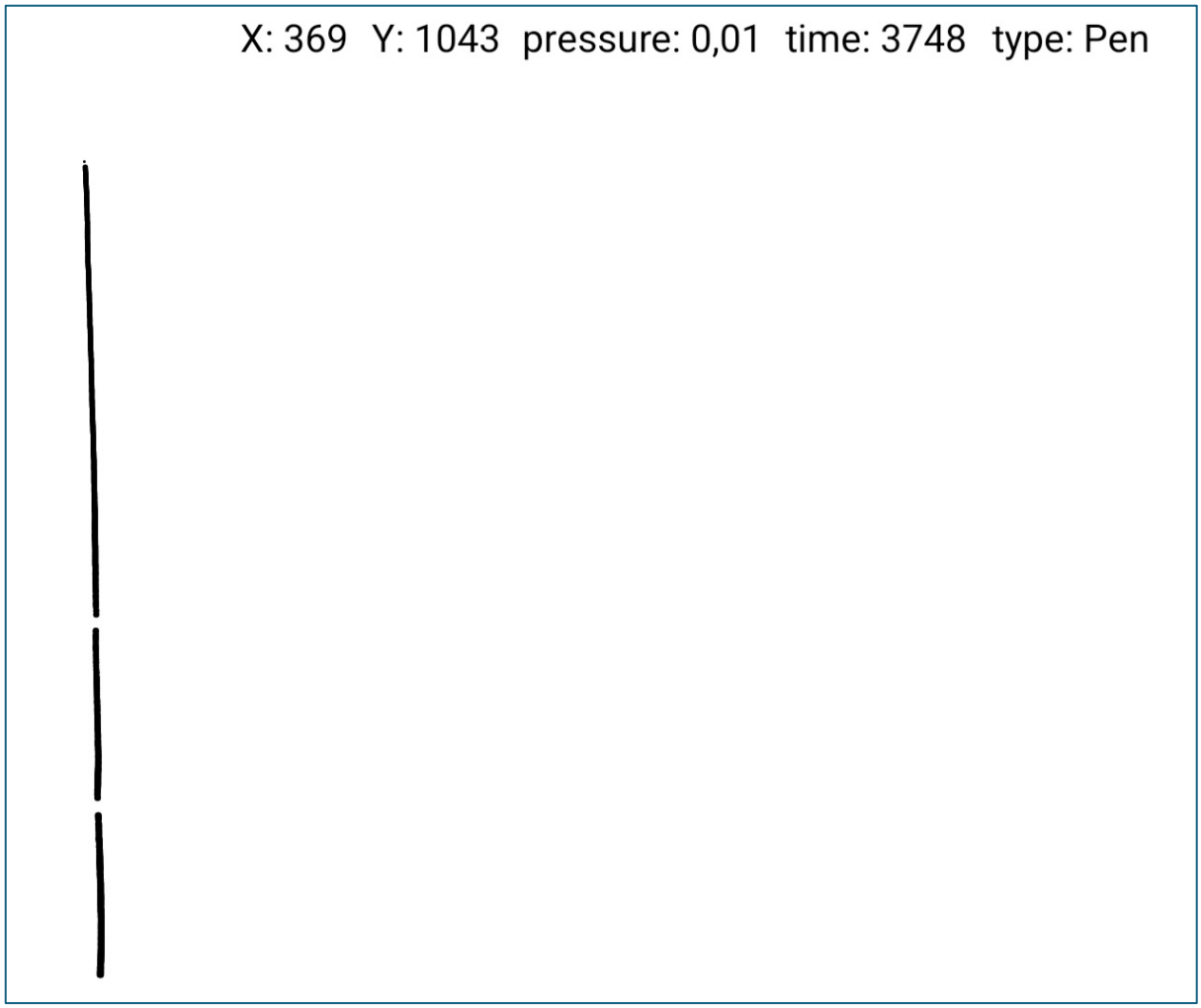

Figure 6.5 Observation of discontinuity in line executed without loss of contact.

Figure 6.5 depicts the visualization of a straight line executed in one stroke, i.e. without lifting the tip of the stylus from the glass surface of the digitizer, as captured with Software 2 on Samsung SM-P610 Galaxy S6 Lite with its stylus. It can be observed that the segments appear as if without contact of the tip of the stylus. This artefact constitutes a big problem as the motion of the stylus during the execution of the signature movement is not faithfully captured and represented in the data and cannot be accurately reconstructed from them. The same

phenomenon was observed during testing with volunteer writers executing their normal signature formation (see Figure 6.6).

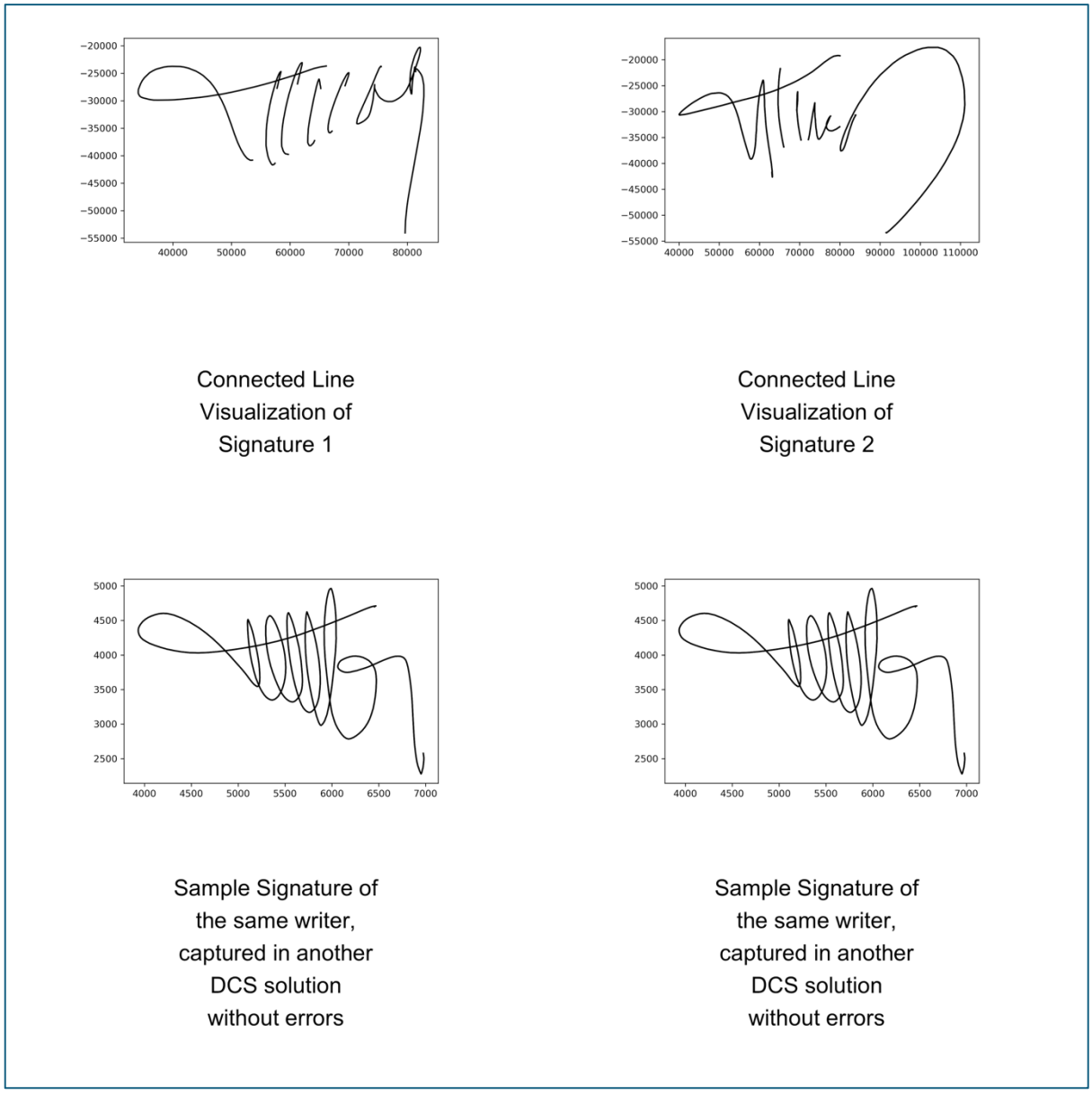

Figure 6.6 Comparison of DCS samples.

As observed on Figure 6.6, two signatures of the same writer exhibit the discontinuity and appear as if executed in 5 and 6 strokes respectively. This

behaviour is differentiated from the normal behaviour of the writer who executes their normal signature in one stroke only, as can be observed from samples captured with other solutions. The signature of the specific writer is executed in one stroke on paper as well and therefore these “breaks” in the continuity of the stroke are artefacts for the tested solution.

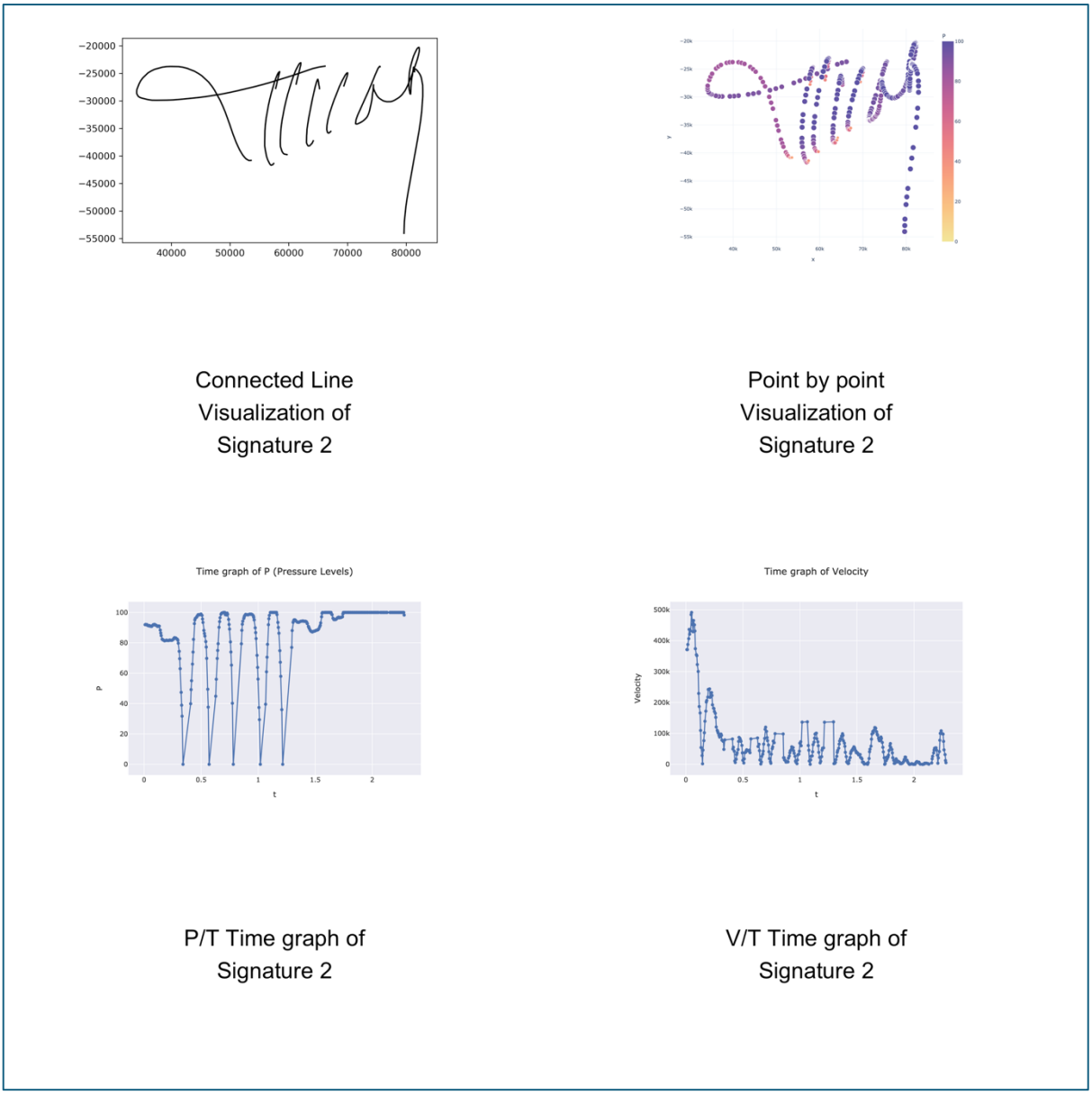

Figure 6.7 Visualizations of Test Signature 2.

As can be observed on Figures 6.7 and 6.8, this solution not only does not record events whilst the stylus is slowing down, but also introduces zero force artefacts in the data, creating the illusion of change of stroke number – which explains the large temporal gaps in the data. Apparently, Software 2 considers the stylus to have been removed away from the active area and stops recording its positions.

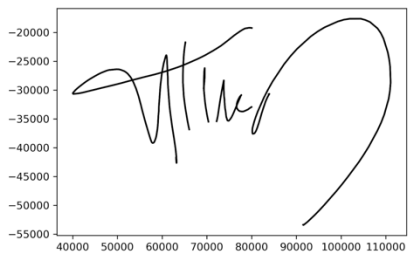

Connected Line Visualization of Signature 2

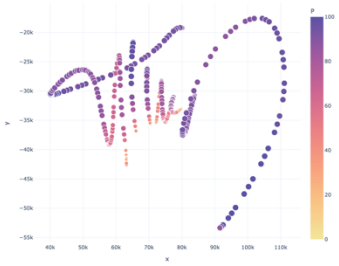

Point by point Visualization of Signature 2

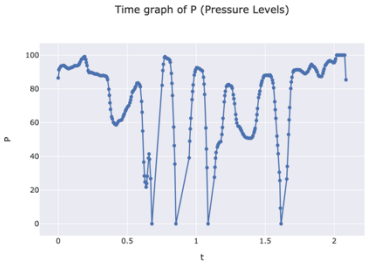

P/T Time graph of Signature 2

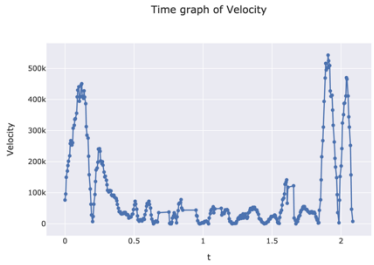

V/T Time graph of Signature 2

Figure 6.8 Visualizations of Reference signature 2.

Observation of these characteristics and the corresponding visualizations of the reference samples of the same writer prove that these findings cannot be attributed to the writer but are due to the software.

Repeated testing with Software 2 with a Samsung SM-P610 Galaxy S6 Lite stylus (S pen) but also with other Wacom Styli (UP4, UP6, LM1 and LTW1) exhibited the same behaviour, proving that the stylus was not the source of the error.

To determine the source of the problem, testing was carried out with software from a different manufacturer, and specifically App Graphosign, and this error was not observed. This finding pinpoints the source of error to Software 2. This defect was also communicated to the software manufacturer and was corrected with the subsequent version of the app (see Figures 6.9 and 6.10).

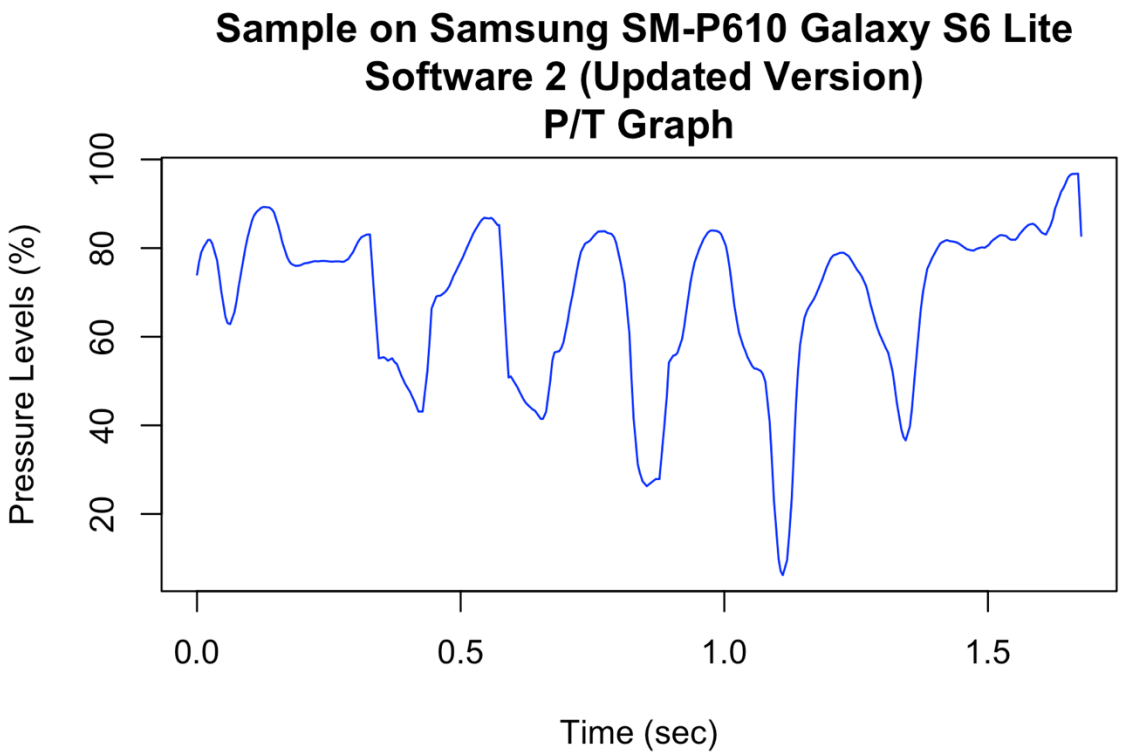

Figure 6.9 Pressure Levels / Time graph – updated version.

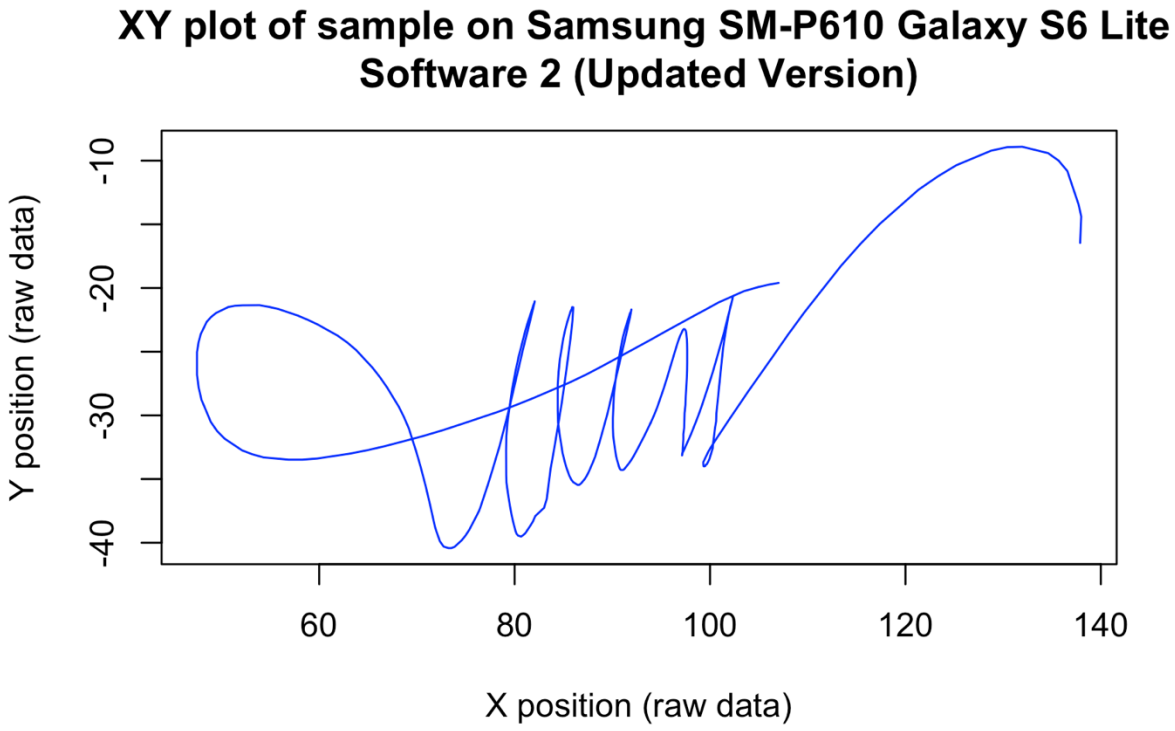

Figure 6.10 XY plot – updated version.

6.4.2.2.3. Error 3: Loss of events on T channel

The T channel shows a variable frequency of capturing events with a minimum value of 3 msec and maximum value of 13 msec. This type of variable frequency is typical for standalone digitizers as the clock used is that of the processor of the tablet (e.g. iPad Pro). As a result of the errors mentioned previously, incidents of large gaps in time capturing were observed, with events captured as far as 40 msec apart. This finding is not observed with the updated version of Software 2 that corrected the previously mentioned errors.

6.4.3. Discussion

The accuracy of the captured data in all data channels (X, Y, F and T) is clearly a very important aspect in the forensic examination of authenticity of DCS. As it was shown, the evaluation of the suitability of two already deployed DCS solutions and the calibration of the Force data channel led to the discovery of serious errors in the accuracy and fidelity of the captured data.

In the case of Hardware 1, the calibration revealed a serious error in the assignment of Pressure Levels, that allowed the same value to be assigned for two different Force values, and hence not allowing a faithful visualization of the exercise Force, nor the calculation of the inverse Zeta Function (which would be required for the normalization of Pressure Level values to Newtons).

In the case of the Samsung SM-P610 Galaxy S6 Lite with Software 2, several errors were uncovered that may impact the validity of expert opinions on the authenticity of DCS.

It is already mentioned that not recording IATs hinders the application of the established scientific methodology for the determination of authenticity of biometric signature. Furthermore, the discontinuity error by default shows inadequate capturing of the handwriting motion and subsequent erroneous visualizations of the signing product.

In both examples, the evaluation and calibration of the deployed solution by forensic scientists was necessary to reveal aspects of their validity (or lack of). It is clear that this should be considered a standard practice in the deployment of DCS solutions, but more importantly it should be clear that the investigation of the accuracy of a given deployed solution is necessary for the accurate interpretation of the captured DCS data from the forensic examiner. In the case of the Samsung SM-P610 Galaxy S6 Lite, the hardware itself was not malfunctioning, but Software 2 was; meaning that the inclusion of a trusted and tested hardware in a given DCS solution does not necessary mean that the solution in its entirety is trusted (if it is not properly tested).

6.5 Linear or logarithmic?

It was observed how the dynamic parameter of signing – the Z axis coefficient – can be quantified either in a pseudo logarithmic way (when expressed in pressure levels for EMR solutions) or in a linear way (when normalized in Newtons). Furthermore, it was established that in order to proceed with the forensic examination of authenticity of DCS, in correspondence to the method used for PPS, the FHE has to engage in the production and examination of multiple different visualizations – all derived from X, Y, F and T data – to have access to the same level of information as with PPS. But which mode of representation of the Z axis coefficient of writing is best for this task?

As the study of “pressure” in the traditional method of PPS examination has been based on qualitative examination of the ink dispersion and paper surface deformation under magnification, there is no theoretical model that can be employed to answer this question.

During delivery of a workshop on the use of the Zeta Function (Kalantzis, 2021h), 51 FHEs were given two PPS signature samples from different authors to evaluate as per their dynamics and “pressure profile”, and each FHE received a different sample per author. These samples were actually hybrid DCS samples, i.e. they were executed oon paper and in DCS recorded. After examination of the paper version of the signatures, the FHEs were asked to write down their observations (to commit) and then they were given XY point by point visualizations of the same signatures, with association of colour as per their F data channel values, in both unnormalized (pseudo logarithmic) and normalized (linear) modes. The FHEs were then asked to re-evaluate their opinion regarding the dynamics of their signature samples and complete an online questionnaire.

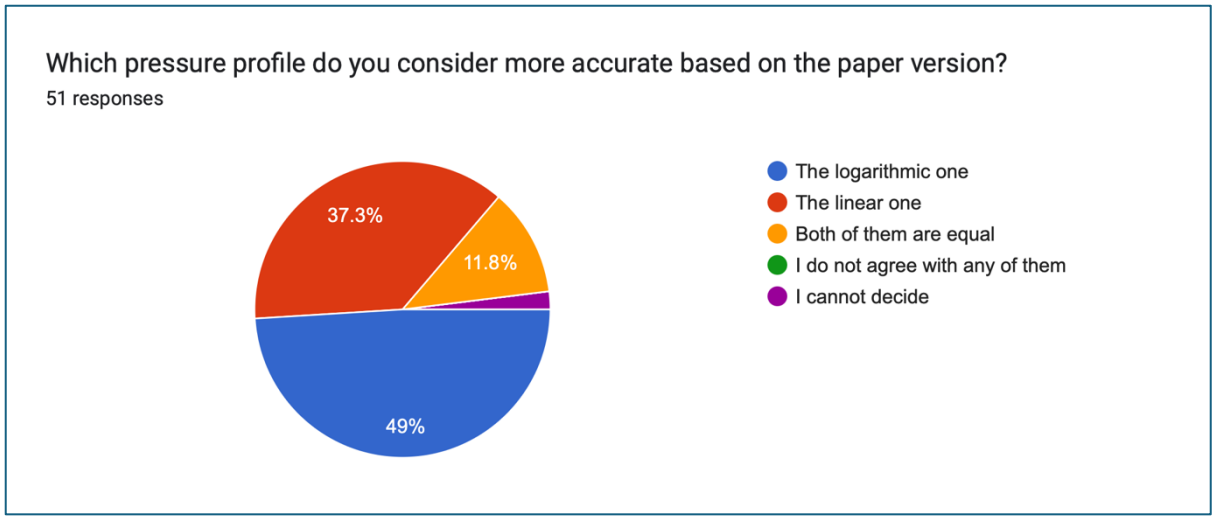

Figure 6.11 Sample 1

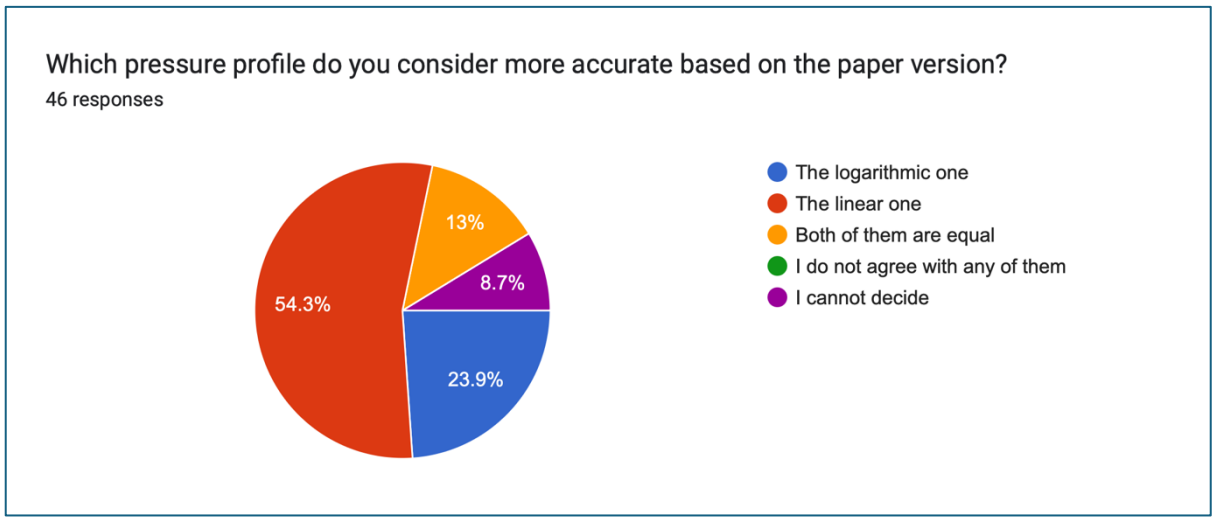

Figure 6.12 Sample 2

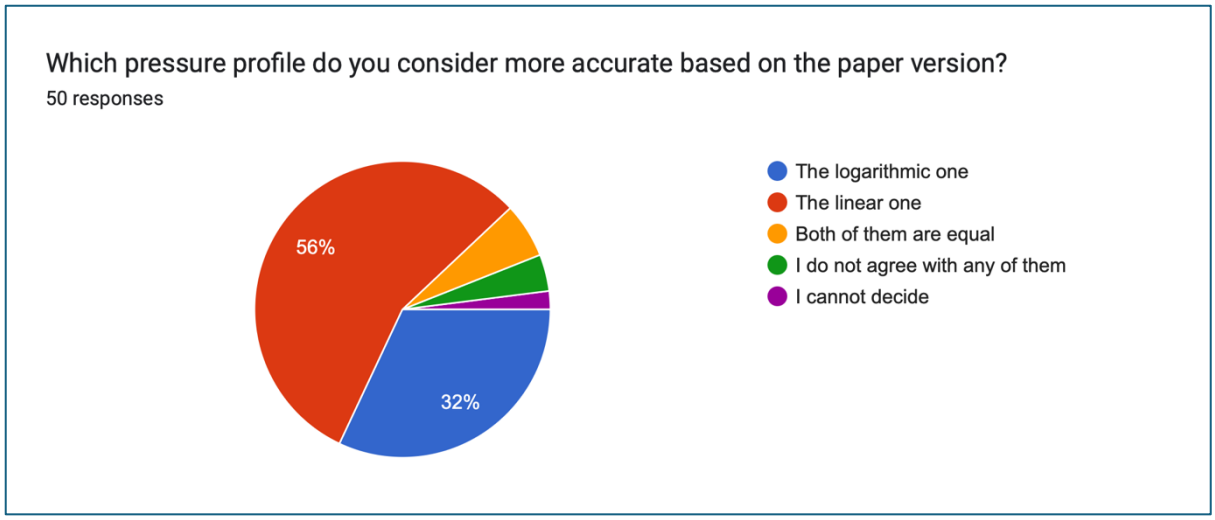

Figure 6.13 Sample 3

Looking at the responses (figures 6.11 – 6.13) there is a preference towards the linear one in two out of three samples.

In another workshop (Kalantzis, 2021i), 13 FHEs examined one sample and gave a clear preference to the logarithmic one.

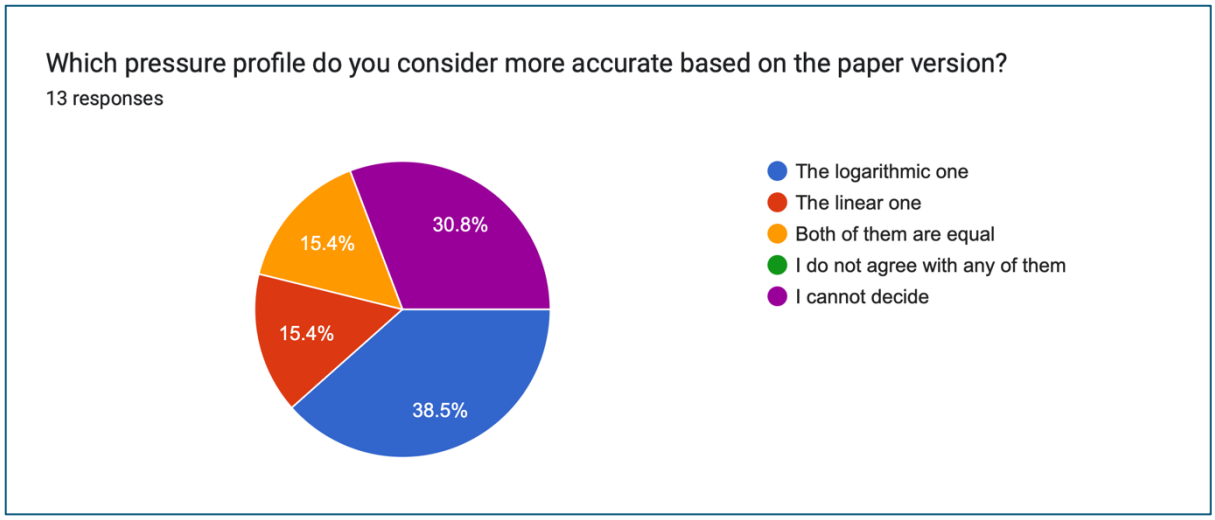

Figure 6.14

The argument can be made for the preference towards the logarithmic visualization as the logarithmic nature of the intensity of human sensation according to Fechner's law may be reflected in the writing product (Kalantzis, 2021f). The relationship between external stimuli and human perception is logarithmic and therefore this could be reflected in the writing product and hence identified by the FHEs.

On the other hand, as signature samples from different authors were used, the preference may be connected to the dynamics of the signature sample – different per author.

This is an aspect of the (now quantified) dynamics of signature execution that should be investigated further.

6.6. Chapter 6 References

Kalantzis, N. (2020) 'The question of comparability of digitally captured signatures from the aspect of normalization & stability of used hardware/software solutions', paper presented at the 78th Annual General Meeting of the American Society of Questioned Document Examiners (ASQDE), 10–14 August, Virtual.

Kalantzis, N. (2021a) 'Normalization and comparability of digitally captured signatures (DCS)', paper presented at the American Academy of Forensic Sciences 73rd Annual Scientific Meeting, 15–19 February, Virtual.

Kalantzis, N. (2021b) 'Pressure measurements in DCS: A study of Wacom STU530 & STU540 digitizers', paper presented at the Australasian Society of Forensic Document Examiners Inc. 2021 Annual Scientific Meeting, 24–28 May, Virtual.

Kalantzis, N. (2021c) 'Training workshop on the analysis, comparison and evaluation of digitally captured signatures', ENFHEX 13th Conference & Business Meeting, 16–18 June, Virtual.

Kalantzis, N. (2021d) 'Alternative styli for DCS execution: A study of the LAMY Al-star black EMR stylus', ENFHEX 13th Conference & Business Meeting, 16–18 June, Virtual.

Kalantzis, N. (2021e) 'Studying pressure through DCS technology: A gateway to population data', ENFHEX 13th Conference & Business Meeting, 16–18 June, Virtual.

Kalantzis, N. (2021f) 'An in-depth exploration of pressure measurements and force recording factors in EMR technology digitizers', 2nd International Webinar on Forensic Research and Toxicology, 15–16 July, Virtual.

Kalantzis, N. (2021g) 'Use of 3rd party EMR styli for digitally captured signature execution: A study of the LAMY Al-star black EMR stylus', 2nd International Webinar on Forensic Research and Toxicology, 15–16 July, Virtual.

Kalantzis, N. (2021h) 'Pressure measurements in DCS: A study of Wacom STU530 & STU540 digitizers (with a twist)', paper presented at the 5th International Conference of the Arab Society for Forensic Sciences and Forensic Medicine, 23–25 November, Riyadh, Saudi Arabia.

Kalantzis, N. (2021i) 'Evaluating pressure: Recalibration of the expert's analysis of writing pressure with the use of DCS technology', workshop presented at the 5th International Conference of the Arab Society for Forensic Sciences and Forensic Medicine, 23–25 November, Riyadh, Saudi Arabia.

Kalantzis, N. and Platt, A.W.G. (2020) 'Digitally captured signatures (biometric signatures) and forensic handwriting examination: A short introduction', *Penal Justice/Ποινική Δικαιοσύνη*, 10, pp. 1006–1012.

Kalantzis, N. and Platt, A.W.G. (2022) 'Digitally captured signatures: A method for the normalization of force through calibration and the use of the zeta function', *Journal of Forensic Sciences*, 67, pp. 651–668. doi:10.1111/1556-4029.14927.

Kalantzis, N. (2022a) 'Pressure evaluation training & calibration workshop: Application of digitally captured signature technology to everyday casework', ENFHEX 14th Conference, 21–23 September, Zagreb, Croatia.

Kalantzis, N. (2022b) 'Zeta function and the normalization of pressure levels to Newtons: Looking at the truly exercised force of writing', ENFHEX 14th Conference, 21–23 September, Zagreb, Croatia.

Kalantzis, N. (2023) 'Setting up laboratories to deal with & take advantage of DCS technology', Ras Al Khaimah First International Forensic Sciences Conference, 30 October–1 November, Ras Al Khaimah, UAE.

European Network of Forensic Science Institutes (2022) *Best practice manual for the forensic handwriting examination (ENFSI-BPM-FHX-01)*. Wiesbaden: ENFSI.

Zimmer, J. *et al.* (2021) 'The challenge of comparing digitally captured signatures registered with different software and hardware', *Forensic Science International*, 327, p. 110945. doi:10.1016/j.forsciint.2021.110945.

Dzieździc, T. and Ferenc, A. (2020) 'Evaluation of the suitability of digitally captured signatures collected in the Electronic Confirmation of Receipt program for forensic handwriting examination', *Problems of Forensic Sciences*, 122–123, pp. 89–109.

Dziedzic, T. and Radwan, K. (2024) 'A tool for automatic normalization of DCS force data', paper presented at ENFHEX 2024 Conference, Stockholm, Sweden.

Namirial (no date) *Forensic Release Notes (Version 1.2.7.6)*.

Harley, J.A. *et al.* (2014) *United States Patent No. US 8,638,320 B2*.

Geistová Čakovská, B. *et al.* (2021) 'Recommendations for capturing signatures digitally to optimize their suitability for forensic handwriting examination', *Journal of Forensic Sciences*, 66, pp. 743–747. doi:10.1111/1556-4029.14627.

Appendix – Calibration Tables

Equipment Technical Report			
Tablet Manufacturer	Samsung	Model	Galaxy S6 Lite
Stylus Manufacturer	Samsung	Model	S6
Software used for measurements		STYLUSIS	
# Pressure Levels		100 (4096 normalized as 100 levels)	
Tilt Capture	No	In Air Trajectory Capture	Yes
Minimum Force Threshold (Newtons)	0.12	Maximum Force Threshold (Newtons)	3.61
Ascending Load Zeta Function			
$Z_{ascending}(x) = -11171.8 + 53854.8x - 39361.5x^2 + 20839.6x^3 - 7233.7x^4 + 1402.5x^5 - 112.6x^6$			
Ascending Load Inverse Zeta Function			
$Z^{-1}_{ascending}(x) = 2.4 * 10^{-1} + 3.003 * 10^{-5}x + 1.78 * 10^{-9}x^2 - 4.021 * 10^{-13}x^3 + 3.775 * 10^{-17}x^4 - 1.4 * 10^{-21}x^5 + 1.929 * 10^{-29}x^6$			
Descending Load Zeta Function			
$Z_{descending}(x) = -18194.85 + 90717x - 86913.56x^2 + 50382.41x^3 - 17114.54x^4 + 3121.29x^5 - 235.66x^6$			
Descending Load Inverse Zeta Function			
$Z^{-1}_{descending}(x) = 4.584 * 10^{-1} - 2.02 * 10^{-4}x + 6.317 * 10^{-8}x^2 - 7.477 * 10^{-12}x^3 + 4.277 * 10^{-16}x^4 - 1.163 * 10^{-20}x^5 + 1.22 * 10^{-25}x^6$			

Appendix Table 1 Technical Report

Calibration Curve
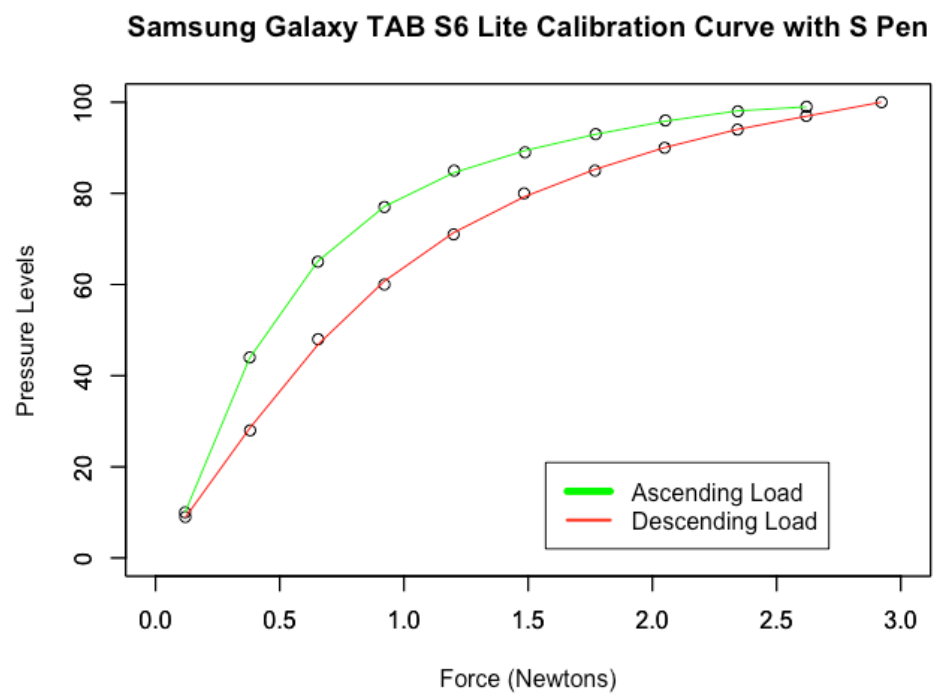
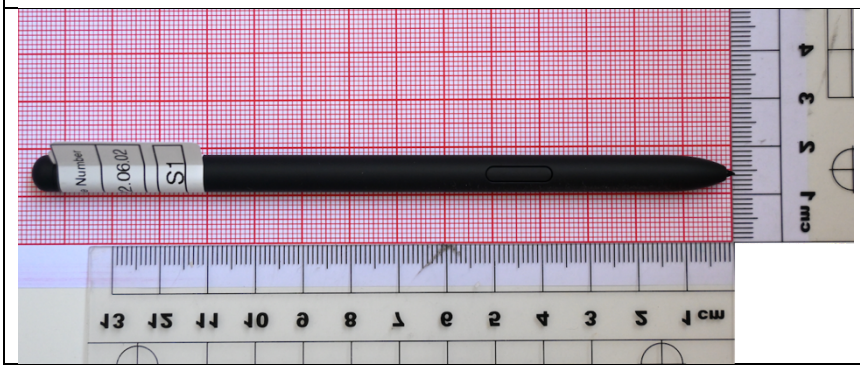

Appendix Table 2 Calibration Curve

Equipment Technical Report

Tablet Manufacturer	Samsung	Model	Galaxy S6 Lite
Stylus Manufacturer	Wacom	Model	UP61089A1
Software used for measurements		STYLUSIS	
# Pressure Levels		100 (4096 normalized as 100 levels)	
Tilt Capture	No	In Air Trajectory Capture	Yes
Minimum Force Threshold (Newtons)	0.37	Maximum Force Threshold (Newtons)	3

Ascending Load Zeta Function

$$Z_{ascending}(x) = -39.017 + 148.329x - 17.56x^2 - 81.763x^3 + 67.685x^4 - 21.196x^5 + 2.37x^6$$

Ascending Load Inverse Zeta Function

$$Z^{-1}_{ascending}(x) = 5.718 - 9.462 * 10^{-1}x + 5.688 * 10^{-2}x^2 - 1.602 * 10^{-3}x^3 + 2.338 * 10^{-5}x^4 - 1.708 * 10^{-7}x^5 + 4.95 * 10^{-10}x^6$$

Descending Load Zeta Function

$$Z_{descending}(x) = -30.501 + 175.243x + 36.688x^2 - 224.117x^3 + 173.405x^4 - 54.929x^5 + 6.368x^6$$

Descending Load Inverse Zeta Function

$$Z^{-1}_{descending}(x) = 1.115 * 10 \quad - 2.748x + 1.834 * 10^{-1}x^2 - 5.306 * 10^{-3}x^3 + 7.657 * 10^{-5}x^4 - 5.434 * 10^{-7}x^5 + 1.517 * 10^{-9}x^6$$

Appendix Table 3 Technical Report

Calibration Curve
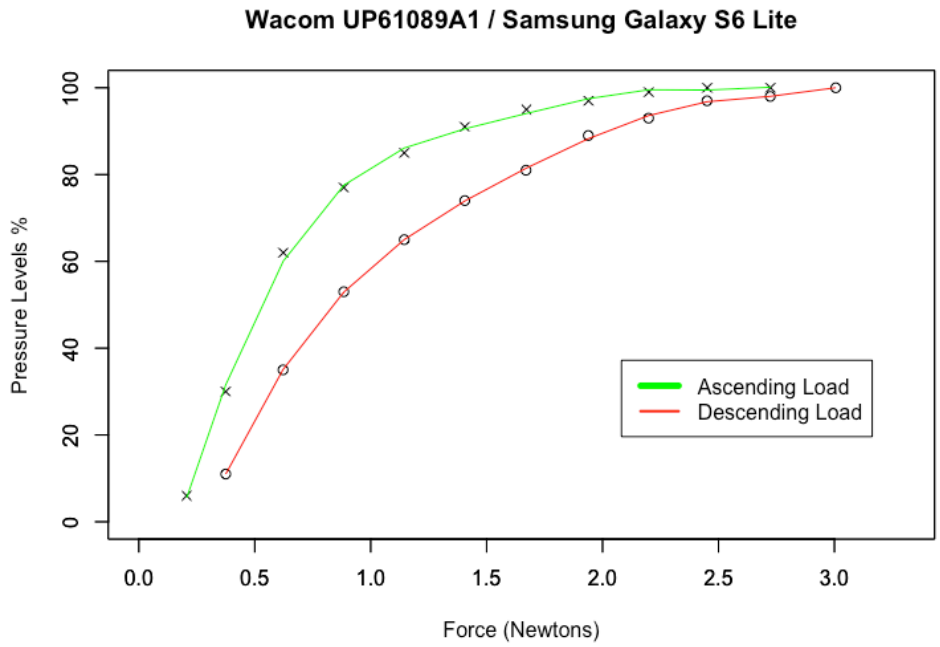
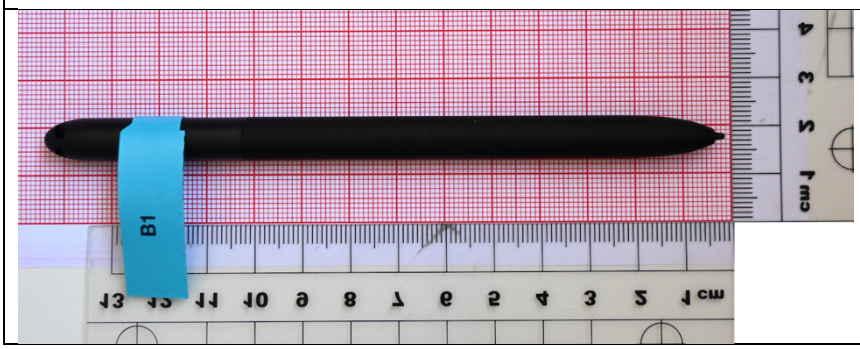

Appendix Table 4 Calibration Curve

Equipment Technical Report

Tablet Manufacturer	Samsung	Model	Galaxy S6 Lite
Stylus Manufacturer	Wacom	Model	UP6710
Software used for measurements		STYLUSIS	
# Pressure Levels		100 (4096 normalized as 100 levels)	
Tilt Capture	No	In Air Trajectory Capture	Yes
Minimum Force Threshold (Newtons)	0.2	Maximum Force Threshold (Newtons)	2.67

Ascending Load Zeta Function

$$Z_{ascending}(x) = -27.95 + 186.385x - 220.782x^2 + 210.393x^3 - 118.209x^4 + 33.655x^5 - 3.753x^6$$

Ascending Load Inverse Zeta Function

$$Z^{-1}_{ascending}(x) = 1.802 * 10^{-1} + 9.787 * 10^{-3}x - 1.341 * 10^{-4}x^2 + 9.319 * 10^{-6}x^3 - 1.606 * 10^{-7}x^4 + 1.093 * 10^{-9}x^5 - 1.336 * 10^{-12}x^6$$

Descending Load Zeta Function

$$Z_{descending}(x) = -43.04 + 333.93x - 594.04x^2 + 713.92x^3 - 474.57x^4 + 156.66x^5 - 20.07x^6$$

Descending Load Inverse Zeta Function

$$Z^{-1}_{descending}(x) = 2.52 * 10^{-1} - 1.377 * 10^{-2}x + 1.368 * 10^{-3}x^2 - 4.135 * 10^{-5}x^3 + 7.327 * 10^{-7}x^4 - 6.994 * 10^{-9}x^5 + 2.794 * 10^{-11}x^6$$

Appendix Table 5 Technical Report

Calibration Curve
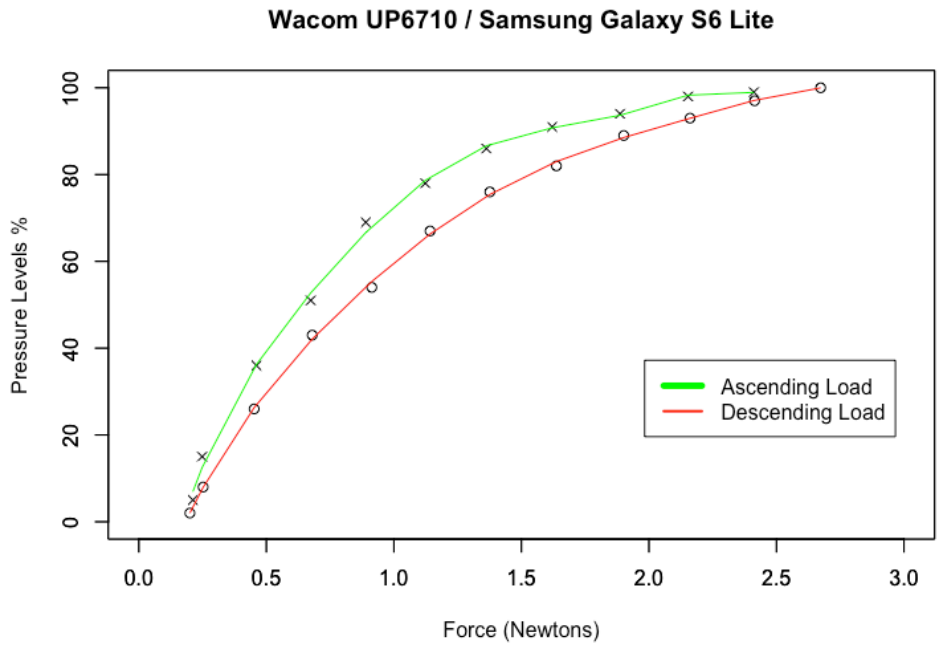
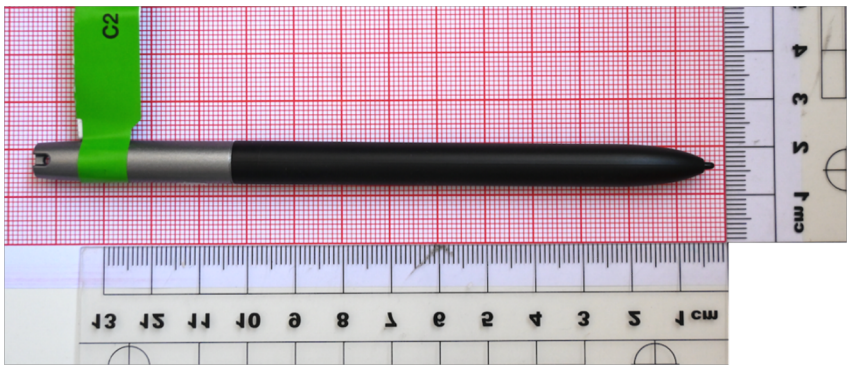

Appendix Table 6 Calibration Curve

Equipment Technical Report

Tablet Manufacturer	Samsung	Model	Galaxy S6 Lite
Stylus Manufacturer	Lamy	Model	Al-Star Black EMR (Glossy Surface)
Software used for measurements		STYLUSIS	
# Pressure Levels		100 (4096 normalized as 100 levels)	
Tilt Capture	No	In Air Trajectory Capture	Yes
Minimum Force Threshold (Newtons)	0.3	Maximum Force Threshold (Newtons)	3.68

Ascending Load Zeta Function

$$Z_{ascending}(x) = -1.859 + 41.7373x + 93.1571x^2 115.4016x^3 + 53.4598x^4 - 11.2732x^5 + 0.9026x^6$$

Ascending Load Inverse Zeta Function

$$Z^{-1}_{ascending}(x) = -6.477 * 10^{-2} + 4.792 * 10^{-2}x - 2.653 * 10^{-3}x^2 + 9.48 * 10^{-5}x^3 - 1.711 * 10^{-6}x^4 + 1.498 * 10^{-8}x^5 - 4.806 * 10^{-11}x^6$$

Descending Load Zeta Function

$$Z_{descending}(x) = -26.1183 + 261.8627x - 282.2287x^2 + 169.7686x^3 - 56.1098x^4 + 9.4886x^5 - 0.6391x^6$$

Descending Load Inverse Zeta Function

$$Z^{-1}_{descending}(x) = 1.275 * 10 \quad - 2.726x + 1.589 * 10^{-1}x^2 - 4.169 * 10^{-3}x^3 + 5.602 * 10^{-5}x^4 - 3.773 * 10^{-7}x^5 + 1.015 * 10^{-9}x^6$$

Appendix Table 7 Technical Report

Calibration Curve
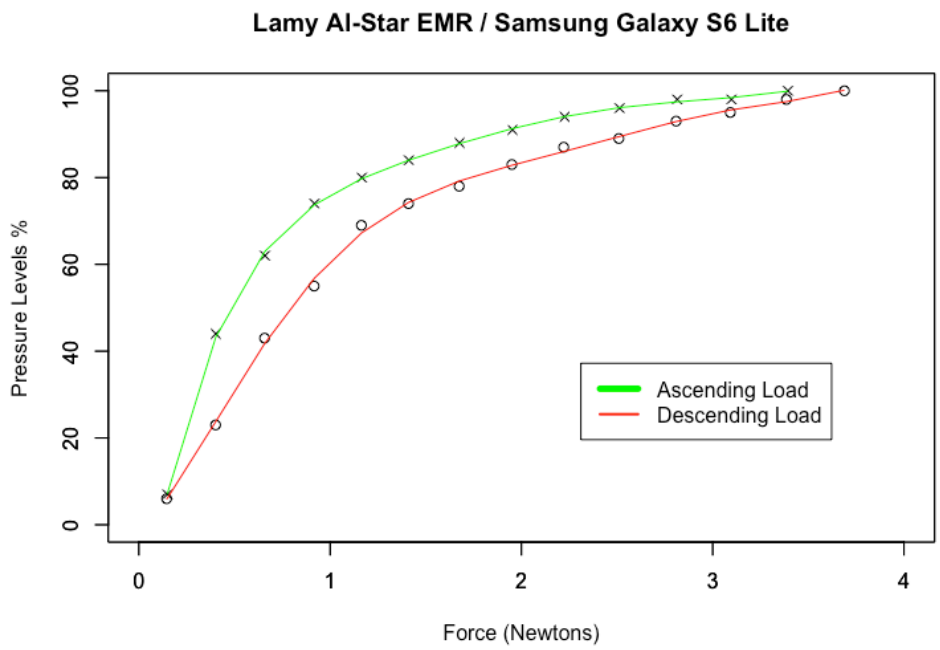


Appendix Table 8 Calibration Curve

Equipment Technical Report

Tablet Manufacturer	Samsung	Model	Galaxy S6 Lite
Stylus Manufacturer	Lamy	Model	LAMY safari twin pen all black EMR
Software used for measurements		STYLUSIS	
# Pressure Levels		100 (4096 normalized as 100 levels)	
Tilt Capture	No	In Air Trajectory Capture	Yes
Minimum Force Threshold (Newtons)	0.1	Maximum Force Threshold (Newtons)	5

Ascending Load Zeta Function

$$Z_{ascending}(x) = -0.9275 + 12.5808x + 88.9644x^2 - 76.4433x^3 + 27.3288x^4 - 4.5936x^5 + 0.2976x^6$$

Ascending Load Inverse Zeta Function

$$Z^{-1}_{ascending}(x) = 1.229 * 10^{-1} + 5.002 * 10^{-3}x + 3.267 * 10^{-3}x^2 - 2.106 * 10^{-3}x^3 + 5.498 * 10^{-6}x^4 + 6.297 * 10^{-8}x^5 + 2.657 * 10^{-10}x^6$$

Descending Load Zeta Function

$$Z_{descending}(x) = -12.0374 + 99.2725x + 53.6294x^2 - 118.574x^3 + 63.4626x^4 - 14.3357x^5 + 1.1896x^6$$

Descending Load Inverse Zeta Function

$$Z^{-1}_{descending}(x) = 6.595 * 10^{-1} - 3.458 * 10^{-1}x + 4.003 * 10^{-2}x^2 - 1.687 * 10^{-3}x^3 + 3.305 * 10^{-5}x^4 - 3.064 * 10^{-7}x^5 + 1.090 * 10^{-9}x^6$$

Appendix Table 9 Technical Report

Calibration Curve
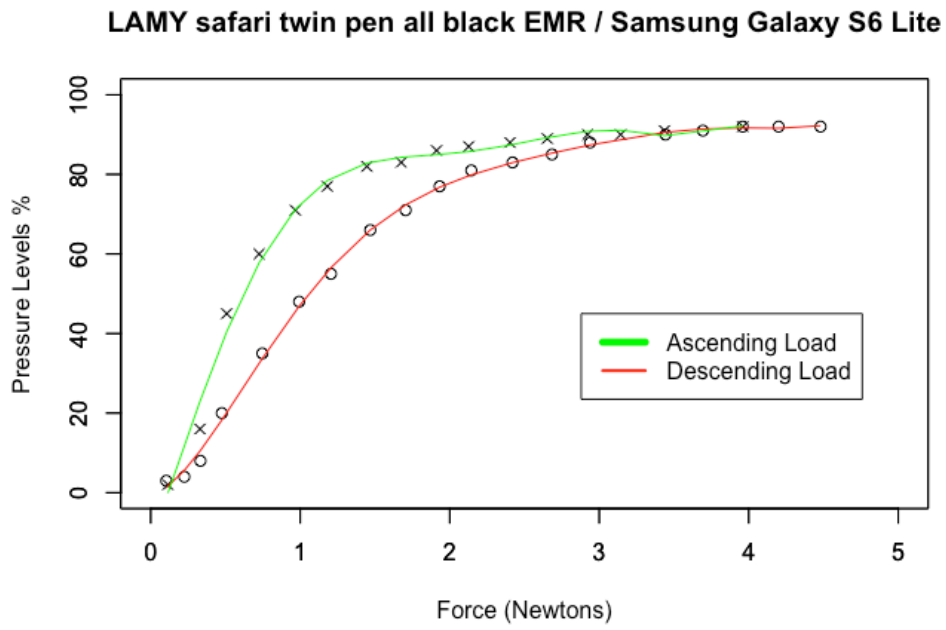


Appendix Table 10 Calibration Curve

Equipment Technical Report

Manufacturer	Wacom	Model	STU530
Stylus Manufacturer	Wacom	Model	Wacom UP61089A1 pen
Software used for measurements		STU SDK version 2.15.4. Wacom Co., Ltd., 2020.	
# Pressure Levels		1024	
Tilt Capture	No	In Air Trajectory Capture	Yes
Minimum Force Threshold (Newtons)	0.14	Maximum Force Threshold (Newtons)	3.5

Ascending Load Zeta Function

$$Z_{ascending}(x) = -273.122 + 2351.661x - 2182.893x^2 + 1150.935x^3 - 341.306x^4 + 53.126x^5 - 3.387x^6$$

Ascending Load Inverse Zeta Function

$$Z^{-1}_{ascending}(x) = 14.74 - 1.713 * 10^{-1}x + 8.007 * 10^{-4}x^2 - 1.898 * 10^{-6}x^3 + 2.434 * 10^{-9}x^4 - 1.608 * 10^{-12}x^5 + 4.318 * 10^{-16}x^6$$

Descending Load Zeta Function

$$Z_{descending}(x) = -179.926 + 3971.228x - 6205.921x^2 + 5091.719x^3 - 2237.698x^4 + 498.409x^5 - 44.15x^6$$

Descending Load Inverse Zeta Function

$$Z^{-1}_{descending}(x) = 59.94 - 7.151 * 10^{-1}x + 3.279 * 10^{-3}x^2 - 7.547 * 10^{-6}x^3 + 9.327 * 10^{-9}x^4 - 5.926 * 10^{-12}x^5 + 1.524 * 10^{-15}x^6$$

Appendix Table 11 Technical Report

Calibration Curve

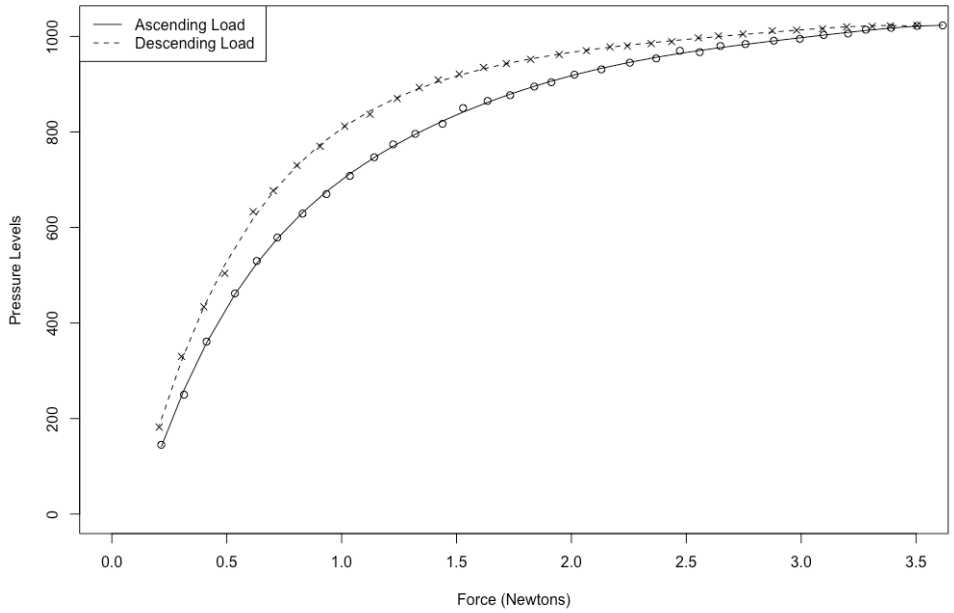

Appendix Table 12 Calibration Curve

Abbreviations

AES: Advanced Electronic Signatures as per the eIDAS definition

BPM: Best Practices Manual

CSV: Comma separated value file

DCS: Digitally Captured Signature (DCS, a.k.a. electronic handwritten signatures or biometric signatures

EMR: Electromagnetic Resonance

ENFHEX: European Network of Forensic Handwriting Experts

ENFSI: European Network of Forensic Science Institutes

F: Force

FCF: Firma Certa Forensic software

FHE: Forensic Handwriting Expert

g: Gravitational Constant (9.81 m/sec^2)

IAT: In air trajectories (i.e. the movement of the stylus over the active area when not in contact)

Kg: Kilograms

m: Mass

N: Newtons

P: Pressure

PPI: Points per inch (resolution)

PPS: Pen and paper signature

QES: Qualified Electronic Signatures as per the eIDAS definition

SDK: Software Developer's Kit

T: Time. Even though in the SI time is symbolized by the small letter "t", due to the ISO19794-7 abbreviations and its adoption by the industry, time will be denoted with the capital letter "T".

WWS: Wacom Signature Scope software

X: Horizontal coordinates on the plane

XY position: the horizontal and vertical coordinates on the plane

Y: Vertical coordinates on the plane

Z: Perpendicular coordinates for 3-dimensional space

ZF: Zeta Function

ZF^{-1}: Inverse Zeta Function

ΔF: Difference in Force values